

This electronic thesis or dissertation has been downloaded from the King's Research Portal at <https://kclpure.kcl.ac.uk/portal/>



## **New Stability Analysis Results on Switched Systems and Fuzzy Systems**

Yang, Xiaozhan

*Awarding institution:*  
King's College London

The copyright of this thesis rests with the author and no quotation from it or information derived from it may be published without proper acknowledgement.

### **END USER LICENCE AGREEMENT**



This work is licensed under a Creative Commons Attribution-NonCommercial-NoDerivatives 4.0 International licence. <https://creativecommons.org/licenses/by-nc-nd/4.0/>

You are free to:

- Share: to copy, distribute and transmit the work

Under the following conditions:

- Attribution: You must attribute the work in the manner specified by the author (but not in any way that suggests that they endorse you or your use of the work).
- Non Commercial: You may not use this work for commercial purposes.
- No Derivative Works - You may not alter, transform, or build upon this work.

Any of these conditions can be waived if you receive permission from the author. Your fair dealings and other rights are in no way affected by the above.

### **Take down policy**

If you believe that this document breaches copyright please contact [librarypure@kcl.ac.uk](mailto:librarypure@kcl.ac.uk) providing details, and we will remove access to the work immediately and investigate your claim.

*A thesis submitted for the degree of  
Doctor of Philosophy*

# **New Stability Analysis Results on Switched Systems and Fuzzy Systems**

Author : Xiaozhan Yang

Student Number : 1421446

First Supervisor : Dr. Hak-Keung Lam

Second Supervisor : Prof. Kaspar Althoefer

February 4, 2019

Ph.D. in Robotics

Department of Informatics

Faculty of Natural & Mathematical Sciences

King's College London

# Acknowledgment

Without the help of many people, it would not have been possible for me to complete the research in this thesis. It is a pleasure to express my gratitude to those who have offered help and contributed to this research.

Firstly I would like to express my sincere and deep gratitude to my supervisor Dr. Hak-Keung Lam who has been a responsible supervisor and also a dear friend to me. His patient and professional guidance was a constant support through the duration of my PhD research. His generous suggestions and assistance also allowed me to explore more broadly as a researcher.

In this regard, I would also like to thank Prof. Ligang Wu of Harbin Institute of Technology (China), Prof. Jian S. Dai of King's College London and Prof. Kaspar Althoefer of Queen Mary University of London for their insightful discussions and helpful comments to improve the work in this research. I am also delighted to express my thanks to Dr. Jie Sun and many other colleagues in King's College London Centre for Robotics Research (CoRe) group for the helpful discussions and fruitful cooperation in our lab which led to some of the results in this thesis.

I would also like to thank my parents, King's-CSC PhD scholarship program and many friends for the financial and emotional support during my PhD study, which made it possible for me to live and study without much worry.

Many special gratitudes are also given to my colleagues in King's College London Students' Union (KCLSU). It's their events, training and collaboration that made King's College a great community and allowed me to grow comprehensively as a student during the academic research.

I also extend my sincere gratitude to many of my friends in London and also the United Kingdom for their encouragement and for being such great examples for me to improve myself. It is with their help, sharing and activities that I had the opportunity to further understand different cultures and conduct my scientific research with a greater awareness of humanity.

I am also grateful to the teachings of Falun Dafa practice, with which I can be more truthful, compassionate and forbearing of the difficulties I encountered in the course of my research and study.

# Abstract

The switched systems and fuzzy systems are common models to describe the non-linear dynamics in practical engineering. And the problem of stability analysis of those systems is of paramount importance. In this thesis we intend to analyze the relationship between some existing methods of stability analysis on switched systems and fuzzy systems, and investigate new approaches to improve these results in term of simplicity and conservativeness. The main content of this thesis can be divided into two branches: stability analysis of second-order switched systems and stability analysis of Takagi-Sugeno (T-S) fuzzy systems.

On the topic of stability analysis of switched systems, we will start from the Lyapunov theory and then propose the concept of phase function. By exploring the properties of phase function, the phase-based stability analysis will be made. And a unified approach for the stability analysis of second-order switched system will be obtained. Compared with existing works, the stability condition obtained here shows advantages in terms of theoretical analysis and numerical computation.

In addition, we will use the phase-based method to see whether the existence of common quadratic Lyapunov functions (CQLFs) for every pair of subsystems can ensure the overall system stability. With additional properties of phase function, the previous stability condition can be further extended. By analysing the equivalent algebraic and linear matrix inequality (LMI) expression of such a new condition, it can be verified that the existence of CQLF for every pair of subsystems will be sufficient for the system stability.

Regarding the stability analysis of T-S fuzzy systems, we will describe the distribution of membership functions in a unified membership space. In this way, a graphical approach is provided to analyse the conservativeness of membership-dependent stability conditions. Following this idea, we will use membership function extrema to construct a simple and tighter convex polyhedron, which encloses the membership trajectory and generates less conservative LMI condition.

As an application of the above membership-dependent analysis method, we will investigate the stability problem of a reconfigurable metamorphic palm control system based on its T-S fuzzy model. Firstly the obtained dynamic model of the metamorphic palm will be transformed to a T-S fuzzy model. Then the palm dynamic boundaries will be used as extrema to reduce the conservativeness in palm

controller design and ensure a wider range of palm re-configuration operations.

Overall, the research in this thesis provides a basic theoretical review of existing stability analysis approaches on specific switched systems and fuzzy systems, and novel approaches have been proposed as an improvement. The results will be of potential use for researchers in the area of systems engineering.

# Contents

<b>Acknowledgment</b>	<b>2</b>
<b>Abstract</b>	<b>3</b>
<b>Contents</b>	<b>5</b>
<b>Author's Publication</b>	<b>8</b>
<b>List of Figures</b>	<b>10</b>
<b>List of Tables</b>	<b>13</b>
<b>Notations and Acronyms</b>	<b>14</b>
<b>1 Introduction and overview</b>	<b>15</b>
1.1 Introduction . . . . .	15
1.1.1 Hybrid systems . . . . .	16
1.1.2 Fuzzy systems . . . . .	18
1.1.3 The issue of stability analysis . . . . .	22
1.1.4 Metamorphic robotic palm as an application . . . . .	24
1.2 Overview on existing stability approaches . . . . .	26
1.2.1 Stability of switched systems . . . . .	26
1.2.2 Stability of T-S fuzzy systems . . . . .	28
1.3 Objective and thesis structure . . . . .	30
1.4 Outline of contributions to knowledge . . . . .	32
<b>2 Preliminaries</b>	<b>33</b>
2.1 The problem of system stability . . . . .	33
2.2 Stability analysis for switched systems under arbitrary switching . . .	36
2.2.1 Polyhedral Lyapunov function [1] . . . . .	38
2.2.2 Polynomial Lyapunov function [2] . . . . .	40
2.2.3 Brief summary . . . . .	41
2.3 Stability analysis for T-S fuzzy systems with membership information	41
2.3.1 Membership function approximation methods [3, 4] . . . . .	42
2.3.2 Membership-bound-dependent relaxation method [5] . . . . .	46

2.3.3	Brief summary . . . . .	47
<b>3</b>	<b>Phase-based stability analysis of switched systems</b>	<b>48</b>
3.1	Introductory remarks . . . . .	48
3.2	Problem formulation . . . . .	49
3.3	The concept of phase function . . . . .	50
3.3.1	Definition of phase function . . . . .	50
3.3.2	Properties of phase function for linear systems . . . . .	51
3.4	Stability analysis under arbitrary switching . . . . .	55
3.4.1	Lyapunov function existence condition in the form of phase function . . . . .	55
3.4.2	Stability condition in the form of phase function . . . . .	57
3.5	Verification examples . . . . .	59
3.5.1	Application of the phase-based condition . . . . .	59
3.5.2	Comparison with existing results . . . . .	60
3.6	Conclusions . . . . .	64
<b>4</b>	<b>Extended results of the phase-based stability condition</b>	<b>65</b>
4.1	Introduction . . . . .	65
4.2	Problem formulation and preliminaries . . . . .	66
4.2.1	Problem formulation . . . . .	66
4.2.2	Preliminaries about phase function . . . . .	67
4.3	Main results . . . . .	69
4.3.1	Further analysis of the phase-based stability condition . . . . .	69
4.3.2	Transformation of the phase-based stability condition . . . . .	74
4.4	Special case: positive switched systems . . . . .	78
4.5	Conclusions . . . . .	80
<b>5</b>	<b>Membership dependent stability analysis of T-S fuzzy systems</b>	<b>81</b>
5.1	Introduction . . . . .	81
5.2	Framework of conservativeness analysis . . . . .	82
5.2.1	Unified space for membership functions . . . . .	82
5.2.2	Membership-dependent conditions as points in the member- ship space . . . . .	84
5.2.3	The extrema-based convex polyhedron construction method . . . . .	86
5.2.4	Extension to the case of interval type-2 T-S fuzzy systems . . . . .	91
5.3	Extrema-based stability conditions . . . . .	93
5.4	Comparison of different membership-dependent methods . . . . .	94
5.4.1	Get the checking points for existing membership dependent methods . . . . .	94
5.4.2	Numerical test for the checking points of different methods . . . . .	97
5.5	Further discussion . . . . .	99

5.6	Conclusions . . . . .	101
<b>6</b>	<b>Fuzzy model based stability analysis of the metamorphic robotic palm</b>	<b>102</b>
6.1	Introduction . . . . .	102
6.2	Kinematic analysis and dynamic modeling of the metamorphic palm .	103
6.2.1	Kinematics analysis of the partial reconfigurable palm . . . . .	105
6.2.2	Lagrangian method based dynamic modeling of the partial reconfigurable palm . . . . .	107
6.2.3	Geometrical constraints based palm kinematics analysis . . . . .	108
6.2.4	Dynamic modeling of the reconfigurable palm . . . . .	109
6.3	Geometry variation based controller design of the metamorphic palm	110
6.3.1	Controller design based on inertia and gravity compensation .	110
6.3.2	Dynamic performance analysis . . . . .	113
6.4	Fuzzy model based stability analysis . . . . .	113
6.5	Conclusions . . . . .	118
<b>7</b>	<b>Conclusions and future work</b>	<b>119</b>
7.1	Main findings . . . . .	119
7.2	Original contributions to knowledge . . . . .	120
7.3	Limitations of the work . . . . .	120
7.4	Suggestion for future research . . . . .	121
	<b>Appendices</b>	<b>122</b>
<b>A</b>	<b>Proofs in Chapter 3</b>	<b>123</b>
A.1	Proof of Proposition 2 . . . . .	123
A.2	Proof of Lemma 4 . . . . .	125
A.3	Proof of Theorem 3 . . . . .	127
<b>B</b>	<b>Proofs in Chapter 4</b>	<b>133</b>
B.1	Proof of Lemma 6 . . . . .	133
B.2	Proof of Lemma 7 . . . . .	135
<b>C</b>	<b>Explanation of the algorithms in Chapter 5</b>	<b>138</b>
C.1	Explanation of Algorithm 1 . . . . .	138
C.2	Explanation of Algorithm 2 . . . . .	139
<b>D</b>	<b>Values of the parameters in Chapter 6</b>	<b>141</b>
	<b>Bibliography</b>	<b>143</b>



# Author's Publication

(Publications during PhD Research):

1. **Xiaozhan Yang**, Hak-Keung Lam, and Ligang Wu. Membership-dependent stability conditions for type-1 and interval type-2 T-S fuzzy systems. *Fuzzy Sets and Systems*, 2018, DOI: 10.1016/j.fss.2018.01.018
2. **Xiaozhan Yang**, Hak-Keung Lam, and Ligang Wu. Necessary and sufficient stability condition for second-order switched systems: a phase function approach. *International Journal of Control*, 2017, DOI: 10.1080/00207179.2017.1375157
3. **Xiaozhan Yang**, Jie Sun, Hak-Keung Lam, and Jian S. Dai. Fuzzy model based stability analysis of the metamorphic robotic palm, *IFAC-Papers - OnLine*, vol. 50, no. 1, pp. 8630–8635. 2017.
4. Bo Xiao, Hak-Keung Lam, **Xiaozhan Yang**, Yan Yu, and Hongliang Ren. Tracking control design of interval type-2 polynomial-fuzzy-model-based systems with time-varying delay, *Engineering Applications of Artificial Intelligence*, vol. 75, pp. 76–87. 2018.
5. Ge Song, Hak-Keung Lam, and **Xiaozhan Yang**. Membership-function-dependent stability analysis of interval type-2 polynomial fuzzy-model-based control systems. *IET Control Theory & Applications*. vol. 11, no. 17, pp. 3156–3170. Nov. 2017.
6. Jianxing Liu, Wensheng Luo, **Xiaozhan Yang**, and Ligang Wu. Robust model-based fault diagnosis for PEM fuel cell air-feed system. *IEEE Transactions on Industrial Electronics*, vol. 63, no. 5, pp. 3261–3270, Feb. 2016.
7. **Xiaozhan Yang**, Hak-Keung Lam, and Ligang Wu. Novel membership-function-dependent stability condition for T-S fuzzy systems, *2016 IEEE World Congress on Computational Intelligence (WCCI2016)*, Vancouver, Canada, July 24-29, 2016.

8. **Xiaozhan Yang**, Hak-Keung Lam, and Ligang Wu. Extended results of phase-function-based stability condition: for second-order switched systems, ***Engineering Applications of Artificial Intelligence***, ready for submission.

# List of Figures

1.1	Graphical representation of the temperature control hybrid automaton model. . . . .	17
1.2	Block diagram of a switched system. . . . .	17
1.3	Gear-box speed control system [6]. . . . .	18
1.4	Motor engine efficiency for different gear ratios $\eta_1, \eta_2, \eta_3$ [7]. . . . .	18
1.5	Membership function of the fuzzy set “temperature is high”. . . . .	19
1.6	Equivalent membership function of the switching rule of hybrid systems. . . . .	19
1.7	Basic structure of fuzzy systems . . . . .	20
1.8	Type-2 membership function of “temperature is high”. . . . .	23
1.9	Robotiq gripper [8]. . . . .	25
1.10	Shadow dexterous hand [9]. . . . .	25
1.11	Metamorphic robotic hand. . . . .	25
1.12	Research topics and their relation in this thesis . . . . .	31
2.1	Concepts of stability . . . . .	34
2.2	Illustration of Lyapunov function $V(x)$ . . . . .	35
2.3	Illustration of the level surfaces of a Lyapunov function $V(x)$ . . . . .	36
2.4	$A_{\sigma(t)} = A_1$ (blue) . . . . .	37
2.5	$A_{\sigma(t)} = A_2$ (green) . . . . .	37
2.6	$A_{\sigma(t)} = A_3$ (red) . . . . .	37
2.7	$A_{\sigma(t)}: A_1 \rightarrow A_2 \rightarrow A_3$ . . . . .	37
2.8	Converging quivers of $A_1x, A_2x, A_3x$ for system states on a level surface of $V(x)$ . . . . .	38
2.9	Level surface of the polyhedral Lyapunov function . . . . .	39
2.10	Illustration of staircase approximation. . . . .	43
2.11	Illustration of piecewise linear approximation. . . . .	44
2.12	Comparison of the minimum $r_1$ in staircase (right) and piecewise linear (left) approximation methods. The dashed smooth gray lines are the trajectories of $h_1(x_1)$ , the solid lines are the layouts of approximated function $\hat{h}_1(x_1)$ , the dotted red lines are the layouts of $\hat{h}_1(x_1) + r_1$ , where $r_1 \geq h_1(x_1) - \hat{h}_1(x_1)$ . . . . .	46

3.1	Definition of phase functions $\phi_\sigma(x)$ and $\phi_p^*(x)$ at point $x$ , with the oval curve being the level-surface of Lyapunov function $V(x)$ and $p(x)$ being the normal of level surface at $x$ . . . . .	51
3.2	Relation of right and left polar decompositions . . . . .	54
3.3	Review of a point on the level surface in Figure 2.8 . . . . .	56
3.4	Magnified micro-space of the considered point in Figure 3.3 and explanation of Criterion (3.12) . . . . .	57
3.5	Layouts of $\varphi_{\min}(\theta)$ and $\varphi_p^*(\theta)$ with different $a$ value and $m$ , (*PLF is the acronym of polynomial Lyapunov function) . . . . .	61
3.6	Phase functions of the subsystem matrices $A_1$ and $A_2$ and their CQLF $\varphi_p^*(\theta)$ (The gray area shows the allowable region for $\varphi_p^*(\theta)$ determined by Conditions (3.11) and (3.12)) . . . . .	62
3.7	Relation of $k$ and $\int_0^{2\pi} \cot \varphi_{\max}(\theta) d\theta$ . . . . .	62
3.8	Comparison among polynomial Lyapunov function [2], piecewise Lyapunov function [10], and phase-based condition in Theorem 3 . . . . .	63
4.1	Definition of phase function $\varphi(A, \theta)$ based on the trajectory of system $\dot{x} = Ax$ . Right: Layout of phase function $\varphi(A, \theta)$ with respect to $\theta$ . . . . .	68
4.2	Layout of phase functions $\hat{\varphi}_{\max}(\theta)$ and $\hat{\varphi}_{\min}(\theta)$ . . . . .	72
4.3	Feasible region of $(a, b)$ : red dots for [11] (every three-tuple of subsystems share a CQLF), blue circles for Theorem 6 (every two-tuple of systems share a CQLF) . . . . .	77
5.1	$h(x)$ with one degree of freedom. The dotted line is the trajectory of $h(x)$ . $\eta_1, \eta_2, \eta_3$ are the vertices of a convex polyhedron enclosing $h(x)$ . . . . .	83
5.2	$h(x)$ with two degrees of freedom. The dotted area is the layout $h(x)$ . $h(x)$ is constrained in the area $0.14 \leq h_1(x) \leq 0.48$ and $0.11 \leq h_2(x) \leq 0.47$ with $h_3(x) = 1 - h_1(x) - h_2(x)$ . . . . .	84
5.3	Feasible values of $(A_1, A_2)$ in the case of $p = 2$ and $n = 1$ , ( $A_1, A_2 \in \mathbb{R}^{1 \times 1}$ ). Points $\eta_1, \eta_2$ are the bounds of $h(x)$ . . . . .	85
5.4	Convex polyhedron obtained by the minimum values of $h_i(x)$ , with the dotted line being the trajectory of $h(x)$ . . . . .	87
5.5	Convex polyhedron obtained by the extrema of $h_i(x)$ , with the dotted line being the trajectory of $h(x)$ . . . . .	87
5.6	Flow chart of Steps 2–4 in Algorithm 1, explaining the calculation of $\alpha_{qk}$ and $\beta_{qmk}$ . . . . .	90
5.7	Possible distribution of an interval type-2 membership function with one degree of freedom, yellow dotted area is the hypercube formed by $(h_1^L(x^*), h_2^L(x^*))$ and $(h_1^U(x^*), h_2^U(x^*))$ . . . . .	92

5.8	Checking points of different methods (piecewise linear approximation method [4] with $d = 3$ : red circle points; bound-dependent method [5]: green triangle points; Theorem 9 with $d = 3$ : blue square points).	98
5.9	Feasible regions of different methods (piecewise linear approximation method [4] with $d = 3$ : red dots; bound-dependent method [5]: small green circles; Theorem 9 with $d = 3$ : big blue circles).	99
5.10	Both polyhedrons $\mathcal{P}_1$ and $\mathcal{P}_2$ have intersection with surface (5.19), but their overlapping area $\mathcal{P}$ is on only one side of surface (5.19). Here $A_i \in \mathbb{R}^{1 \times 1}$ for all $i = 1, 2, \dots, p$	101
6.1	Parameters and frames of the metamorphic hand with a reconfigurable palm [12]	104
6.2	Relationship between parameters gravity vector $\mathbf{g}(p)$ and joint state $p$	111
6.3	Relation between the parameters in inertia matrix $\mathbf{D}(p)$ and joint state $p$	112
6.4	Maximum and minimum values of $h_i(x)$ , $i = 1, 2, \dots, 16$	116
6.5	Dynamic trajectories of joint angles $\theta_1(t)$ and $\theta_5(t)$ under the given control parameters $\mathbf{k}_1$ and $\mathbf{k}_2$	117
6.6	Control inputs $\mathbf{u}(x)$ , $\mathbf{u}_1(x)$ and $\mathbf{u}_2(x)$ under the given control parameters $\mathbf{k}_1$ and $\mathbf{k}_2$	117
A.1	Layouts of functions $\varphi_{\max}(\theta)$ , $\varphi_{\max \epsilon}(\theta)$ and $\varphi_{\max_1}(\theta)$	128

# List of Tables

3.1	Maximum values of $a^*$ obtained by different polynomial Lyapunov functions [13]	60
5.1	Relation of the intermediate variables in Algorithm 1	89
6.1	Parameter definitions of the metamorphic palm	104
6.3	Maximum and minimum values of the parameters $\mathbf{m}_{ij}(x)$ , $i, j = 1, 2$	114
D.1	Parameter values of the metamorphic palm	141

# Notations and Acronyms

## Notations

$A^T$	Transposition of matrix $A$
$\mathbb{R}^n$	$n$ -dimensional Euclidean space
$\mathbb{R}_{>0}$ ( $\mathbb{R}_{<0}$ )	the set of positive (negative) real numbers
$\mathbb{N}$	the set of all natural numbers excluding 0
$\mathbb{N}_0$	the set of non-negative integers
$\mathbb{Z}^+$	the set of positive integers
$P > 0$ ( $P \geq 0$ )	$P$ is real symmetric and positive definite (semi-definite)
$a \stackrel{2\pi}{=} b$	$(a \bmod 2\pi) = (b \bmod 2\pi)$
$\ x\ _2$	the 2nd norm of vector $x$
$x \cdot y$	the scalar product of vectors $x$ and $y$
$\cot(\cdot)$	the usual cotangent function

## Acronyms

CQLF	Common quadratic Lyapunov function
FOU	Footprint of uncertainty
LMI	Linear matrix inequality
LTI	Linear time invariant
MLF	Multiple Lyapunov function
N/A	Not applicable
SOS	Sum of squares
T-S	Takagi-Sugeno

# Chapter 1

## Introduction and overview

*This chapter provides an overview of the background knowledge and elaborates some of the issues associated with the stability analysis of switched systems and fuzzy systems. It also establishes the motivation for the research and outlines the work contained in the reminder of this thesis.*

### 1.1 Introduction

The dramatic development in computing capabilities and engineering materials has resulted in the synthesis and implementation of increasingly complex dynamic systems [14]. One common characteristic of these complex dynamic systems is the high nonlinearities in their system models. However the mathematical tools for nonlinear system analysis are usually restricted in terms of generality and practical applicability. Alternatively, another way to analyze these nonlinear models is by describing their local or transient dynamics as simplified (such as linear) local models and considering the overall model as the hybrid or fuzzy combination of the individual local models. More specifically we name them as hybrid systems [15] and fuzzy systems [16].

These two groups of systems share similarities as both of them describe the original complex dynamics by typical continuous-time local dynamical models and the interacting behavior which is governed by logic rules. But they also have their own distinct characteristics as the logic rules of hybrid dynamical system emphasize more on the discrete-time crisp switching behavior which can be described as instantaneous switching event, while the logic rules of fuzzy systems emphasize more on the continuous smooth blending effect of local dynamics.

The idea of the above multi-model approaches for complex nonlinear system makes the modeling possible to be an art in theory, as we can easily perceive and describe the dynamic behavior around us by the mathematical tools we have. It also provides us the practical analysis act to understand things directly, rather than simply identifying and reproducing the input-output relation by computer.

Among all aspects we want to understand for a system, the characteristic of



stability is probably the most fundamental and important one [17]. If the considered equilibrium point of a system is unstable, a small input perturbation will result in an output with a large amplitude that may or may not converge to the original state, consequently resulting in a number of practical issues. For example, the unstable thermostat may produce the undesirable high heat that causes electric fire, the unstable engine speed control system of a vehicle could be a potential reason for traffic accident, and without stability, it would be impossible for a robotic hand to grab things properly. Motivated by this necessity, different approaches have been proposed for the stability analysis of hybrid systems and fuzzy systems.

In the following part, we will briefly introduce the models of hybrid systems and switched systems, and elaborate on the stability issues that are related with them.

### 1.1.1 Hybrid systems

In practical engineering, many systems that typically exhibit simultaneous discrete and continuous dynamics can be described as hybrid dynamical systems [14]. Examples include the switched electrical circuit [18] where voltages and currents change continuously following the classical electrical network law and also change discontinuously due to switches opening or closing [19]. Some other applications can be found in manufacturing systems [20], automotive engine control [21], air traffic management [22], chemical processes [23], thermostat control systems [15], engine speed control [7] etc. Among those systems, two typical classes can be formed based on the relationship between their continuous states and discrete states, namely hybrid automata [15] and switched systems [24].

#### 1.1.1.1 Hybrid automata

Some models of hybrid systems explicitly partition the system state into a continuous state  $x_c$  which describes the primary system dynamic, and a discrete state  $x_d$  which describes the mode of the system [19]. This group of systems are generally called *hybrid automata* [15]. For this group of systems, each mode in  $x_d$  is associated with constraints within which the continuous state  $x_c$  can evolve. Edges between modes in  $x_d$  are annotated with guards that indicate the conditions for the mode transition to be triggered. Each edge is also associated with a reset map explaining how the continuous state  $x_c$  is being updated after transition of  $x_d$  [15].

For example, in the temperature control systems, state  $x_d$  can be described as the “on” and “off” working modes of thermostat; state  $x_c$  can be applied to represent the room temperature which follows different evolving dynamics depending on whether the heater is on or off. Assume that the heater is initially off and the room temperature is  $x_c = 15^\circ\text{C}$ . We set the desired room temperature as  $x_{\text{desire}} = 25 \pm 1^\circ\text{C}$ . Then the guard is  $x_c < 24^\circ\text{C}$  which triggers the transition of  $x_d$  from “off” to “on”. The reset map of  $x_c$  will be continuous as  $x_c := x_c$ . After a period of time when the

room temperature  $x_c$  hits the threshold  $26^\circ\text{C}$ , transition of  $x_d$  from “on” to “off” will be triggered by guard  $x_c > 26^\circ\text{C}$ , and reset map will still be continuous as  $x_c := x_c$ . The graphical representation of this example can be found in Figure 1.1.

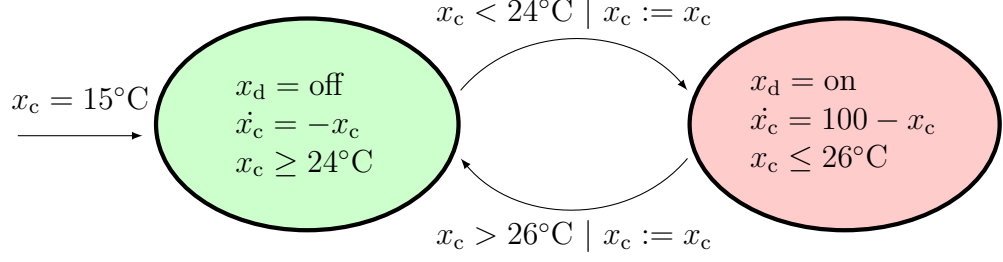


Figure 1.1: Graphical representation of the temperature control hybrid automaton model.

### 1.1.1.2 Switched systems

If the dynamics of a hybrid system are described by a differential equation whose right-hand side is chosen from a family of functions based on a switching signal, then we can call it a *switched system* [24]. In this case, the state  $x$  in the system is continuous. The *switching signal* will be a logic rule that orchestrates the switching between the functions of subsystems.

Mathematically, a switched system can be written as

$$\dot{x} = f_{\sigma(t)}(x), \quad (1.1)$$

where  $\sigma(t) \in \mathcal{Q} = \{1, 2, \dots, q\}$  is the switching signal,  $f_{\sigma(t)}(x) : \mathbb{R}^n \rightarrow \mathbb{R}^n$  is a continuous  $n$ -dimensional function describing the system structure under the switching signal  $\sigma(t)$ . The block diagram of a switched system can be depicted as Figure 1.2.

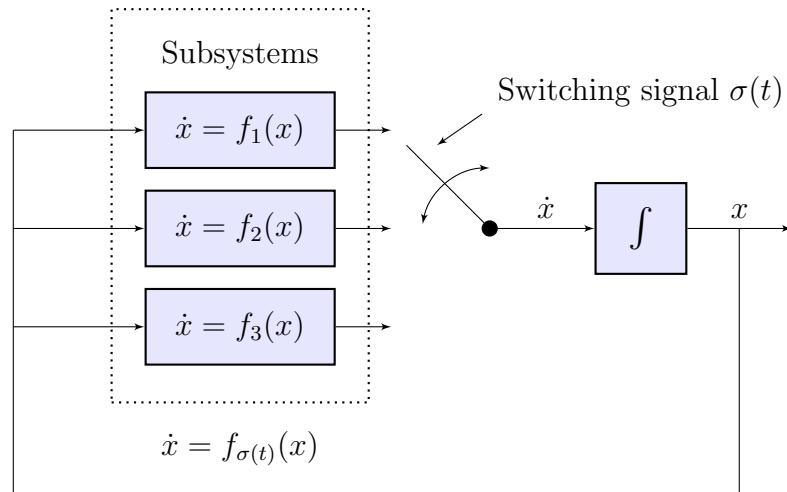


Figure 1.2: Block diagram of a switched system.

An example of the switched system is the gear-box speed control system of motor engine, see Figure 1.3.



Figure 1.3: Gear-box speed control system [6].

Generally the motor engine efficiency of a vehicle has different optimal efficiency zones [7] under different gear ratios  $\eta_1$ ,  $\eta_2$ ,  $\eta_3$ , see Figure 1.4. As a result, with the increase of velocity, switching from lower to higher gear ratios will be necessary for the optimal motor operation. The corresponding system dynamics under each gear ratio can be viewed as the subsystem  $\dot{x} = f_i(x)$  ( $i = 1, 2, 3$ ) of the motor engine system. The switching signal  $\sigma(t)$  comes from the gear stick, as shown in Figure 1.3.

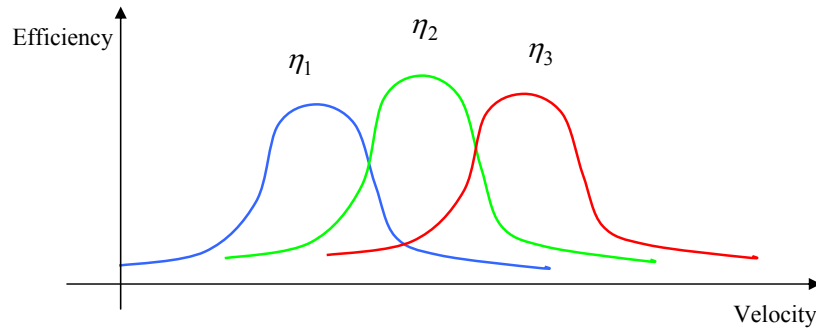


Figure 1.4: Motor engine efficiency for different gear ratios  $\eta_1$ ,  $\eta_2$ ,  $\eta_3$  [7].

### 1.1.2 Fuzzy systems

The concept of “fuzzy set” was first introduced by L. A. Zadeh in his manuscript [25] in 1965. Let  $X$  be a space of points (objects), with a generic element of  $X$  denoted by  $x$ . Then a fuzzy set can be defined as:

**Definition 1.** [25] A **fuzzy set (class)**  $A$  in  $X$  is characterized by a membership (characteristic) function  $h_A(x)$  which associates each point in  $X$  with a real number in the interval  $[0, 1]$ , with the value of  $h_A(x)$  at  $x$  representing the “grade of membership” of  $x$  in  $A$ .

And the term *membership function* we mentioned above is defined as:

**Definition 2.** For any set  $A$ , a **membership function**  $h_A(x)$  on  $X$  is any function from  $X$  to the real number unit interval  $[0, 1]$ .

What makes the fuzzy sets different from the switching rules mentioned in the hybrid system above is the membership function associated with it. In other words, such a set is characterized by a membership characteristic function which assigns to each object a grade of membership ranging continuously between zero and one. For example, the set “room temperature is high” can be a fuzzy set with membership function whose input is “room temperature” and output is a continuous value between zero and one, see Figure 1.5. Intuitively we know that, in the concerned range, the output value will increase monotonously with the increase of temperature.

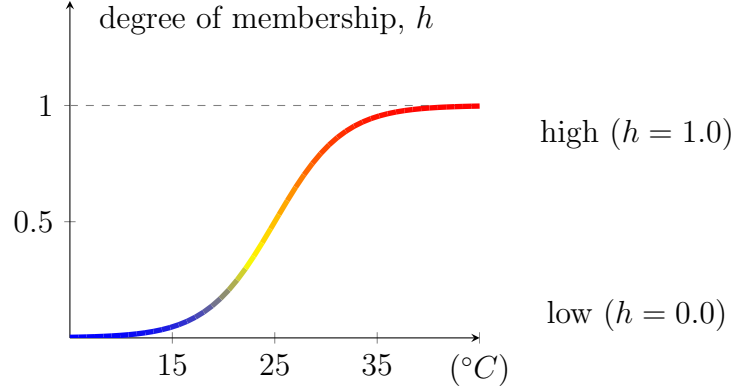


Figure 1.5: Membership function of the fuzzy set “temperature is high”.

The various types of switches, or “on-off” of hybrid systems can be also viewed as a group of sets, but such kind of sets will always have a truth membership value equal to either one or zero. In this sense, the hybrid systems can be dealt with as fuzzy systems with simplified membership functions that happen to be either one or zero, see Figure 1.6.

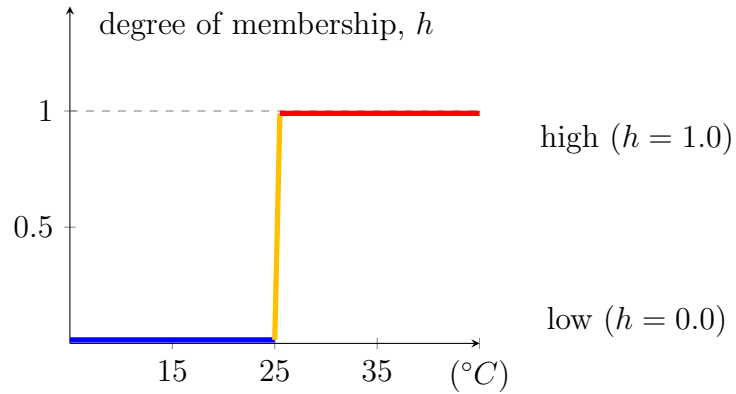


Figure 1.6: Equivalent membership function of the switching rule of hybrid systems.

In fuzzy systems, the membership function will determine the “mappings” from input variable to a truth value between zero and one. Based on the generated membership value on each rule, the fuzzy logic then makes decisions for what action to take. This process can be conceptually divided into three stages: input stage, processing stage, and output stage. The input stage will involve a process called *fuzzification*, which can be explained as below,

**Definition 3. Fuzzification** is a process that maps sensor input to the appropriate truth values by the membership function.

The processing stage is based on a collection of logic rules in the form of IF-THEN statement, which are defined as *fuzzy rules* here. In each of these rules, the IF part is called the “antecedent” and the THEN part is named as “consequent”. Finally the output state is a process of *defuzzification* that can explained as below,

**Definition 4. Defuzzification** is a process that converts the fuzzy result back to a specific control value, see Figure 1.7.

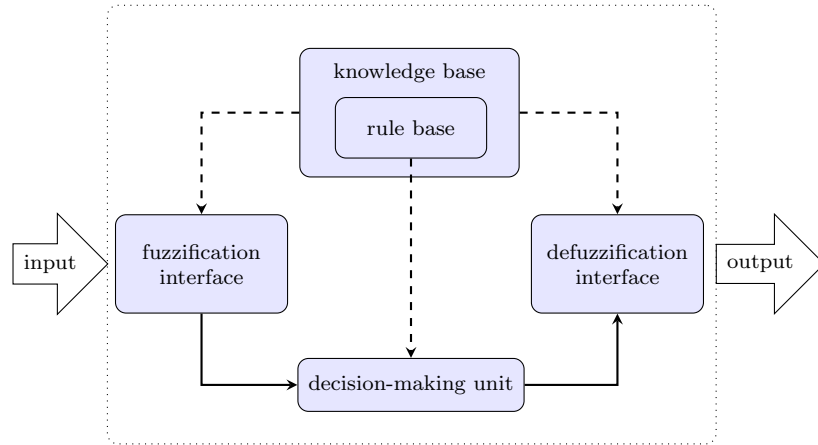


Figure 1.7: Basic structure of fuzzy systems

Following this concept, a simple fuzzy rule of a thermostat can be stated as [26]:

**IF** (temperature is high) **THEN** (turn the heater off),  
**IF** (temperature is low) **THEN** (turn the heater on).

Fuzzy rules play a key role in connecting the input and output variables by the expert knowledge and experience. Theoretically there are two commonly used types of fuzzy rules, namely, Mamdani fuzzy rules [27,28] and Takagi-Sugeno (T-S) fuzzy rules [29]. We will discuss them briefly in the following section.

#### 1.1.2.1 Mamdani fuzzy systems

The typical rule of a Mamdani fuzzy model [27,28] can be viewed as the logical extension of the above rule for thermostat. What makes it different is the *Mamdani fuzzy system*, whose reasoning process can be presented as below,

**Definition 5.** Normally, the **standard reasoning process in a Mamdani fuzzy system** can be achieved in the following six steps:

1. Determining a set of fuzzy rules,
2. Fuzzifying the inputs using the input membership functions,

3. Combining the fuzzified inputs according to the fuzzy rules to establish a rule strength,
4. Finding the consequence of the rule by combining the rule strength and the output membership function,
5. Combining the consequences to get an output distribution,
6. Defuzzifying the output distribution.

In the above example of the thermostat, we assume that the power of a heater can be continuously tuned. Then part of the Mamdani fuzzy rules can be described as:

**IF** (temp. is high) **AND** (temp. is increasing) **THEN** (heater is low)  
**IF** (temp. is high) **AND** (temp. is decreasing) **THEN** (heater is modest)

For this example, we have multiple variables, “temperature” and “temperature changing trend”, as input variables. And the fuzzy sets represented by them are connected by the **AND** logic operator. In Mamdani fuzzy rules, the variables as well as linguistic terms such as “high” can be represented by mathematical symbols [30]. So, a general *Mamdani fuzzy rule* for fuzzy modeling can be described as follows:

$$\mathbf{IF} (x_1 \text{ is } M_1) \mathbf{AND} (x_2 \text{ is } M_2) \mathbf{THEN} (u_1 \text{ is } M_3) \mathbf{AND} (u_2 \text{ is } M_4) \quad (1.2)$$

where  $M_1$ ,  $M_2$ ,  $M_3$ , and  $M_4$  are fuzzy sets,  $x_1$  and  $x_2$  are input variables,  $u_1$  and  $u_2$  are output variables.

#### 1.1.2.2 T-S fuzzy systems

As we can see in rule (1.2), the Mamdani systems provide directly the linguistic action (or output) in the rule consequent, without the need of mathematical models. So it is termed as a model-free control approach. Different from the Mamdani fuzzy rules, the rules in T-S fuzzy model [29] use functions of variables as the rule consequent, thus are model-based. We can formal present it as

**Definition 6.** *The T-S fuzzy model is a fuzzy model that is described by IF-THEN rules (like (1.2)), and uses functions of input variables as the rule consequent.*

In this way, the model description will be more consistent and stability analysis will be made easier. A typical T-S fuzzy rule corresponding to the Mamdani rule in (1.2) can be presented as

$$\mathbf{IF} (x_1 \text{ is } M_1) \mathbf{AND} (x_2 \text{ is } M_2) \mathbf{THEN} u_1 = f(x_1, x_2) \mathbf{AND} u_2 = g(x_1, x_2) \quad (1.3)$$

where  $f(\cdot)$  and  $g(\cdot)$  are two real functions describing the system output.

In the practical case, when the T-S fuzzy model is used to represent a nonlinear system, the input variables of the rule antecedents are specially named as *premise variables*, denoted as  $z = \{z_1, z_2, \dots, z_p\}$ , which may be functions of state variables, input variables, or external disturbances. With the given value of premise variables and corresponding degree of memberships, it will be possible for us to work out the contribution made by each rule. As a result, the dynamics of a nonlinear system can be described as an average weighted sum of the local subsystems where the weights are characterized by the contribution of each rule [31].

### 1.1.2.3 Type-2 fuzzy systems

The fuzzy systems we mention before have a grade of membership that is crisp. They have been successfully used in many practical applications. However, such kind of membership functions are not capable of handling the data uncertainties of the grade itself. For example, the linguistic term “high temperature” can mean different values to different people, or a certain value of the temperature can be described as different degree of “high” by different people. To solve this problem, the *type-2 fuzzy sets*, which can be also called “fuzzy-fuzzy set”, were proposed in 1957 in [32]. This concept provides the possibility to measure the uncertainty in a single membership function. The definition of *type-2 fuzzy sets* can be highlighted as below:

**Definition 7.** *A type-2 fuzzy set is a fuzzy set that incorporates uncertainty about the membership function into fuzzy set theory.*

The type-2 fuzzy membership function actually has a 3-D layout. While a common way to visualize such a type-2 fuzzy set is to plot its *footprint of uncertainty* (FOU) on its 2-D domain [33]. In this way, all the possible uncertain area of the membership can be depicted. For example, the expected value of a high temperature for people in south China is generally several degrees higher than that of people in north China. Thus, to have all the Chinese considered, we can design the temperature membership function as a combination of a lower membership function  $h^L(x)$ , based on the feeling of people in south China, and an upper membership function  $h^U(x)$ , based on the feeling of people in north China, see Figure 1.8. The area between  $h^L(x)$  and  $h^U(x)$  is the FOU that has been widely used in the system analysis.

### 1.1.3 The issue of stability analysis

As a fundamental problem of system analysis, the stability of a system relates to its response to inputs or disturbances. A stable system will remain in a constant state unless it is affected by an external action, and it will return to a constant state when the external action is removed. By practical test, we can find whether a system is

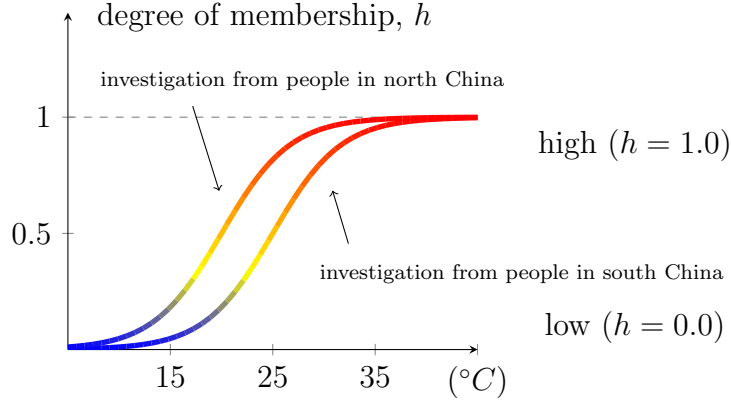


Figure 1.8: Type-2 membership function of “temperature is high”.

stable or not in some special cases. But that is not sufficient in the real case, for the damage would have already been caused when we see the unstable reaction. As a result, there is a need for *stability analysis* in theory to investigate whether a system is stable or not.

For a linear time invariant (LTI) system, there are a number of classical methods to determine the stability property. For example, Routh-Hurwitz stability condition [34], root locus method [35], and also Nyquist diagram [36] and Bode Plot [37] via frequency domain techniques. With these methods, not only can we see whether a system is stable, but also determine how close the system is to instability and the margin for disturbances.

However, it is not easy to find the counter part of those methods for complex nonlinear systems. In such cases, we need to see the stability problem as a typical phenomenon of the dynamical system concerning its equilibrium point  $x_e$ <sup>1</sup>. In simple terms, if the solutions that start out near an equilibrium point  $x_e$  stay near  $x_e$  forever, then  $x_e$  is *Lyapunov stable*<sup>2</sup>. More strongly, if  $x_e$  is Lyapunov stable and all solutions that start out near  $x_e$  converge to  $x_e$ , then  $x_e$  is *asymptotically stable*<sup>3</sup> [38]. Since the idea of Lyapunov stability can be extended to infinite-dimensional manifolds, it is a general way for the stability analysis of complex systems such as hybrid systems and fuzzy systems.

Let’s take the temperature controller as an example. Considering that we set the desired temperature as  $x_{\text{desire}} = 25^\circ\text{C}$ , if any temperature starting near  $x_{\text{desire}}$  can be regulated back to  $x_{\text{desire}}$ , we can say that the temperature control system is stable. In this thesis we consider the stability problem of hybrid systems and fuzzy systems. And we will specially focus on the general forms of these two branches of systems, namely the switched systems and T-S fuzzy systems.

<sup>1</sup>Throughout this thesis, the stability property of we considered for a nonlinear system is with respect to its equilibrium point. For example, by saying “the stability of a switched system”, we mean the stability of the equilibrium of such a switched system.

<sup>2</sup>Formal definition can be found in the Definition 8 of Chapter 2.

<sup>3</sup>Formal definition can be found in the Definition 9 of Chapter 2.



### 1.1.3.1 Stability issues for switched systems

For switched systems, stability issues include several interesting phenomena which show that the stability of a switched system depends not only on the dynamics of each subsystem but also on the properties of switching signals [39]. In the example of the gearbox speed control system in Figure 1.3, the motor engine is generally stable at each constant gear ratio. But the instant switching action between different gear ratios may cause an engine flameout problem.

Another phenomenon can be noticed in the temperature control system, see Figure 1.1. It is obvious that such a system will be unstable if we leave the heater constantly on or constantly off. But by the autonomous switching mechanism between on and off, the temperature can be regulated gradually back to the desired value  $x_{\text{desire}}$ .

In this sense, the stability issues for switched systems can be roughly classified into two categories. One category is the stability analysis of switched systems under given switching signals (such as arbitrary switching, slow switching etc). Another category is the synthesis of stabilizing switching signals for a given group of dynamical systems [39].

### 1.1.3.2 Stability issues for T-S fuzzy systems

As we have mentioned in Section 1.1.2, the switched system can be treated as a special kind of fuzzy system with crisp fuzzy sets. Therefore, the stability analysis methods for switched systems and fuzzy systems share similarities. Specifically, some linear matrix inequality (LMI) stability conditions for switched systems under arbitrary switching can be well extended to analyze the stability property of T-S fuzzy systems with similar LTI subsystems. In this case the stability condition is not dependent on the membership functions of T-S fuzzy systems.

The analysis result in such case is generally conservative<sup>4</sup> since the membership grade information is not considered in the stability condition. While for the membership-dependent approach, the systems structural information will be taken into account. More general ways of membership-dependent analysis will be made possible especially when the membership functions fulfill some constraints that can help to relax the LMI-problem formulation [40].

## 1.1.4 Metamorphic robotic palm as an application

As the end-effector of a robot, a robotic hand is a critical component between the robot and environment. In terms of application fields, robotic hands have two typical categories: grippers [41] (see Figure 1.9) and dexterous hands [42] (see Figure

---

<sup>4</sup>By *conservativeness* (or being *conservative*), we describe the degree of unnecessary restriction in the stability result. For example, a necessary and sufficient condition will be less conservative than a sufficient but unnecessary condition.

1.10). The gripper has a generally simple structure but is not very flexible to fulfill complex grasping tasks. On the contrary, a dexterous hand is highly flexible in terms of grasping and manipulation tasks, while the complexity in theoretical and computational analysis will make it less reliable in practical cases.



Figure 1.9: Robotiq gripper [8].



Figure 1.10: Shadow dexterous hand [9].

As a trade-off of these two design approaches, a metamorphic robotic hand with a reconfigurable palm was developed by taking advantages of intelligent mechanisms [43–45], see Figure 1.11. The design of such a reconfigurable palm was originally inspired by origami with a mechanism which relates the panels and crisis to links and joints respectively [46].

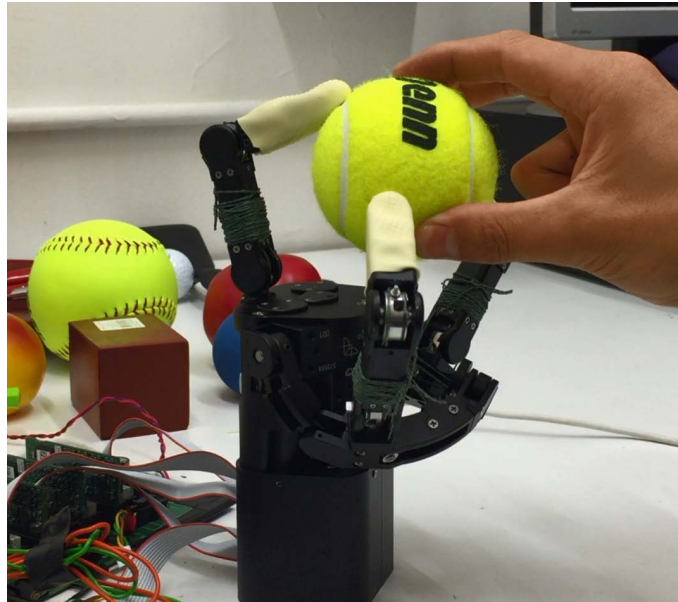


Figure 1.11: Metamorphic robotic hand.

As we can see, by introducing a reconfigurable palm, this metamorphic hand retains the robustness property of grippers and at the same time, can generate flexible and delicate motions as a dexterous hand [47]. Compared with the dexterous robotic hand, the structural complexity of each finger has been greatly reduced,

because the finger orientation can be directly changed by the reconfigurable palm. While to ensure the practical reliability and applicability of this metamorphic hand, the stability of reconfigurable palms should be an important issue. In Chapter 6, we will discuss more on this issue based on the T-S fuzzy model of this device.

## 1.2 Overview on existing stability approaches

In this thesis we focus on the general forms of hybrid systems and fuzzy systems, namely the switched system and the T-S fuzzy system, to consider the improved approaches for their stability analysis. Before that, we will review some existing approaches of stability analysis for switched systems and T-S fuzzy systems.

### 1.2.1 Stability of switched systems

In recent decades, the stability issues of switched systems have drawn much attentions in the field of system engineering. There are several excellent surveys and reviews on the stability of switched systems explaining the large amount of applications and existing results, see for example the survey papers [39, 48–50] and introductory book [24].

We will briefly overview some existing research results to provide the background information to readers. As we have discussed in Section 1.1.3.1, the stability problems of switched systems can be divided into two aspects: stability analysis and stabilization. Within the problems of stability analysis, we can further separate them based on the property of switching signals: systems under arbitrary switching and systems under restricted switching. Under each group of research topics, we will discuss the methods that are specific to them.

#### 1.2.1.1 Stability analysis under arbitrary switching

By arbitrary switching, here we mean that there is no restriction on the switching signals. For such a switching system, the activated system can be any of the subsystems at anytime. The necessity for investigating this problem comes from the fact that, even though all the subsystems are stable individually, it is still not sufficient to ensure the overall system stability, just like the case of the gear ratio switching system that we mentioned in Section 1.1.3.1. Meanwhile, based on the Lyapunov theory, we also know that a common Lyapunov function for all the subsystems can guarantee the system state convergence under arbitrary switching. So this gives us a practical way to consider this kind of stability problems.

Among the various approaches, common quadratic Lyapunov function (CQLF) has been widely considered and attracted much research efforts due to its advantages in practice. One advantage of this approach is that the conditions for the existence

of a CQLF can be expressed as LMIs [51]. Numerical methods have been used for solving these LMIs, for example the standard interior point methods [52] and interactive gradient decent algorithm [53] which can converge to the desired CQLF in finite steps.

The numerical methods for solving LMIs of CQLF have contributed a lot towards solving practical problems, especially with the development of computer softwares such as Matlab toolbox. But research on algebraic conditions for the existence of CQLF remains a challenging task. Various attempts have been made in this direction because this kind of results are easier to verify and also provide valuable insights in the stability property of a given switched system [39]. Especially for the second-order switched LTI systems with two modes, the concept of matrix pencil [54] has been adopted to investigate the algebraic conditions that can be necessary and sufficient for system stability.

It is worth mentioning that the existence of a CQLF is only sufficient for system stability under arbitrary switching. The conservativeness here generally comes from the restricted flexibility of the quadratic Lyapunov function. To improve this, some novel ideas have been proposed to give greater freedom for the construction of the Lyapunov function, such as the norm-based Lyapunov function [55], polyhedral Lyapunov function [1], line-integral Lyapunov function [56], and polynomial Lyapunov function [2].

When the investigated switched systems are restricted to the class of second-order, some special techniques can be also applied. For example, analysis based on the polar coordinate transformation [57–60], the algebraic analysis for the existence of CQLF [11] as we mentioned before, analysis by means of the generalized first integral [61] and the geometry-based algorithm [62].

#### 1.2.1.2 Stability analysis under restricted switching

For some switched systems, the switching behavior might not be arbitrary but restricted to a special group of signals. For example the automobile gear switching system in some cases is restricted naturally by physical constraints, and a particular sequence/order (from first gear to the second gear then to the third gear, rather than directly to the third gear) must be followed; the mode switching in the temperature control system cannot change too fast because of the delay of heat transmission.

With such kind of prior knowledge about the switching signals, we can obtain much stronger and less conservative stability conditions for a given switched system than that in the arbitrary switching case. This is generally achieved by considering worst case scenarios, based on the necessity property [39].

By solving this problem, one may find the answer to whether the system is stable under the restricted switching, or what restrictions should be applied on switching signals in order to guarantee the stability of switched systems. The restrictions

on switching signals may be either state space restrictions (such as abstractions from partitions of the state space, trajectory dependent switching), or time domain restrictions (such as dwell-time, average dwell-time switching signals).

Based on the investigation in [49], one may find that an unstable state is usually the result of failure to absorb the energy generated by switching or unstable subsystems. Therefore, an intuitive idea would be whether the stable subsystems can be activated relatively long enough, so that the energy increase caused by switching or unstable subsystems can be traded off. This idea has been proven to be reasonable and can be realized by concepts such as dwell time and average dwell time of switching signals [63]. Readers may refer to [64,65] for detailed results on this topic.

For systems where switching is restricted in the state space, one basic idea to consider the system stability is to construct multiple Lyapunov functions (MLFs). And each of these functions is related with each single subsystem or certain region in the state space described by the switching restriction. Then a non-traditional Lyapunov function can be constructed by concatenating the MLFs together. This theory has been studied and excellent reviews can be found in [48–50,64].

### 1.2.2 Stability of T-S fuzzy systems

As we have mentioned in Section 1.1.2.2, it is generally not easy to analyze the stability property of Mamdani-type fuzzy systems, for they are based on linguistic description rather than a precise mathematical model. While the model-based rules in T-S fuzzy model can precisely capture the dynamics behavior of a nonlinear system by describing its local dynamics as subsystems. By considering the contribution of each rule at specific time, the T-S fuzzy model can be further expressed as a weighted summation of the local subsystems. As a result, the stability analysis for T-S fuzzy model will be made possible.

A necessary step for stability analysis is to find the equivalent fuzzy model of the nonlinear system. Techniques for constructing a T-S fuzzy model can be classified into three branches [31]: (1) system identification techniques based on experimental data [29,66], (2) sector nonlinearity techniques [67], (3) model approximation by combining linearized models at the chosen operating points of membership functions [68].

With the constructed T-S fuzzy model in the form of multiple linear subsystems, stability analysis of the original system would be made easier. Generally there are two streams of analysis approaches, namely the membership-independent and membership-dependent analysis approaches [69], which are all based on the Lyapunov stability theory.

### 1.2.2.1 Membership-independent approach

For the membership-independent stability analysis, the shapes of membership functions are not considered in the stability analysis. Once the T-S fuzzy system is verified to be stable by the membership-independent stability condition, system stability can be guaranteed regardless of the expression of membership functions [31]. Since the information we use in stability analysis is just the expression of multiple subsystems, to some extent, the analysis process will be quite similar to that of switched systems under arbitrary switching. To reduce the conservativeness in stability analysis, an intuitive idea is to construct more flexible Lyapunov function covering a wider range of subsystems.

Similar to the analysis for switched systems, various types of Lyapunov functions have been constructed for stability analysis of T-S fuzzy systems. Among them, the quadratic Lyapunov function in [70, 71] is the basic and simple approach and the LMI stability condition can be derived directly from the analysis. This method can be easily extended to other system analysis problems such as passivity and  $H_\infty$  performance. But on the other hand, flexibility will be greatly restricted by its simplicity and thus conservativeness can be relatively big.

A direct way to improve the flexibility of Lyapunov function is to increase the mathematical order of its expression. Following this idea, the polynomial Lyapunov function has been proposed in [2]. With this method, we can clearly see in the example of [2] that, conservativeness of stability analysis can be gradually minimized by increasing the order of polynomial Lyapunov function. However, the computational efforts in practical cases will increase accordingly.

If we think from a mathematical point of view, an alternative way of improving flexibility would be increasing the number of candidate terms for constructing an overall Lyapunov function. The advantage of this approach comes from the fact that the individual candidate may not be positive monotonic decreasing globally, but by proper combination of their local decaying area, the joint function would ensure the global energy convergence.

The different ways of connecting these candidate terms would result in different sub-classes of MLF candidates, for example, the piecewise-linear Lyapunov function [72, 73] or switching Lyapunov function [74, 75] candidate divides the operating domain in the state space into a number of operating sub-domains and would choose a different local Lyapunov function candidate [31] in different sub-domains.

### 1.2.2.2 Membership-dependent approach

In the membership-independent stability analysis approach, the way to reduce analysis conservativeness is to improve the Lyapunov function itself, such that a wider range of subsystems can be covered. But actually, we can make use of the system information to avoid invalid combinations of subsystems, thus reduce the range of

subsystems variation to be considered in the analysis. In this way, it will be relatively easy for us to find a proper Lyapunov function and consequently reduce the conservativeness in analysis.

For the switched system we mentioned before, we can further consider the switched signal as additional information. Here for the T-S fuzzy system, additional information can be found in the membership function of each fuzzy rule. It would be impractical to consider all the membership information in the stability analysis since the membership functions might be continuously changing in the whole domain. A feasible and practical way to make use of membership function is to find the relative simple characteristic information of it.

Generally there are two ways to do this. One approach of characterizing the membership function is to find its simplified approximation [3, 4, 76, 77] that can be easily described and combined in the system analysis. Of course, we also need to find the boundary of approximation error, such that sufficiency can be ensured in the stability result. Following this approach, different functions have been used to approximate the original complex membership functions, for example, staircase function in [3], piecewise linear function in [4] and polynomial function in [76–78].

In the approximation approach we mentioned above, a simplified approximated function is designed and an error bound is used together to include the exact original membership function. We can say that this is from inside (the approximated function can be viewed as the center) to outside (the error bound can be viewed as the radius). Another approach is to start from the opposite direction. That is, we start from the highest and lowest membership values ( $h = 1$  and  $h = 0$ ) and gradually shrink them to find the upper-bound and lower-bound of the membership function. Then the boundary information can be applied in the stability analysis [5]. Sufficiency in this approach can be also ensured since the exact original membership function is still included in the region between upper-bound and lower-bound.

### 1.3 Objective and thesis structure

In this thesis we will focus on the stability problems of switched systems and T-S fuzzy systems. As we mentioned above, for both switched systems and T-S fuzzy systems, there are generally two approaches to improve the stability analysis. In the first approach, the research point is the Lyapunov function itself. By finding a new method to construct a proper and flexible Lyapunov function, a wide range of subsystems can be included and less conservative results can be obtained.

In the second approach, the main idea is to improve the analysis results by making use of system information (which is the switching signal for switched systems and the membership function for T-S fuzzy systems). We can also understand it as: reduce the range of subsystem variation by making use of the switching signals or

membership functions, such that it will be easier for us to construct an appropriate Lyapunov function.

Here we will investigate the new research methods in both approaches, such that improved results can be obtained. Specifically, for the first approach, we will investigate the stability analysis problem of switched systems under arbitrary switching. In this case if the conservativeness is reduced to a minimum for the given subsystems, we can say the result is necessary and sufficient condition.

And for the second approach, we will consider the membership-dependent stability analysis methods in a new framework. In this way we can see clearly how the range of subsystem variation can be reduced by considering the membership information, which will make it easier for us to construct a proper Lyapunov function.

As the sub-branches of our main research directions, we will also consider the further extension of the analysis result obtained in the first approach and apply analysis result of the second approach in the metamorphic robotic palm. An outline of our research topics can be found below in Figure 1.12.

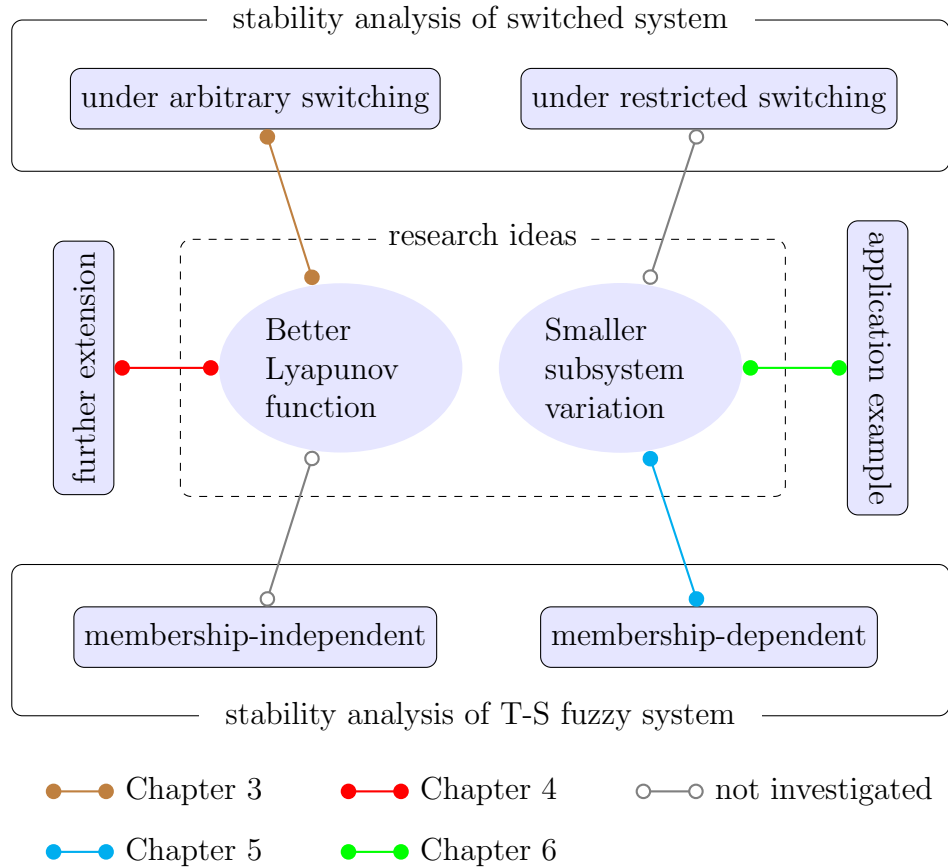


Figure 1.12: Research topics and their relation in this thesis

Specifically in Chapter 2, we will elaborate the preliminary knowledge about system stability analysis. Based on that, firstly we will introduce the existing research ideas on how to construct a better Lyapunov function for multiple subsystem



models, e.g. switched systems. Secondly we will discuss the existing approaches to reduce conservativeness in stability analysis of T-S fuzzy systems by considering membership information.

Chapter 3 follows the preliminary on the stability problem of switched systems in Chapter 2 to discuss the new phase-based approach of stability analysis for second-order switched systems under arbitrary switching. The idea here is based on the existence condition of a hypothetical ultimate flexible Lyapunov function.

In Chapter 4, the phase-based stability condition in Chapter 3 will be extended to analyze whether the existence of CQLF for every pair of subsystems will ensure the overall stability of switched systems under arbitrary switching.

Chapter 5 changes the research topic from switched systems to T-S fuzzy systems and discusses the membership dependent approaches to reduce conservativeness in stability analysis. A new framework will be provided in this chapter to compare the effectiveness of different membership dependent stability conditions and explain how the membership-dependent approach can be explained as reducing subsystem variation.

Chapter 6 will present the modeling and stability analysis problem of a metamorphic robotic palm, which can be treated an example application of the theoretical results in Chapter 5.

The concluding remarks of this thesis and potential directions of future work will be provided in Chapter 7.

## 1.4 Outline of contributions to knowledge

Within the thesis structure mentioned in Section 1.3, our main contributions to knowledge have been presented in Chapters 3 to 6. Their novelty and importance are listed as below:

1. The new concept of Phase Function has been proposed in Chapter 3. By using this concept, a necessary and sufficient stability condition of switched systems has been obtained.
2. It has been verified in Chapter 4 that the existence of CQLF for every two tuples of subsystems can ensure stability of the whole switched system.
3. An efficient algorithm has been designed in Chapter 5 to get the less conservative membership dependent stability condition for T-S fuzzy systems.
4. The membership dependent stability analysis method in Chapter 5 has been applied to a robotic palm in Chapter 6, which ensures the wider range of re-configuration of the robotic palm.

# Chapter 2

## Preliminaries

*This chapter elaborates the background knowledge of system stability analysis. As the preliminaries of latter chapters, it will also discuss the existing methods on stability analysis of switched systems under arbitrary switching and on stability analysis of T-S fuzzy system by considering membership information.*

### 2.1 The problem of system stability

A general continuous-time nonlinear system can be described in the following form,

$$\dot{x}(t) = f(x(t), t), \quad (2.1)$$

where  $f : (\mathbb{R}^n, \mathbb{R}) \rightarrow \mathbb{R}^n$  is be a nonlinear function of both system state  $x(t)$  and time  $t$ . For any initial system state  $x(0)$ , the function  $f(x(t), t)$  will determine the subsequent dynamic evolution of state  $x(t)$ .

If on the state domain  $x(t) \in \mathbb{R}^n$  we can find a point  $x_e$  such that  $f(x_e, t) = 0$  for all  $t \in \mathbb{R}^+$ , we then call it the *equilibrium point* of system (2.1). From the system expression in (2.1), at this specific equilibrium point  $x_e$ , the differential equation  $\dot{x}(t) = 0$  means that the state  $x(t)$  can stay here forever in the ideal case. While in the practical case, such a point is not isolated and the state must go through its surrounding area to reach that specific point, which means the stability property of the equilibrium is closely related with the state dynamic in its surrounding area. As a result the stability property of an equilibrium point can be formally described as

**Definition 8.** [79] (**Stable Equilibrium**) *A system equilibrium point  $x_e$  is stable if for each  $\epsilon > 0$ , there exists  $\delta > 0$ , such that*

$$\|x(0) - x_e\| < \delta \quad \Rightarrow \quad \|x(t) - x_e\| < \epsilon, \quad \forall t > 0. \quad (2.2)$$

Conceptually, the above definition means that a starting point “close enough” to the equilibrium (within a distance  $\eta$  from it) remains “close enough” forever (within

a distance  $\delta$  from it). If the above condition is not satisfied, then the equilibrium point is said to be **unstable**. If an equilibrium point  $x_e$  is both stable and *convergent*, then it is said to be *asymptotically stable*. Formally we can define it as

**Definition 9.** [79] (**Asymptotically Stable**) A system equilibrium point  $x_e$  is asymptotically stable if it is stable and there exists  $\delta > 0$ , such that

$$\|x(0) - x_e\| < \delta \quad \Rightarrow \quad \lim_{t \rightarrow \infty} x(t) = x_e. \quad (2.3)$$

It means that a starting point close enough to  $x_e$  not only remains close enough to  $x_e$  but also eventually converges to this equilibrium. Graphically, the behavior of stable, unstable and asymptotically stable can be illustrated as Figure 2.1.

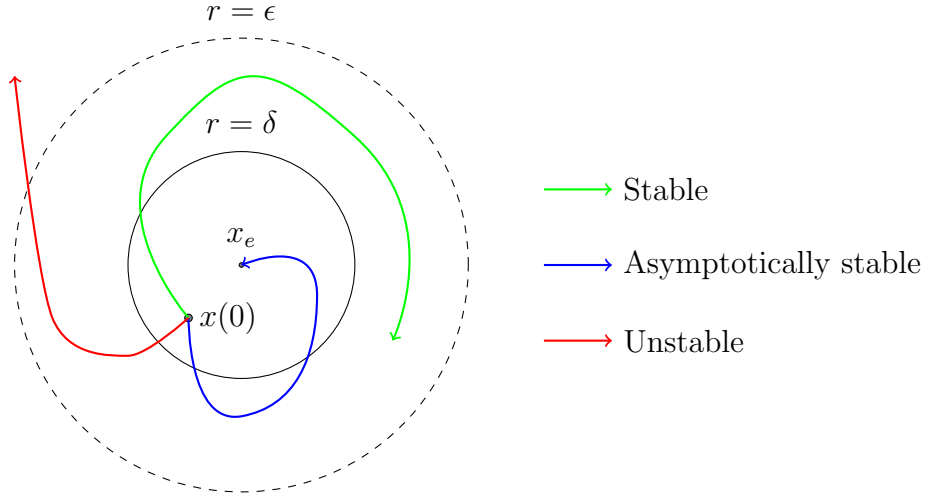


Figure 2.1: Concepts of stability

A widely used effective method to visualize the above stability property is the second method proposed by A. M. Lyapunov [80] for demonstrating stability, which we commonly refer to as *Lyapunov stability criterion*. In this method, a *Lyapunov function*  $V(x) : \mathbb{R}^n \rightarrow \mathbb{R}$  is designed as an analogy to the potential function of classical system dynamics. It can be formally defined as,

**Definition 10.** [81] A **Lyapunov function** is a scalar function  $V(x) : \mathbb{R}^n \rightarrow \mathbb{R}$  that is continuous, positive-definite and has continuous first-order partial derivatives at every point of  $\mathbb{R}^n$ .

The stability condition corresponding to the definition of “stable” can be presented as

**Theorem 1.** [82] (**Stability**) Let  $x = 0$  be an equilibrium point of system (2.1). Let  $V(x) : \mathbb{R}^n \rightarrow \mathbb{R}$  be a continuously differentiable function. Then  $x = 0$  is stable if

1.  $V(0) = 0$ ,
2.  $V(x) > 0$  for  $x \neq 0$ ,
3.  $\dot{V}(x) \leq 0$  for  $x \neq 0$  (negative semidefinite).

Accordingly, the stability condition for definition of “asymptotically stable” can be described as

**Theorem 2.** [82] (**Asymptotic Stability**) Let  $x = 0$  be an equilibrium point of system (2.1). Let  $V(x) : \mathbb{R}^n \rightarrow \mathbb{R}$  be a continuously differentiable function. Then  $x = 0$  is asymptotically stable if

1.  $V(0) = 0$ ,
2.  $V(x) > 0$  for  $x \neq 0$ ,
3.  $\dot{V}(x) < 0$  for  $x \neq 0$  (negative definite).

To conclude the global stability (or similarly global asymptotic stability), an additional condition called “properness” or “*radial unboundedness*” is required. The above analysis method can be visualized by considering the Lyapunov function  $V(x)$  as the energy of the concerned system, see Figure 2.2 as an illustration of  $V(x) = x_1^2 + 1.3x_2^2$ . If the system loses energy over time and energy is never restored then the system state will grind to a stop and reach its equilibrium point.

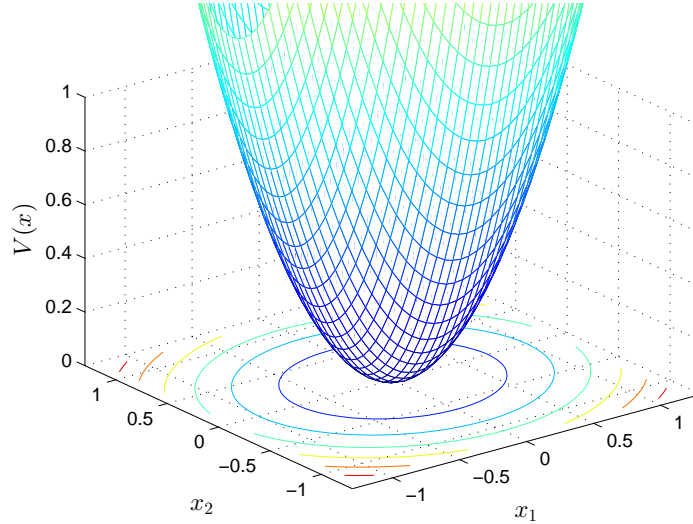


Figure 2.2: Illustration of Lyapunov function  $V(x)$

A level-surface of Lyapunov function with energy  $\mathcal{E}$  can be found by solving the state space solution of equation  $V(x) = \mathcal{E}$ . The illustration of such a surface on the state space will be an enclosed contour, see Figure 2.3 as an illustration of  $V(x) = 0.1, 0.3, 0.6, 1, 1.4$ . The level-surface closer to the equilibrium point would

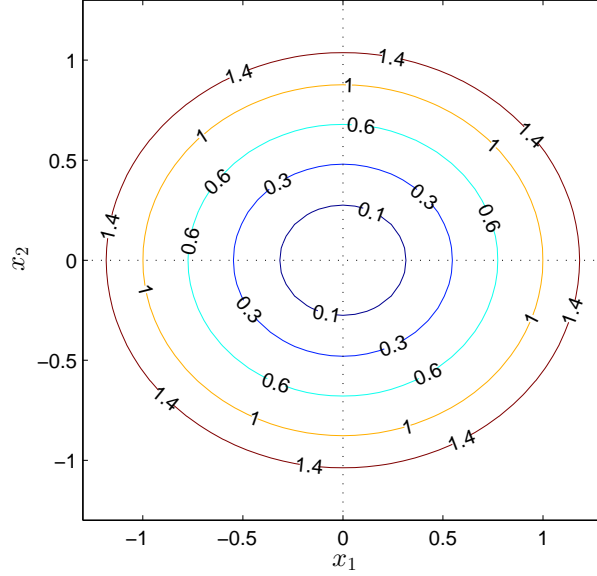


Figure 2.3: Illustration of the level surfaces of a Lyapunov function  $V(x)$

have less energy. In other words, if a system state on the level surface is stable, it would go inside the contour of such a level surface along the system equation.

In the following sections, we will consider the stability problem of switch systems and fuzzy systems based on the idea of Lyapunov function. Some existing methods will be discussed accordingly.

## 2.2 Stability analysis for switched systems under arbitrary switching

In this part we will briefly discuss the existing approaches for stability analysis of switched systems under arbitrary switching. Here we consider the switched linear system that consists of a finite set of linear time-invariant (LTI) systems,

$$\dot{x}(t) = A_{\sigma(t)}x(t), \quad (2.4)$$

where  $A_{\sigma(t)}$  can switch among a given collection of matrices  $A_1, A_2, \dots, A_q$  in  $\mathbb{R}^{n \times n}$ . Denote  $\mathcal{Q} \triangleq \{1, 2, \dots, q\}$  as the set of indexes of subsystems, then the switching signal in (2.4) can be constrained as  $\sigma(t) \in \mathcal{Q}$ .

For a switched system under arbitrary switching, the system matrix  $A_{\sigma(t)}$  can be any matrix among  $A_1, A_2, \dots, A_q$ . The stability under arbitrary switching would require that the system state can always go to the equilibrium point  $x = 0$  regardless of the switching signal  $\sigma(t)$ . To see this on the state space, we can consider

a switched system with  $q = 3$  and  $n = 2$ . Corresponding subsystems are chosen as

$$A_1 = \begin{bmatrix} -1 & 0.5 \\ -1.5 & -3 \end{bmatrix}, \quad A_2 = \begin{bmatrix} -1 & 0 \\ -0.5 & -3 \end{bmatrix}, \quad A_3 = \begin{bmatrix} -1 & -1.5 \\ 0.5 & -3 \end{bmatrix}$$

In Figures 2.4–2.7, the converging directions as well as the magnitudes of  $A_1x$ ,  $A_2x$ ,  $A_3x$  are illustrated as the blue, green and red quivers correspondingly. The state trajectories along  $\dot{x}(t) = A_1x(t)$ ,  $\dot{x}(t) = A_2x(t)$ ,  $\dot{x}(t) = A_3x(t)$  are plotted in Figures 2.4–2.6 separately. The state trajectory under switching  $A_{\sigma(t)}$ :  $A_1 \rightarrow A_2 \rightarrow A_3$  is explained in Figure 2.7.

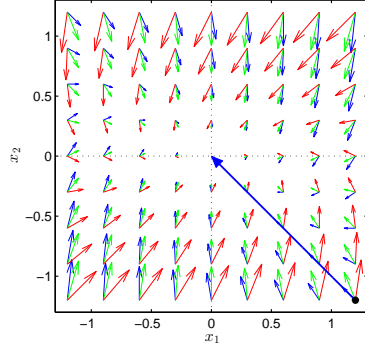


Figure 2.4:  $A_{\sigma(t)} = A_1$  (blue)

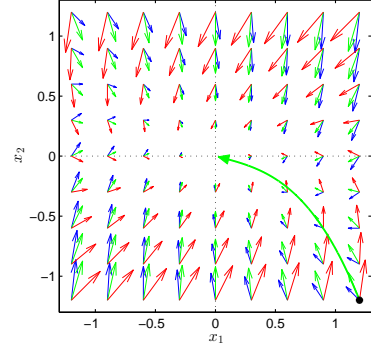


Figure 2.5:  $A_{\sigma(t)} = A_2$  (green)

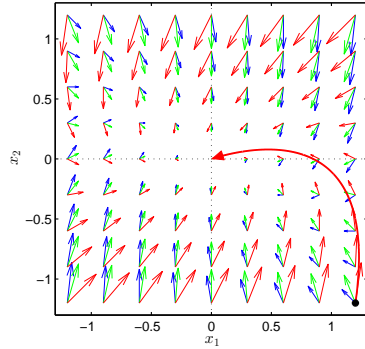


Figure 2.6:  $A_{\sigma(t)} = A_3$  (red)

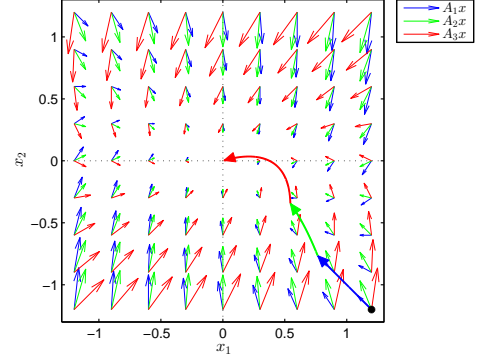


Figure 2.7:  $A_{\sigma(t)}$ :  $A_1 \rightarrow A_2 \rightarrow A_3$

If this system is asymptotically stable under arbitrary switching, the system state will gradually converge to  $x = 0$  no matter which quiver it travels along at a specific point of the state space. To ensure this, we can consider the Lyapunov function we mentioned in Section 2.1. That is, if there is a Lyapunov function, such that, for a system state on a specific level surface of this function, all converging quivers of subsystems would point inside this level surface, then the system state would always travel from high energy level surface to low energy level surface, see Figure 2.8. The system state would finally reach and stay at the equilibrium and consequently the system would be stable. In other words, we can also explain it as, if we can find a common Lyapunov function for all the subsystem matrices  $A_1$ ,  $A_2$  and  $A_3$ , then the switched system would be stable under arbitrary switching.

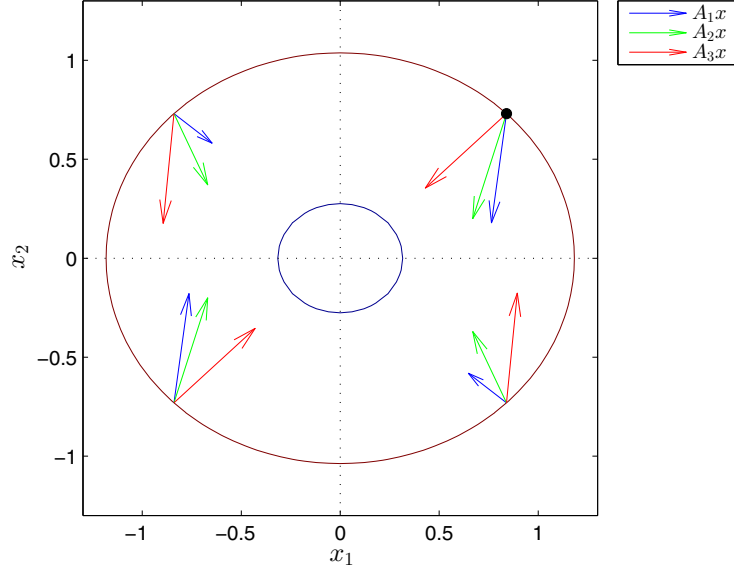


Figure 2.8: Converging quivers of  $A_1x$ ,  $A_2x$ ,  $A_3x$  for system states on a level surface of  $V(x)$

As we have mentioned in Chapter 1, Figure 1.12, there are two approaches to improve the results of stability analysis. We can either reduce the variation of subsystem quivers  $A_1x$ ,  $A_2x$ ,  $A_3x$  by making use of the information of switching signal  $\sigma(t)$ , or we can find a more flexible Lyapunov function  $V(x)$  such that all the subsystem quivers can be enclosed (pointing inward) by the level surface of such a Lyapunov function. Obviously, for the switching system under arbitrary switching, it is impossible for us to reduce the subsystem variation by switching signal information. Thus a more practical approach is the construction of a highly flexible Lyapunov function.

Following this idea, various methods have been considered to improve the flexibility of Lyapunov function. Among them we will briefly discuss the typical approaches: polyhedral Lyapunov function, polynomial Lyapunov function.

### 2.2.1 Polyhedral Lyapunov function [1]

The definition of *polyhedral Lyapunov function* can be introduced as,

**Definition 11.** *The polyhedral Lyapunov function is a special class of piecewise linear Lyapunov function that is defined as,*

$$V_{\mathcal{P}}(x) = \max\{\xi_1^T x, \xi_2^T x, \dots, \xi_m^T x\}, \quad (2.5)$$

where  $\xi_i \in \mathbb{R}^n$  is the parameter determining the direction, or the normal of level surface in region  $i$  ( $i = 1, 2, \dots, m$ ), see Figure 2.9.

This function is induced by a *polyhedral set* in the following form,

$$\mathcal{P} = \{x \in \mathbb{R}^n : \xi_i^T x \leq 1, i = 1, 2, \dots, s\}, \quad (2.6)$$

which is compact and contains the origin  $x = 0$  in its interior. The linear functions  $\xi_i^T x$  ( $i = 1, 2, \dots, m$ ) are called the *generators* of polyhedral function  $V_{\mathcal{P}}(x)$ .

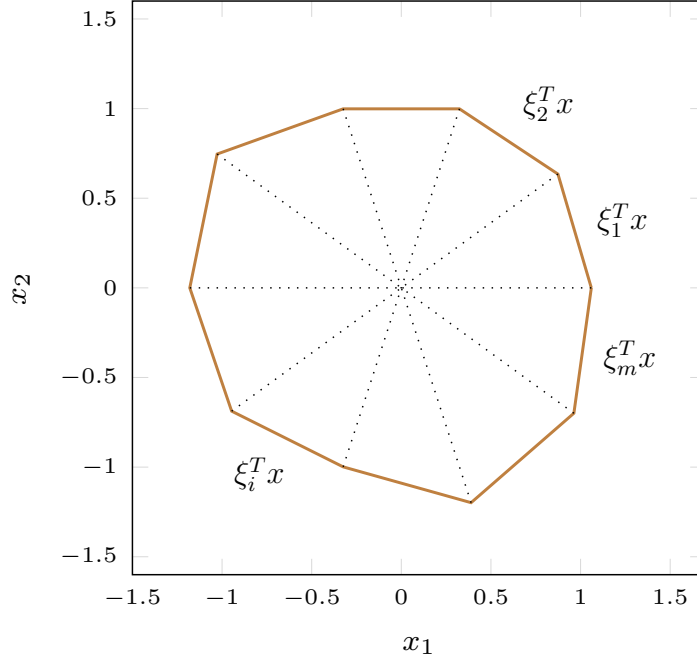


Figure 2.9: Level surface of the polyhedral Lyapunov function

To get the proper polyhedral Lyapunov function ensuring the stability of the equilibrium of system (2.4) under arbitrary switching, we need to find generators such that all the subsystem quivers  $A_i x$  ( $i \in \mathcal{Q}$ ,  $x \in \mathcal{P}$ ) point inward the polyhedral set  $\mathcal{P}$ . This can be formally described as the *positive invariance principle* [83],

**Definition 12.** A polyhedral set  $\mathcal{P}$  is called **positively invariant** with respect to the trajectories of a dynamical system if for all  $x(0) \in \mathcal{P}$  the solution  $x(t) \in \mathcal{P}$  for  $t > 0$ .

Then following the same idea as in [84], the stability condition can be formulated by the polyhedral Lyapunov function (2.5) as follows

**Lemma 1.** For the function (2.5) to be a common Lyapunov function for subsystem matrices  $A_i$  ( $i \in \mathcal{Q}$ ) (and the polytope  $\mathcal{P}$  to be invariant under the dynamics of (2.4)) it is necessary and sufficient that

$$\xi_i^T \cdot A_j x \leq 0, \quad \forall x \in \partial \mathcal{P}, \quad i \in \mathcal{J}(x), \quad j \in \mathcal{Q} \quad (2.7)$$

where  $\mathcal{J}(x) = \{i \in 1, 2, \dots, m : \xi_i^T \cdot x = V_{\mathcal{P}}(x)\}$  is a set of indexes corresponding to the active constraints.



The way to increase the flexibility of polyhedral Lyapunov function is to find the proper partitions of the state space, such that the invariant condition (2.7) can be satisfied as much as possible and complexity of the Lyapunov function is acceptable for practical calculation. One well-established example of this should be the *ray partition* approach in [1], where the flexibility can be improved by increasing the number of partition rays.

### 2.2.2 Polynomial Lyapunov function [2]

If we see the commonly used quadratic Lyapunov function,  $V(x) = x^T P x$ , from the mathematic point of view, we will find that it is actually a second order polynomial function. Then an alternative idea to improve the flexibility of a Lyapunov function would be increasing the mathematical order of it.

Following this idea, we can increase the mathematical order of quadratic Lyapunov function  $V(x)$  to get a *polynomial Lyapunov function*. We can formal introduce it as the following definition,

**Definition 13.** [2] *A polynomial Lyapunov function is a function designed in the following form,*

$$V(x) = \hat{x}^T(x) \mathbf{P} \hat{x}(x) \quad (2.8)$$

where  $\mathbf{P} \in \mathbb{R}^{N \times N}$  is positive definite,  $\hat{x}(x) \in \mathbb{R}^N$  is a column vector whose entries are all monomials in  $x$  and satisfies that

$$\hat{x}(x) = 0 \quad \text{iff} \quad x = 0. \quad (2.9)$$

By the term “monomial in  $x$ ” we mean a function of the form  $x_1^{\alpha_1} x_2^{\alpha_2} \cdots x_n^{\alpha_n}$ , whose order is  $\alpha_1 + \alpha_2 + \cdots + \alpha_n$  with  $\alpha_1, \alpha_2, \cdots, \alpha_n$  being nonnegative integers.

The stability condition in this case is still ensuring the positive definite property of  $V(x)$  and negative definite property of  $\dot{V}(x)$ . But to make the computation easier, the sum of squares (SOS) decomposition of multivariate polynomials would be applied. A multivariate polynomial  $f(x)$  is an SOS if there exist polynomials  $f_1(x), f_2(x), \cdots, f_m(x)$  such that  $f(x) = \sum_{i=1}^m f_i^2(x)$ . Equivalence between an SOS expression and the quadratic form in (2.8) can be stated as the following proposition.

**Proposition 1.** [85] *Let  $V(x)$  be a polynomial in  $x \in \mathbb{R}^n$  of order  $2d$ . In addition, let  $\hat{x}(x)$  be a column vector whose entries are all monomials in  $x$  with order no greater than  $d$ . Then  $V(x)$  is an SOS iff there exists a positive semidefinite matrix  $\mathbf{P}$  such that*

$$V(x) = \hat{x}^T(x) \mathbf{P} \hat{x}(x). \quad (2.10)$$

The stability of a given system at equilibrium  $x = 0$  can be ensured if for all  $x$  both  $V(x)$  and  $-\dot{V}(x)$  are SOS [2].

### 2.2.3 Brief summary

In the above existing research methods, ideas have been discussed to improve the flexibility of Lyapunov function, consequently reducing the conservativeness in stability analysis. Ideally, we may think that the ultimate flexible Lyapunov function would ensure the necessary and sufficient property of our stability results. But in the practical case, it would mean the infinite partition rays for polyhedron Lyapunov function and infinite high order for the polynomial Lyapunov function, which are unlikely to be achieved.

While, if we consider one step further, we may realize that, our purpose of constructing flexible Lyapunov function is still to see the possibility of existence of a proper Lyapunov function, rather than actual existence of it. With this thought, we may possibly avoid the construction of a Lyapunov function by analyzing the criteria of its existence. This will be the focus of our research in Chapter 3.

## 2.3 Stability analysis for T-S fuzzy systems with membership information

In the previous section, we focused on the construction of flexible Lyapunov function to improve the results of system stability analysis. The system switching information was not considered in the analysis. While in this part we change our topic to the stability analysis of T-S fuzzy systems. Instead of improving the result by constructing flexible Lyapunov function, this time we will focus on the application of system membership information to reduce stability analysis conservativeness, in other words, as we mentioned in Figure 1.12, we use the membership information to ensure smaller subsystem variation.

Before the explanation on how to reduce subsystem variation by membership information, we would like to briefly introduce some existing membership-dependent methods. The relation between membership-dependent results and reducing subsystem variation will be explained based on the new analysis framework in Chapter 5.

To make it easier to follow, the main ideas of these methods will be reviewed based on a simple T-S fuzzy system and a commonly used Lyapunov function, i.e., the quadratic Lyapunov function. Consider the following T-S fuzzy system

$$\dot{x} = \sum_{i=1}^p h_i(x) A_i x, \quad (2.11)$$

where  $x \in \mathbb{R}^n$  is the system state,  $p \in \mathbb{Z}^+$  is the number of fuzzy rules,  $h_i(x) : \mathbb{R}^n \rightarrow \mathbb{R}$  is the membership function in the  $i$ -th rule,  $A_i \in \mathbb{R}^{n \times n}$  is the system matrix in the  $i$ -th rule. Choose the Lyapunov function as

$$V(x) = x^T P x. \quad (2.12)$$

with  $P \in \mathbb{R}^{n \times n}$  being a symmetric matrix satisfying  $P > 0$ .

In the existing research, there are two effective branches of membership-dependent methods, namely the membership function approximation methods [3,4] which consider the membership information by using alternative simpler functions, and the membership-bound-dependent method [5] which applies the bound information of membership function into stability analysis. We start with the introduction of membership function approximation methods and explain how to get corresponding LMI conditions. Firstly the staircase and piecewise linear approximation methods will be reviewed. And after that, in the subsequent subsection, the introduction to membership-bound-dependent method will be provided.

### 2.3.1 Membership function approximation methods [3,4]

Here the term “membership function approximation” means that, the actual membership functions in the T-S fuzzy systems will be replaced by the alternative functions whose layouts are pretty close to the original ones and are relatively easier to describe by mathematical expressions. In this way, with those alternative approximated functions, it will be possible for us to combine their membership information into the system stability analysis. And the obtained stability condition will be membership-dependent. In the following part we will discuss the general membership approximation idea of staircase approximation in [3] and piecewise linear approximation in [4]. Based on that, the corresponding membership-dependent stability conditions will be provided.

#### 2.3.1.1 Membership function approximation ideas

For both the staircase and piecewise approximation methods, the whole domain of premise variable  $x$  is divided into gridded sub-regions, and in the  $i$ -th dimension of  $x$ , these sub-regions are separated by sample points satisfying  $x_i(t) = x_i^{(\tau)}$  ( $\tau = 1, 2, \dots, d+1$ ). The regional approximation of  $h_i(x)$ ,  $i = 1, 2, \dots, p$ , is described by the values of  $h_i(x)$  at the surrounding sample points. To make it simple and highlight the main idea, we consider the special case  $h_i(x) = h_i(x_1)$  ( $i = 1, 2, \dots, p$ ) as an example, which means the membership function has one degree of freedom and only depends on  $x_1(t)$ . For the definition of approximation functions with more degrees of freedom the idea is same, and readers can refer to [4] for more details.

Define  $\hat{h}_i(x)$  as the approximated membership function. For the staircase ap-

proximation, the approximated function in sub-region  $(x_1^{(\tau)}, x_1^{(\tau+1)}]$  can be chosen as any value of  $h_i(x_1)$  ( $i = 1, 2, \dots, p$ ) in this region.

To facilitate the comparison, without loss of generality, the *staircase approximation* would be presented as,

**Definition 14.** *The **staircase approximation** of a membership function  $h_i(x_1)$  in region  $(x_1^{(\tau)}, x_1^{(\tau+1)}]$  is a function designed as*

$$\hat{h}_i^{(\tau)}(x_1) = \mu_\tau^-(x_1)h_i(x_1^{(\tau)}) + \mu_\tau^+(x_1)h_i(x_1^{(\tau+1)}) \quad (2.13)$$

for all  $i = 1, 2, \dots, p$ , where  $\mu_\tau^-(x_1) = e(\frac{x_1^{(\tau)} + x_1^{(\tau+1)}}{2} - x_1)$  is a step function changing value at sub-region center  $x_1 = \frac{x_1^{(\tau)} + x_1^{(\tau+1)}}{2}$ ,  $\mu_\tau^+(x_1) = 1 - \mu_\tau^-(x_1)$  is the counter-part of  $\mu_\tau^-(x_1)$ , and  $e(t)$  is the step function satisfying  $e(t) = 1$  for  $t \geq 0$  and  $e(t) = 0$  for  $t < 0$ .

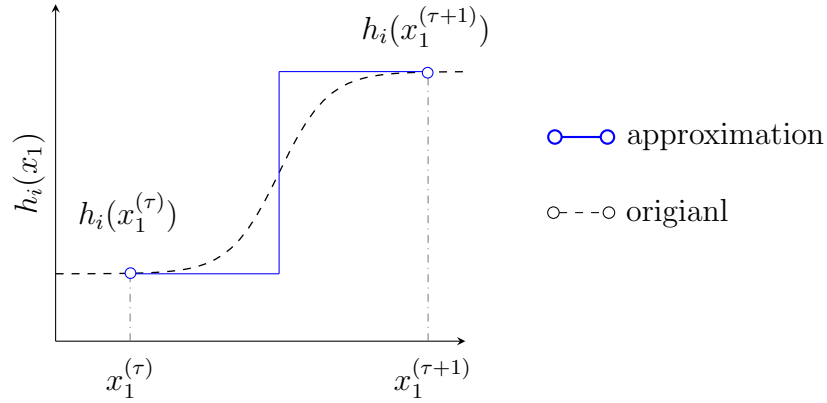


Figure 2.10: Illustration of staircase approximation.

On the other hand, the piecewise linear approximation would be presented as,

**Definition 15.** *The **piecewise linear approximation** of a membership function  $h_i(x_1)$  in region  $(x_1^{(\tau)}, x_1^{(\tau+1)}]$  is a function designed as*

$$\hat{h}_i^{(\tau)}(x_1) = v_\tau^-(x_1)h_i(x_1^{(\tau)}) + v_\tau^+(x_1)h_i(x_1^{(\tau+1)}) \quad (2.14)$$

for all  $i = 1, 2, \dots, p$ , where  $v_\tau^-(x_1) = \frac{x_1 - x_1^{(\tau+1)}}{x_1^{(\tau)} - x_1^{(\tau+1)}}$  satisfying  $v_\tau^-(x_1^{(\tau)}) = 1$  and  $v_\tau^-(x_1^{(\tau+1)}) = 0$ , and  $v_\tau^+(x_1) = 1 - v_\tau^-(x_1)$  is the counter-part of  $v_\tau^-(x_1)$ .

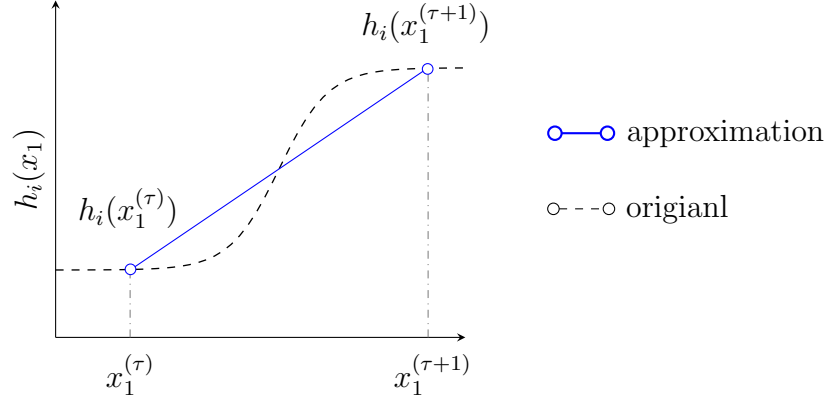


Figure 2.11: Illustration of piecewise linear approximation.

For both staircase and piecewise linear approximations, the obtained function  $\hat{h}_i(x_1)$  has the same value as  $h_i(x_1)$  at the sample points  $x_1^{(\tau)}$ ,  $\tau = 1, 2, \dots, d, d+1$ , see Figure 2.12.

### 2.3.1.2 The obtained membership-dependent stability conditions

For both approximation methods we have  $\sum_{i=1}^p \hat{h}_i(x) = 1$ . Introduce the new matrices  $Q_i \triangleq A_i^T P + P A_i$ , ( $i = 1, 2, \dots, p$ ), then the membership information can be combined in the derivation of Lyapunov function (2.12) with details given below:

$$\begin{aligned}
 \dot{V}(x) &= \sum_{i=1}^p h_i(x) x^T Q_i x \\
 &= \sum_{i=1}^p \hat{h}_i(x) x^T Q_i x + \sum_{i=1}^p (h_i(x) - \hat{h}_i(x)) x^T Q_i x \\
 &\quad + \sum_{i=1}^p (h_i(x) - \hat{h}_i(x)) x^T M x \\
 &= \sum_{i=1}^p \hat{h}_i(x) x^T Q_i x + \sum_{i=1}^p (h_i(x) - \hat{h}_i(x)) x^T (Q_i + M) x \\
 &\quad + \sum_{i=1}^p (r_i - r_i) x^T (Q_i + M) x \\
 &= \sum_{i=1}^p x^T \left( \hat{h}_i(x) Q_i + r_i (Q_i + M) \right) x \\
 &\quad + \sum_{i=1}^p x^T \left( (h_i(x) - \hat{h}_i(x) - r_i) (Q_i + M) \right) x.
 \end{aligned}$$

Overall a sufficient condition for  $\dot{V}(x) < 0$  could be

$$\begin{cases} (h_i(x) - \hat{h}_i(x) - r_i) (Q_i + M) \leq 0, & \forall i = 1, 2, \dots, p \\ \sum_{i=1}^p \hat{h}_i(x) Q_i < - \sum_{i=1}^p r_i (Q_i + M). \end{cases} \quad (2.15)$$

where  $r_i$  is a scalar and  $M$  is a symmetric matrix of appropriate dimension. We can get the following conditions by dividing the first inequality of (2.15) into two inequalities

$$\begin{cases} r_i \geq h_i(x) - \hat{h}_i(x), & \forall i = 1, 2, \dots, p \\ Q_i + M \geq 0, & \forall i = 1, 2, \dots, p \\ \sum_{i=1}^p \hat{h}_i(x) Q_i < - \sum_{i=1}^p r_i (Q_i + M). \end{cases} \quad (2.16)$$

Based on the definition of  $\hat{h}_i(x_1)$  in region  $(x_1^{(\tau)}, x_1^{(\tau+1)}]$ , the conditions in (2.16) can be equivalently illustrated as

$$\begin{cases} r_i \geq h_i(x_1) - \hat{h}_i(x_1), & \forall i = 1, 2, \dots, p \\ Q_i + M \geq 0, & \forall i = 1, 2, \dots, p \\ \sum_{i=1}^p \hat{h}_i^{(\tau)}(x_1) Q_i < - \sum_{i=1}^p r_i (Q_i + M), & \forall \tau = 1, 2, \dots, d. \end{cases} \quad (2.17)$$

Since for any  $\tau = 1, 2, \dots, d+1$ , all  $v_\tau^-(x_1), v_\tau^+(x_1), \mu_\tau^-(x_1), \mu_\tau^+(x_1) \geq 0$  and  $v_\tau^-(x_1) + v_\tau^+(x_1) = \mu_\tau^-(x_1) + \mu_\tau^+(x_1) = 1$ , the linear inequality related with  $\hat{h}_i^{(\tau)}(x_1)$  can be replaced by that related with  $h_i(x_1^{(\tau)})$  and  $h_i(x_1^{(\tau+1)})$ . Thus a sufficient condition for (2.17) could be [3, 4]

$$\begin{cases} r_i \geq h_i(x_1) - \hat{h}_i(x_1), & \forall i = 1, 2, \dots, p \\ Q_i + M \geq 0, & \forall i = 1, 2, \dots, p \\ \sum_{i=1}^p h_i(x_1^{(\tau)}) Q_i < - \sum_{i=1}^p r_i (Q_i + M) \end{cases} \quad (2.18)$$

for all  $\tau = 1, 2, \dots, d, d+1$ , where  $r_i$  ( $i = 1, 2, \dots, p$ ) is a scalar and  $M$  is a symmetric matrix of appropriate dimension. In (2.18), the main difference of staircase and piecewise linear approximation methods is  $\hat{h}_i(x_1)$ , which will result in different  $r_i$  from the first inequality. Consequently, from the third condition of (2.18), we may find that, the inequality with smaller  $r_i$  will be less conservative.

An example from [4] of different approximation methods is provided in Figure 2.12, where  $h_1(x_1) = e^{-(x_1-10)^{1/25}}$  and  $x_1$  is divided into six sub-regions by points  $x_1^{(1)} = -10$ ,  $x_1^{(2)} = -5$ ,  $x_1^{(3)} = 0$ ,  $x_1^{(4)} = 5$  and  $x_1^{(5)} = 10$ . Clearly we can see that, for smooth membership functions, the  $r_i$  value of piecewise linear approximation is generally smaller subject to the same set of sample points, which means less conservative stability conditions. Thus we will choose the piecewise linear approximation method as a representative for the conservativeness comparison in Section 5.4.

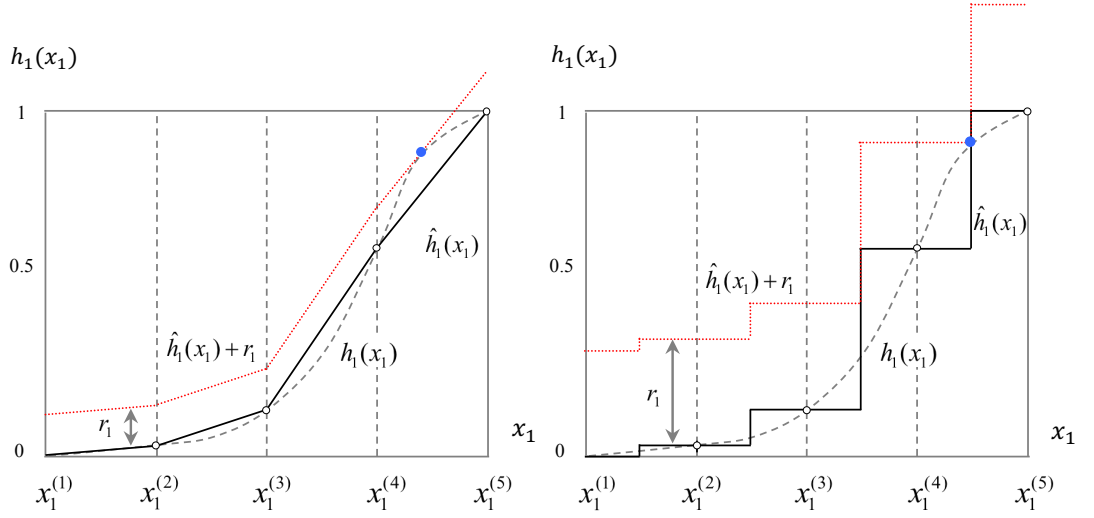


Figure 2.12: Comparison of the minimum  $r_1$  in staircase (right) and piecewise linear (left) approximation methods. The dashed smooth gray lines are the trajectories of  $h_1(x_1)$ , the solid lines are the layouts of approximated function  $\hat{h}_1(x_1)$ , the dotted red lines are the layouts of  $\hat{h}_1(x_1) + r_1$ , where  $r_1 \geq h_1(x_1) - \hat{h}_1(x_1)$ .

### 2.3.2 Membership-bound-dependent relaxation method [5]

Another approach to apply the membership information in the stability results is considering the bound margin value of membership function  $h_i(x)$ . If a bound for  $h_i(x)$  is known, then we can name it as  $\beta_i \in \mathbb{R}$  which satisfies  $h_i(x) \leq \beta_i$  for all  $x$  in the system domain. Directly it holds that

$$h_i(x) \leq \beta_i \sum_{j=1}^p h_j(x).$$

Consider a group of arbitrary positive semi-definite matrices  $N_i \geq 0$ , ( $i = 1, 2, \dots, p$ ). The following expression holds

$$\begin{aligned} \dot{V}(x) &= \sum_{i=1}^p h_i(x) x^T Q_i x \\ &\leq \sum_{i=1}^p h_i(x) x^T Q_i x + \sum_{i=1}^p \left( \beta_i \sum_{j=1}^p h_j(x) - h_i(x) \right) x^T N_i x \\ &= \sum_{i=1}^p h_i(x) x^T Q_i x + \sum_{i=1}^p h_i(x) \left( \sum_{j=1}^p \beta_j x^T N_j x \right) - \sum_{i=1}^p h_i(x) x^T N_i x \\ &= \sum_{i=1}^p h_i(x) x^T \left( Q_i - N_i + \sum_{j=1}^p \beta_j N_j \right) x. \end{aligned}$$

Directly, a sufficient condition for  $\dot{V}(x) < 0$  can be chosen as

$$\begin{cases} \beta_i \geq h_i(x) \\ N_i \geq 0 \\ Q_i - N_i + \sum_{j=1}^p \beta_j N_j < 0 \end{cases} \quad (2.19)$$

for all  $i = 1, 2, \dots, p$ .

Clearly we can see that compared with the direct membership-independent condition

$$Q_i < 0, \quad \forall i = 1, 2, \dots, p,$$

much more information has been combined in the membership-dependent results (2.18) and (2.19). Theoretically conservativeness can be reduced in this way.

### 2.3.3 Brief summary

In the above subsections we have reviewed some typical membership-dependent methods for stability analysis of T-S fuzzy systems. An instinct question would be effectiveness of them. In most existing papers [3, 86, 87], comparisons of different membership-dependent methods are usually analyzed in the numerical approach. Such an approach is simple and direct, and one can compare different methods based on the obtained feasible regions of preset parameters. But the comparison results will be highly dependent on the specific example. And sometimes it is difficult to explain the inner relation of different methods. To avoid those limitations and take one step further, in Chapter 5 we would like to introduce framework *membership space* for the theoretical comparison. This framework is obtained by considering all the membership functions in a joint space. With this idea we will be able to see the whole picture of the membership layouts and conduct analysis that is less dependent on the specific example. What's more, in such a framework, we will also find out how the membership-dependent methods can be explained as the reduction of subsystem variation.



# Chapter 3

## Phase-based stability analysis of switched systems

*This chapter introduces the concept of phase function and applies it to the stability analysis problem of switched systems. Firstly, the basic properties of phase function are explored. Then by following this concept and its properties, the phase-based stability criterion is investigated.*

### 3.1 Introductory remarks

Following the preliminary results in Section 2.2, in this chapter we consider the stability analysis of switched system under arbitrary switching. From Section 2.1, we understand that the stability of a given system can be validated by the existence of an appropriate Lyapunov function for such a system. Furthermore in Section 2.2, we discussed some existing methods to construct flexible Lyapunov function such that it is more likely to be appropriate for the given system and stability can be verified.

However, as we also mentioned in Section 2.2.3, the system stability actually does not dependent on (though can be verified by) the existence of a specific appropriate Lyapunov function. Following this thought, in this chapter, we will not stick to the improvement of Lyapunov function flexibility. Instead, we analyze the necessary requirements for an appropriate Lyapunov function. Then with the new concept of *phase function*, those requirements can be directly related with the system expression, making it easier for us to check the system stability.

The following sections of this chapter are organized as follows. Section 3.2 formulates the problem that we are going to investigate in this chapter. Section 3.3 introduces the concept and mathematical properties of phase function. With this concept, in Section 3.4, we will analyze the necessary requirement for an appropriate Lyapunov function and transform it into stability condition. Application and

comparison examples will be provided in Section 3.5 and conclusion will be drawn in Section 3.6.

## 3.2 Problem formulation

Consider a second-order switched system

$$\dot{x}(t) = f_{\sigma(t)}(x(t)) = A_{\sigma(t)}x(t), \quad (3.1)$$

where  $A_{\sigma(t)}$  can switch among a given collection of matrices  $A_1, A_2, \dots, A_q$  in  $\mathbb{R}^{2 \times 2}$ . Denote  $\mathcal{Q} \triangleq \{1, 2, \dots, q\}$  as the set of indexes of subsystems, then the switching signal in (3.1) can be constrained as  $\sigma(t) \in \mathcal{Q}$ . Throughout this chapter, the input arguments of variables may be omitted to simplify the expressions, for example,  $f_{\sigma(t)}(x(t))$  may be abbreviated as  $f_{\sigma}(x)$  and  $\theta(x)$  may be simplified as  $\theta$ . For the above system, let us construct the following line-integral function [56] which will be used as an ultimate flexible Lyapunov function,

$$V(x) \triangleq \int_{\Gamma(0,x)} p(\psi) \cdot d\psi, \quad (3.2)$$

where  $\Gamma(0, x)$  is a path from the origin 0 to the current state  $x$ ,  $\psi \in \mathbb{R}^2$  is a dummy vector for the integral,  $p(x) \in \mathbb{R}^2$  is a vector function of the state  $x$ , and  $d\psi \in \mathbb{R}^2$  is an infinitesimal displacement vector. If  $p(x)$  is regarded as a force vector at a state  $x$ ,  $V(x)$  in (3.2) can be regarded as the work done from the origin to the current state  $x$ , and is thus an energy-like function. As we have mentioned in Section 2.1, to be an appropriate Lyapunov function candidate,  $V(x)$  has to satisfy the following necessary conditions [82],

- (a)  $V(x)$  is continuously differentiable;
- (b)  $V(x)$  is positive-definite;
- (c)  $V(x)$  is radially unbounded.

Our purpose of this chapter is to find a unified approach for stability analysis of second-order switched systems by applying the ultimate flexible line-integral Lyapunov function. One important medium of this approach will be the new concept of *phase function*. The problems investigated in this chapter can be stated as: Find the phase-based necessary and sufficient condition that guarantees the global stability of switched system (3.1) under arbitrary switching signals. Main contribution of this chapter can be summarized as follows: (1) Analyzing the properties of phase function in the geometric way; (2) Describing the Lyapunov stability criteria in the

form of phase function; (3) Obtaining the necessary and sufficient stability condition based on phase functions of subsystems.

Before discussing the stability analysis problem mentioned above, we will firstly introduce the concept of phase function, and investigate the intrinsic properties of it.

### 3.3 The concept of phase function

#### 3.3.1 Definition of phase function

The concept of phase function of second-order system is illustrated in the following definition. This concept will be used in the later sections as a new approach of stability analysis.

**Definition 16.** *The **phase function** of a state-dependent non-zero vector  $p(x) \in \mathbb{R}^2$  is defined as the angle from vectors  $x$  to  $p(x)$ , for all non-zero  $x \in \mathbb{R}^2$ . In the normal case this function is denoted as  $\phi_p(x)$  with range  $[0, 2\pi)$ . In the symmetric case, it is denoted as  $\phi_p^*(x)$  with range  $[-\pi, \pi)$ , see Figure 3.1.*

Firstly, we construct an angle function that is defined on the domain  $\{x \mid 0 < x_1^2 + x_2^2\}$  and based on the the arctangent function  $\text{atan2}(x_2, x_1)$  [88] in computer science

$$\text{atan}(x) \triangleq \begin{cases} \text{atan2}(x_2, x_1), & x_2 \geq 0; \\ \text{atan2}(x_2, x_1) + 2\pi, & x_2 < 0; \end{cases} \quad (3.3)$$

According to Definition 16, the phase functions of vectors  $f_\sigma(x)$  and  $p(x)$  can be expressed as

$$\begin{aligned} \phi_\sigma(x) &\triangleq \text{atan}(f_\sigma(x)) - \text{atan}(x) \pmod{2\pi}, \\ \phi_p(x) &\triangleq \text{atan}(p(x)) - \text{atan}(x) \pmod{2\pi}, \end{aligned}$$

see Figure 3.1. Note that, since  $(t, x) \rightarrow f_{\sigma(t)}(x)$  is both state- and time-dependent, its phase function  $\phi_\sigma(x)$  would also be time-dependent and is orchestrated by the switching signal  $\sigma(t)$ .

Specially for LTI system with system matrix  $A$ , we give the general expression of phase function with input matrix and angle variables  $A$  and  $\theta$ ,

$$\varphi(A, \theta) \triangleq \text{atan}(A\omega(\theta)) - \theta \pmod{2\pi}. \quad (3.4)$$

The above definitions are dependent on the phase angle  $\theta$  of system state  $x$ . In the

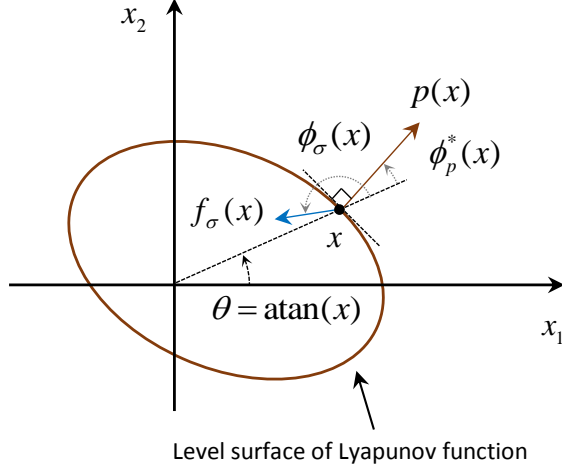


Figure 3.1: Definition of phase functions  $\phi_\sigma(x)$  and  $\phi_p^*(x)$  at point  $x$ , with the oval curve being the level-surface of Lyapunov function  $V(x)$  and  $p(x)$  being the normal of level surface at  $x$ .

subsequent analysis, we will also use their angle-dependent expressions

$$\varphi_p(\theta) \triangleq \phi_p(\omega(\theta)), \quad \varphi_p^*(\theta) \triangleq \phi_p^*(\omega(\theta)), \quad \varphi_\sigma(\theta) \triangleq \phi_\sigma(\omega(\theta))$$

as the simplified versions of  $\phi_p(\omega(\theta))$ ,  $\phi_p^*(\omega(\theta))$ ,  $\phi_\sigma(\omega(\theta))$ , respectively, with

$$\omega(\theta) \triangleq [\cos \theta \quad \sin \theta]^T. \quad (3.5)$$

Generally, the inputs of functions defined with  $\phi$  will be a vector, e.g.,  $\phi_\sigma(x)$ ,  $\phi_p(x)$ ; and input of functions defined with  $\varphi$  will be an angle, e.g.,  $\varphi_\sigma(\theta)$ ,  $\varphi_p(\theta)$ .

### 3.3.2 Properties of phase function for linear systems

To apply phase function into stability analysis, we need to know the the properties of it. Firstly we want to check whether we can move the layout of phase function  $\varphi(A, \theta)$  up, down, left and right by changing the parameters in matrix  $A$ . This shifting property can be analyzed based on the polar decomposition of matrix  $A$ . Clearly for any matrix  $A$ , we can always find its polar decomposition: right polar decomposition,  $A = U_r P_r$ , and left polar decomposition,  $A = P_l U_l$ , with  $U_r$  and  $U_l$  being unitary matrices,  $P_r$  and  $P_l$  being negative semidefinite symmetric matrices. What's more, for the obtained symmetric matrices  $P_r$  and  $P_l$ , we can make further decompositions  $P_r = T_r^T \Lambda_r T_r$  and  $P_l = T_l^T \Lambda_l T_l$ , where  $\Lambda_r$  and  $\Lambda_l$  are diagonal matrices, and  $T_r$  and  $T_l$  are unitary matrices. Overall we have

$$A = U_r P_r = U_r T_r^T \Lambda_r T_r, \quad A = P_l U_l = T_l^T \Lambda_l T_l U_l. \quad (3.6)$$

**Remark 1.** The unitary matrices would be easier to describe if they can be represented as rotation matrices. For the obtained unitary matrix  $U_r$ , one has  $|\det(U_r)| = 1$ . If  $\det(U_r) = 1$ , then  $U_r$  is called a *proper* unitary matrix [89], which means  $U_r$  can be viewed as a rotation matrix. But if  $\det(U_r) = -1$ , then  $U_r$  would contain both rotation and reflection. On the other hand, matrix  $P_r$  is symmetric, so the unitary matrix  $T_r$  can always be intentionally constructed as a proper unitary matrix to express the effect of rotation, regardless of the eigenvalue distribution of  $P_r$ .

Note that  $\det(P_r) \geq 0$  and  $\det(P_l) \geq 0$  because  $P_r$  and  $P_l$  are chosen to be negative semidefinite symmetric. If  $A$  is Hurwitz, both  $U_r$  and  $U_l$  should be proper unitary matrices to ensure the relation that

$$\det(U_r) \det(P_r) = \det(P_l) \det(U_l) = \det(A) > 0.$$

Define a rotation matrix as

$$R(\theta) \triangleq \begin{bmatrix} \cos \theta & -\sin \theta \\ \sin \theta & \cos \theta \end{bmatrix}.$$

Then in the case of Hurwitz  $A$ , the obtained unitary matrices in (3.6) can be expressed by rotation matrix  $R(\theta)$  as

$$U_r \triangleq R(\alpha_r), \quad T_r \triangleq R(\beta_r), \quad U_l \triangleq R(\alpha_l), \quad T_l \triangleq R(\beta_l),$$

where  $\alpha_r, \beta_r, \alpha_l, \beta_l \in [-\pi, \pi)$  are the corresponding rotation angles and the diagonal matrices in (3.6) can be denoted as

$$A_r \triangleq \text{diag}\{\lambda_{r1}, \lambda_{r2}\}, \quad A_l \triangleq \text{diag}\{\lambda_{l1}, \lambda_{l2}\},$$

where  $\lambda_{r1}, \lambda_{r2}, \lambda_{l1}, \lambda_{l2} \in \mathbb{R}_{<0}$ . Based on the decompositions in (3.6), one can find the following facts about the planar shifting property of phase function.

**Lemma 2.** *For any phase function  $\varphi(A, \theta)$  with  $\det(A) > 0$ , the following results hold*

$$(a) \text{ Vertical shifting: } \varphi(A, \theta) \stackrel{2\pi}{=} \varphi(P_r, \theta) + \alpha_r;$$

$$(b) \text{ Diagonal shifting: } \varphi(A, \theta) \stackrel{2\pi}{=} \varphi(P_l, \theta + \alpha_l) + \alpha_l;$$

$$(c) \text{ Horizontal shifting: } \varphi(A, \theta) = \varphi(U_r A_r, \theta + \beta_r) = \varphi(A_l U_l, \theta + \beta_l);$$

where the equation symbol  $a \stackrel{2\pi}{=} b$  means  $(a \bmod 2\pi) = (b \bmod 2\pi)$ .

*Proof.* For (a), we can prove it by

$$\begin{aligned}
\varphi(A, \theta) &\stackrel{2\pi}{=} \text{atan}(U_r P_r \omega(\theta)) - \text{atan}(\omega(\theta)) \\
&\stackrel{2\pi}{=} \text{atan}(U_r^T U_r P_r \omega(\theta)) - \text{atan}(U_r^T \omega(\theta)) \\
&\stackrel{2\pi}{=} \text{atan}(P_r \omega(\theta)) - \text{atan}(\omega(\theta - \alpha_r)) \\
&\stackrel{2\pi}{=} \varphi(P_r, \theta) + \alpha_r.
\end{aligned}$$

Our next step is to prove (b). By simple derivation, one can find

$$\varphi(A, \theta) \stackrel{2\pi}{=} \text{atan}(P_l \omega(\theta + \alpha_l)) - \theta \stackrel{2\pi}{=} \varphi(P_l, \theta + \alpha_l) + \alpha_l,$$

thus (b) is proven. The proof of (c) will be a straightforward combination of (a) and (b). Note that unitary second-order matrices are commutative, which means

$$\varphi(A, \theta) = \varphi(U_r T_r^T \Lambda_r T_r, \theta) = \varphi(T_r^T U_r \Lambda_r T_r, \theta).$$

Combining the results in (a) and (b), one can get

$$\varphi(A, \theta) \stackrel{2\pi}{=} \varphi(U_r \Lambda_r T_r, \theta) - \beta_r \stackrel{2\pi}{=} \varphi(U_r \Lambda_r, \theta + \beta_r),$$

thus the result in (c) is proven.  $\square$

**Remark 2.** All unitary matrices are *commutative*<sup>1</sup>, so we can also write the polar decompositions of  $A$  as

$$A = T_r^T U_r \Lambda_r T_r \quad \text{and} \quad A = T_l^T \Lambda_l U_l T_l.$$

From this point of view, we may find that both  $T_r$  and  $T_l$  result in the horizontal shift of  $\varphi(\cdot, \theta)$ . But the rotation degrees  $\beta_r$  and  $\beta_l$  should be different since  $U_r \Lambda_r \neq \Lambda_l U_l$ . From the perspective of singular-value decomposition (SVD)  $A = W \Sigma V^T$ , we can assert that

$$U_r = U_l = V^T W, \quad T_r = V^T, \quad \text{and} \quad T_l = W^T.$$

What's more,  $\Lambda_r$  and  $\Lambda_l$  should have the same eigenvalues, namely  $\{\lambda_{r1}, \lambda_{r2}\} = \{\lambda_{l1}, \lambda_{l2}\}$ , because both  $\varphi(\Lambda_r, \theta)$  and  $\varphi(\Lambda_l, \theta)$  have the same outline as  $\varphi(A, \theta)$ . Specially, if  $\Lambda_r$  and  $\Lambda_l$  are intentionally obtained as  $\Lambda_r = \Lambda_l = \Lambda$ , we can further get the relation that  $U_l T_l = T_r$  or equivalently  $\alpha_l + \beta_l = \beta_r$ . The above relations are presented in Figure 3.2. From Figure 3.2, we can also confirm that, in vertical direction, rotation matrix with positive angle leads to upper shift. In the horizontal direction, rotation matrix with positive angle gives rise to the left shift.

---

<sup>1</sup>Two elements  $x$  and  $y$  of a set  $S$  are said to be *commutative* under a binary operation  $*$  if they satisfy  $x * y = y * x$ . Definition of this term can be found in [90].

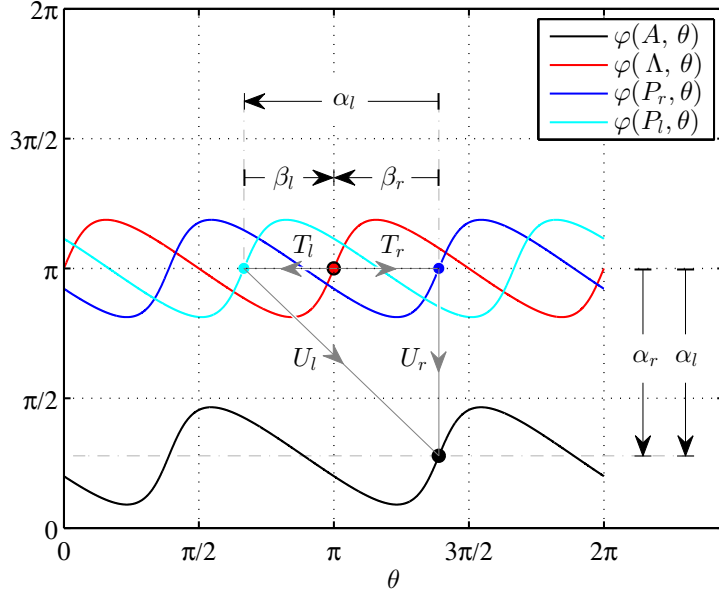


Figure 3.2: Relation of right and left polar decompositions

From Lemma 2 and the subsequent remarks after it, we can get a general impression of the layout and position of phase function  $\varphi(A, \theta)$ , as well as its relation with the polar decomposition of  $A$ . Overall, the outline of  $\varphi(A, \theta)$  can be uniquely determined by parameters  $\alpha_r$ ,  $\beta_r$  and the ratio  $\lambda_{r2}/\lambda_{r1}$ . The properties introduced in the following lemmas will explain the relation between phase function  $\varphi(A, \theta)$  and eigenvalues of matrix  $A$ .

**Lemma 3.** *For any  $A \in \mathbb{R}^{2 \times 2}$  with  $\det(A) > 0$ , the following results hold*

(a) *Positive real eigenvalue of  $A$ :*

$$\varphi(A, \theta^*) = 0 \quad \Leftrightarrow \quad \exists \lambda \in \mathbb{R}_{>0} \quad s.t. \quad A\omega(\theta^*) = \lambda\omega(\theta^*); \quad (3.7)$$

(b) *Negative real eigenvalue of  $A$ :*

$$\varphi(A, \theta^*) = \pi \quad \Leftrightarrow \quad \exists \lambda \in \mathbb{R}_{>0} \quad s.t. \quad A\omega(\theta^*) = -\lambda\omega(\theta^*); \quad (3.8)$$

(c) *Periodicity of  $\varphi(A, \theta)$ :*

$$\varphi(A, \theta + \pi) = \varphi(A, \theta). \quad (3.9)$$

*Proof.* From the definition in (3.4), we can confirm that,  $A\omega(\theta)$  would have the same phase angle as  $\omega(\theta + \varphi(A, \theta))$ . It means that

$$A\omega(\theta) = \|A\omega(\theta)\|_2 \omega(\theta + \varphi(A, \theta)). \quad (3.10)$$

The pre-condition  $\det(A) > 0$  ensures that  $A\omega(\theta)$  is non-zero, then  $\|A\omega(\theta)\|_2 > 0$  for all  $\theta$ . Choosing  $\lambda = \|A\omega(\theta^*)\|_2 > 0$  and considering  $\omega(\theta + \pi) = -\omega(\theta)$ , as we can see in (3.5), the sufficiency part of (3.7) and (3.8) can be easily proven, and their necessity parts would be obvious.

For (3.9), we can find the straight-forward derivation

$$\varphi(A, \theta + \pi) = \varphi(R^T(\pi)AR(\pi), \theta) = \varphi(A, \theta).$$

Thus the proof is completed.  $\square$

### 3.4 Stability analysis under arbitrary switching

Based on the concept of phase function, the main result of stability analysis for system (3.1) under arbitrary switching will be introduced in this part. For the equilibrium of system (3.1) to be stable under arbitrary switching, a necessary condition is that all the subsystems should be stable. Hence it is natural to propose the following assumption in this section.

**Assumption 1.** *Matrices  $A_1, A_2, \dots, A_q$  are all Hurwitz matrices.*

#### 3.4.1 Lyapunov function existence condition in the form of phase function

Under Assumption 1, all system matrices would satisfy  $\det(A_i) > 0$  ( $i \in \mathcal{Q}$ ). As a result, the properties in Lemmas 2 and 3 can be used in the stability analysis. Starting from the line-integral Lyapunov function in (3.2), we would firstly transform the Lyapunov function existence conditions (a), (b) and (c) in Section 3.2 into phase-based criteria. The vector  $p(x)$  considered in the following proposition is designed to be independent on the length  $\|x\|_2$  of vector  $x$ , thus for  $\theta = \text{atan}(x)$  we have

$$\varphi_p^*(\theta)|_{\theta=\text{atan}(x)} = \phi_p^*(\omega(\theta))|_{\theta=\text{atan}(x)} = \phi_p^*(x).$$

Overall the Lyapunov function existence conditions can be described as the criteria of  $\varphi_p^*(\theta)$  and  $\varphi_\sigma(\theta)$  in Proposition 2.

**Proposition 2.** *If there exists  $p(x)$  such that its phase function  $\varphi_p^*(\theta)$  is continuous and satisfies*

$$\varphi_\sigma(\theta) - \frac{3\pi}{2} \leq \varphi_p^*(\theta) \leq \varphi_\sigma(\theta) - \frac{\pi}{2}, \quad (3.11)$$

$$-\frac{\pi}{2} < \varphi_p^*(\theta) < \frac{\pi}{2}, \quad (3.12)$$



for all  $\theta \in [0, 2\pi)$ ,  $\sigma(t) \in \mathcal{Q}$ , and

$$\int_0^{2\pi} \tan \varphi_p^*(\theta) d\theta = 0, \quad (3.13)$$

then function (3.2) can be an appropriate line-integral Lyapunov function to ensure the stability of the equilibrium of system (3.1). Moreover, the equilibrium point of system (3.1) is asymptotically stable if the inequalities in (3.11) are satisfied as strict ones.

*Proof.* See Appendix A.1. □

**Remark 3.** In the conditions of Proposition 2, the reason for using  $\varphi_p^*(\theta)$  instead of  $\varphi_p(\theta)$  is to simplify the expression in (3.11) and (3.12) by the special range property that  $\varphi_p^*(\theta) \in [-\pi, \pi)$ .

**Remark 4.** Based on Figure 3.1 we can find that, condition (3.12) is provided to ensure that Lyapunov function  $V(x)$  is positive definite, in other words, its level surface with lower energy is contained in level surface with higher energy. Condition (3.13) ensures that the level surface of  $V(x)$  with the same energy is a closed circle. Condition (3.11) will guarantee that the system state  $x$  on a level surface moves inside that surface, in other words,  $\dot{V}(x) \leq 0$ .

With Proposition 2, we can understand the stability problem of Figure 2.8 from a new point of view. If we focus on one point on the level surface of the given Lyapunov function and consider the magnified micro-space around that point, we will find the graphical explanation of relation in Condition (3.11), see Figures 3.3 and 3.4.

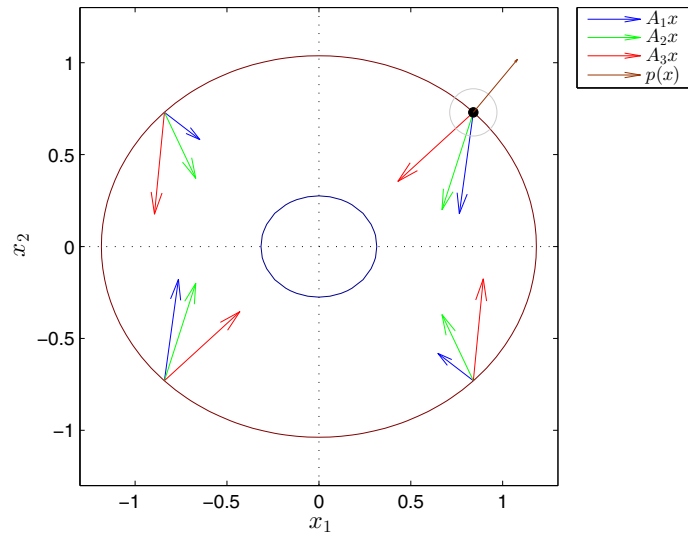


Figure 3.3: Review of a point on the level surface in Figure 2.8



$\varphi(A_i, \theta)$  ( $i = 1, 2, \dots, q$ ), for  $\theta \in [0, 2\pi)$ , then find their maximum and minimum values  $\varphi_{\max}(\theta)$  and  $\varphi_{\min}(\theta)$ . Finally the extreme value  $\sup\{\varphi_{\max}(\theta) - \varphi_{\min}(\theta)\}$  can be obtained. Alternatively, we can also find the equivalent algebraic criterion if (3.14) is a strict inequality. The relation can be described in Lemma 5.

**Lemma 5.** *A necessary and sufficient condition for*

$$\sup\{\varphi_{\max}(\theta) - \varphi_{\min}(\theta)\} < \pi \quad (3.15)$$

*to be satisfied is that  $A_i A_j^{-1}$  has no negative real eigenvalue for all  $1 \leq i < j \leq q$ .*

*Proof.* We choose an  $x$  such that  $A_j x = \omega(\theta)$  can be satisfied. Hurwitz  $A_j$  is invertible, then the value of  $x$  can be obtained as  $x = A_j^{-1} \omega(\theta)$ . Furthermore, the difference of two phase functions  $\varphi(A_i, \theta)$  and  $\varphi(A_j, \theta)$  can be calculated as

$$\varphi(A_i, \theta) - \varphi(A_j, \theta) \stackrel{2\pi}{=} \text{atan}(A_i A_j^{-1} \omega(\theta)) - \text{atan}(\omega(\theta)) = \varphi(A_i A_j^{-1}, \theta). \quad (3.16)$$

Inequality (3.15) means that  $\varphi(A_i, \theta) - \varphi(A_j, \theta) \neq \pi$  for all  $i, j \in \mathcal{Q}$ , equivalently we have  $\varphi(A_i A_j^{-1}, \theta) \neq \pi$  for all  $i, j \in \mathcal{Q}$ . By the relation (3.8) in Lemma 3, we know that matrix  $A_i A_j^{-1}$  has no negative real eigenvalue for  $i, j \in \mathcal{Q}$ , or equivalently for all  $1 \leq i < j \leq q$ . The proof is thus completed.  $\square$

The criterion in (3.14) can be viewed as a combination of (3.11) and (3.12). Our next step is to consider the condition represented by integral equation (3.13), and replace it with integral inequalities of  $\cot \varphi_{\max}(\theta)$  and  $\cot \varphi_{\min}(\theta)$ . Based on the aforementioned phase functions  $\varphi_{\max}(\theta)$  and  $\varphi_{\min}(\theta)$ , the main result of this chapter can be stated as Theorem 3.

**Theorem 3.** *A necessary and sufficient condition for the stability of the equilibrium of system (3.1) under arbitrary switching is that*

$$\sup\{\varphi_{\max}(\theta) - \varphi_{\min}(\theta)\} \leq \pi, \quad (3.17)$$

and

$$\inf\{\varphi_{\max}(\theta)\} \leq \pi \quad \text{or} \quad \int_0^{2\pi} \cot \varphi_{\max}(\theta) d\theta \geq 0, \quad \text{if} \quad \inf\{\varphi_{\max}(\theta)\} > \pi, \quad (3.18)$$

$$\sup\{\varphi_{\min}(\theta)\} \geq \pi \quad \text{or} \quad \int_0^{2\pi} \cot \varphi_{\min}(\theta) d\theta \leq 0, \quad \text{if} \quad \sup\{\varphi_{\min}(\theta)\} < \pi. \quad (3.19)$$

Moreover, the equilibrium of system (3.1) is asymptotically stable if all the involved inequalities are satisfied as strict ones.

*Proof.* See Appendix A.3.  $\square$

To check the stability condition in Theorem 3, firstly we need to get the expressions of  $\varphi_{\max}(\theta)$  and  $\varphi_{\min}(\theta)$  based on phase function  $\varphi(A_i, \theta)$  of each subsystem.

For criterion in (3.18), if the inequality  $\inf\{\varphi_{\max}(\theta)\} \leq \pi$  holds, then there is no need to check  $\int_0^{2\pi} \cot \varphi_{\max}(\theta) d\theta \geq 0$ . Criterion (3.18) does not hold if and only if

$$\int_0^{2\pi} \cot \varphi_{\max}(\theta) d\theta < 0 \quad \text{and} \quad \inf\{\varphi_{\max}(\theta)\} > \pi.$$

It is the same for criterion in (3.19).

**Remark 5.** *From the dynamic point of view, the condition in (3.17) is provided to ensure that all the regional chattering dynamics are stable. Conditions in (3.18) and (3.19) can ensure that system state with spiralling dynamics does not diverge to infinity.*

In Theorem 3, if  $\inf\{\varphi_{\max}(\theta)\} \leq \pi$  then there is no need to check the inequality condition in (3.18). The same holds for  $\inf\{\varphi_{\min}(\theta)\} \geq \pi$ . Thus, as a special case of Theorem 3, we have the following simple sufficient stability condition.

**Corollary 1.** *The equilibrium of system (3.1) is stable under arbitrary switching if the following inequalities are satisfied*

$$\inf\{\varphi_{\max}(\theta)\} \leq \pi, \tag{3.20}$$

$$\sup\{\varphi_{\max}(\theta) - \varphi_{\min}(\theta)\} \leq \pi, \tag{3.21}$$

$$\sup\{\varphi_{\min}(\theta)\} \geq \pi. \tag{3.22}$$

*And the equilibrium of system (3.1) is asymptotically stable if (3.21) is satisfied as strict inequality.*

## 3.5 Verification examples

By two simple examples, now we discuss the application of phase-based condition in Proposition 2 and compare the results in Theorem 3 with several existing methods.

### 3.5.1 Application of the phase-based condition

**Example 1.** *To explain how the stability analysis conservativeness can be reduced by increasing the order of polynomial Lyapunov function, we will describe the phase functions of 2nd, 4th, 6th, 8th order polynomial Lyapunov functions (correspondingly in [13] the value of parameter  $m$  should be set as  $m = 1, 2, 3, 4$ ) based on an example with the following subsystems*

$$A_1 = \begin{bmatrix} -1 & -1 \\ 1 & -1 \end{bmatrix}, \quad A_2 = \begin{bmatrix} -1 & -a \\ \frac{1}{a} & -1 \end{bmatrix}$$

where  $a$  is a parameter. The problem is to determine the maximum value of  $a^*$  for which the system equilibrium is asymptotically stable for arbitrary switching signals. The results obtained by different order polynomial Lyapunov functions are shown in Table 3.1.

Table 3.1: Maximum values of  $a^*$  obtained by different polynomial Lyapunov functions [13]

$m$	1	2	3	4
$a^*$	5.8283	9.2911	9.6825	10.4105

The phase function of each polynomial Lyapunov function is plotted in Figure 3.5. We can find that, with the increase of  $a$ , the minimum value of  $\varphi_{\min}(\theta)$  will move downward. From Proposition 2, it is obvious that, for an appropriate Lyapunov function, its phase layout should be lower than  $\varphi_{\min}(\theta) - \pi/2$  and satisfying  $\int_0^{2\pi} \tan \varphi_p^*(\theta) d\theta = 0$ . By increasing the value of  $m$ , the corresponding polynomial Lyapunov function will be more flexible. Consequently the gap between  $\varphi_{\min}(\theta)$  and  $\varphi_{\min}(\theta) - \pi/2$  can be smaller, and bigger value of  $a$  will be allowed. If we calculate the value of  $a$  by condition  $\int_0^{2\pi} \cot \varphi_{\min}(\theta) d\theta = 0$ , the critical value with 5 decimal places can be obtained as  $a^* = 11.31149$ .

### 3.5.2 Comparison with existing results

**Example 2.** In this example, we will compare the phase-based stability condition in Theorem 3 with some existing methods in literature. Consider the following switched system model

$$\dot{x}(t) = A_{\sigma(t)}x(t), \quad A_{\sigma(t)} \in \{A_1, A_2\},$$

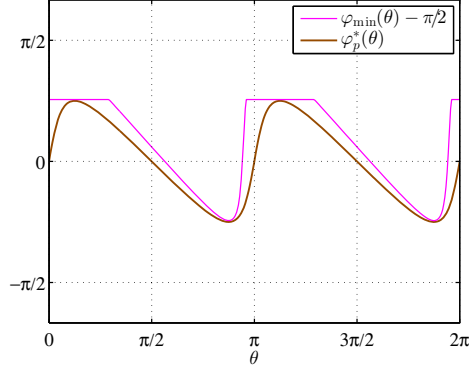
where

$$A_1 = \begin{bmatrix} 0 & 1 \\ -2 & -1 \end{bmatrix}, \quad A_2 = \begin{bmatrix} 0 & 1 \\ -2-k & -1 \end{bmatrix}.$$

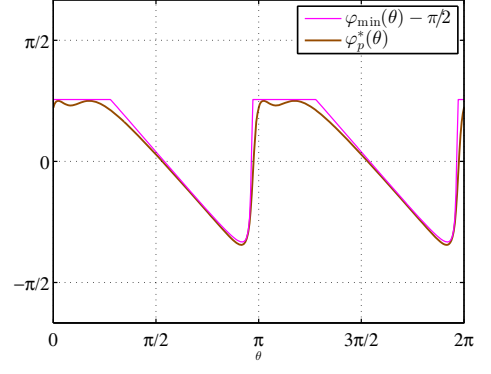
This example has been widely used in literature, e.g. [1, 2, 10], to check the conservativeness of obtained results. Here we also choose it to exemplify the result in Theorem 3 and make comparisons with existing methods.

#### (1). Exemplification of the result in Theorem 3

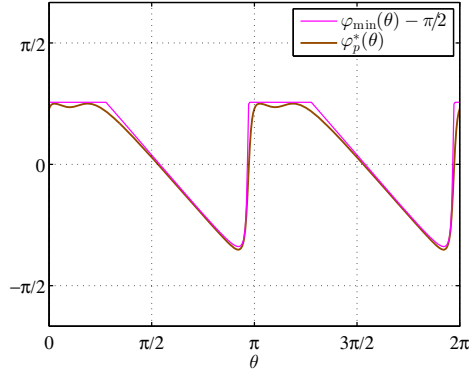
Based on the criteria in Proposition 2, the phase function  $\varphi_p^*(\theta)$  of feasible Lyapunov function must lie within the grey region  $[\varphi_{\max}(\theta) - \frac{3\pi}{2}, \frac{\pi}{2})$  in Figure 3.6, and satisfies the integral condition  $\int_0^{2\pi} \tan \varphi_p^*(\theta) d\theta = 0$ . The condition obtained from quadratic Lyapunov function [2] can guarantee the stability for  $k \leq 3.82$ , and its corresponding phase function is shown in Figure 3.6. For the range  $3.5 \leq k \leq 7.5$ , we get



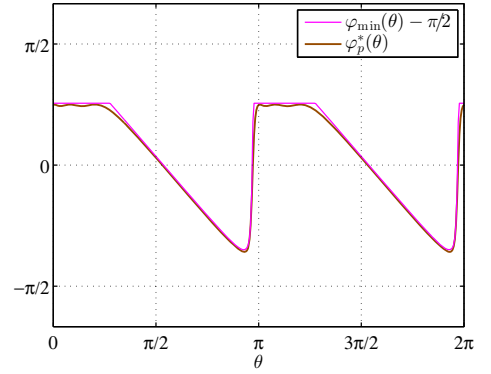
(a)  $m = 1$  (2nd-order PLF\*) and  $a = 5.8283$



(b)  $m = 2$  (4th-order PLF) and  $a = 9.2911$



(c)  $m = 3$  (6th-order PLF) and  $a = 9.6825$



(d)  $m = 4$  (8th-order PLF) and  $a = 10.4105$

Figure 3.5: Layouts of  $\varphi_{\min}(\theta)$  and  $\varphi_p^*(\theta)$  with different  $a$  value and  $m$ , (\*PLF is the acronym of polynomial Lyapunov function)

$\sup\{\varphi_{\max}(\theta) - \varphi_{\min}(\theta)\} \in [1.08, 1.46]$ ,  $\sup\{\varphi_{\min}(\theta)\} = 4.85$  and  $\inf\{\varphi_{\min}(\theta)\} = 3.93$ . Thus conditions (3.17) and (3.19) can be always satisfied, what we need to do is checking the integral condition in (3.18). By setting  $\int_0^{2\pi} \cot \varphi_{\max}(\theta) d\theta = 0$ , one can clearly find in Figure 3.7 that the critical  $k$  value for (3.18) is  $k^* = 6.98513$ .

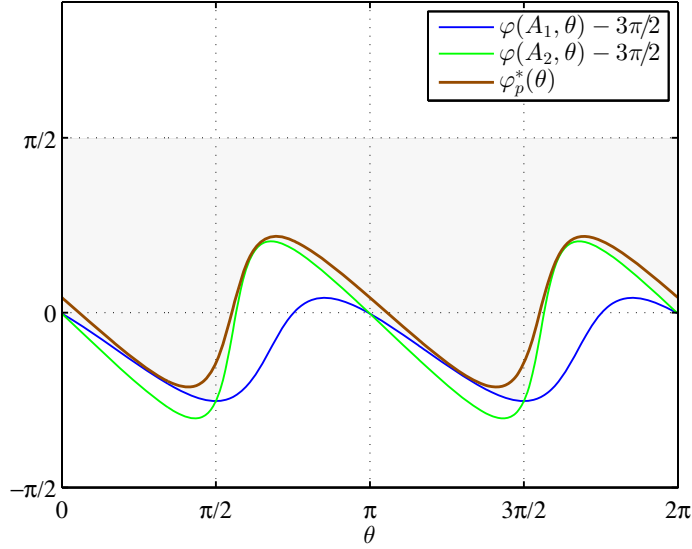


Figure 3.6: Phase functions of the subsystem matrices  $A_1$  and  $A_2$  and their CQLF  $\varphi_p^*(\theta)$  (The gray area shows the allowable region for  $\varphi_p^*(\theta)$  determined by Conditions (3.11) and (3.12))

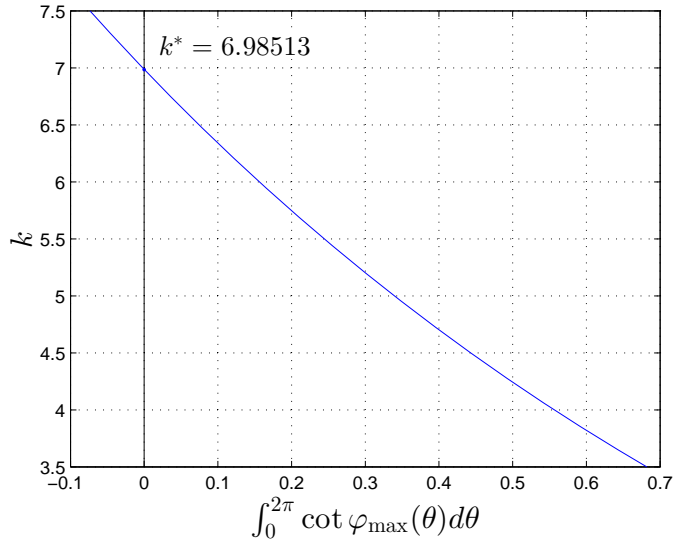


Figure 3.7: Relation of  $k$  and  $\int_0^{2\pi} \cot \varphi_{\max}(\theta) d\theta$

## (2). *Relation with Lyapunov function based methods*

Various novel Lyapunov functions have been proposed to improve the function flexibility. The piecewise Lyapunov function [10] constructed by double quadratic terms guarantees the stability for  $k \leq 4.7$ . Following this method, the result can be further improved to  $k \leq 5.9$  if the nonlinear transformation in [91] is combined.

The method proposed in [2] and [13] is an extension of traditional quadratic Lyapunov function from second-order polynomial function to higher order ones. Theoretically, the conservativeness of stability condition in [2] can be gradually reduced by increasing the order of adopted polynomial Lyapunov function. But when

it is actually solved by the SOS Tools software, the improvement of analysis result will stop at some certain order. If we choose the function order to be even higher, as we can see in Figure 3.8, the algorithm will crash and provide unreasonable results. This is mainly caused by the inevitable calculation-error amplification of high order polynomials during the numerical iteration. The best result of this method is obtained by the tenth-order polynomial Lyapunov function, ensuring the stability for  $k \leq 6.64$  which is below the value obtained by Theorem 3, as is shown in Figure 3.8.

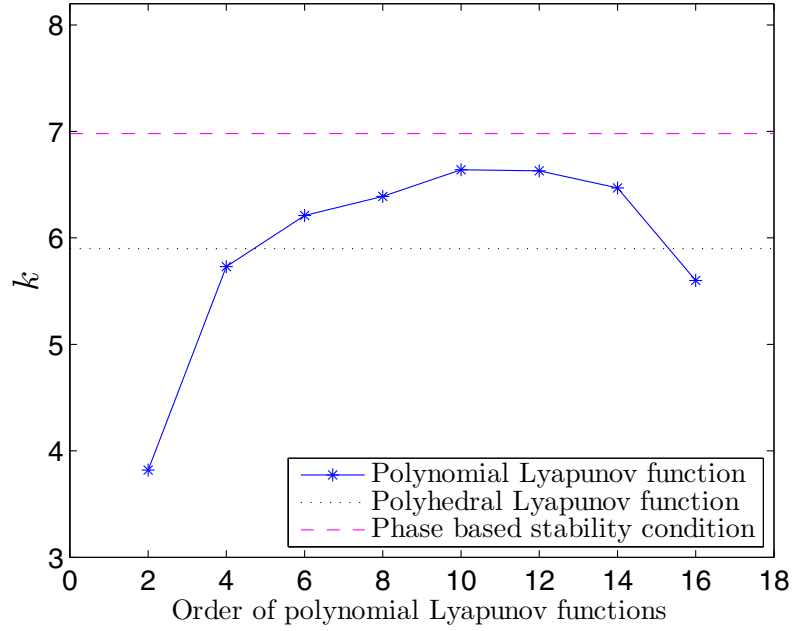


Figure 3.8: Comparison among polynomial Lyapunov function [2], piecewise Lyapunov function [10], and phase-based condition in Theorem 3

### (3). Relation with numerical methods

The numerical approach in [1] originates from the construction of a polyhedral Lyapunov function. Theoretically, the accuracy of  $k^*$  can be gradually improved by progressively choosing a larger number of *partition rays*. But this approach is computationally demanding in practical experiment. As we can see, one needs 40000 rays for a two-digit accuracy of  $k^* = 6.98$ . But to achieve a three-digit accuracy of  $k^* = 6.985$ , the rays number 1500000 is required. The phase-based method in Theorem 3 can achieve results identical to that obtained by numerical method with infinite number of rays, and at the same time can get rid of the heavy burden of computation.

### (4). Relation with polar coordinate based methods

Similar necessary and sufficient condition can be also found in [58], which is obtained based on the polar coordinate model. But that condition is applicable to



systems with only a pair of subsystems. Results in [59] and [60] can be viewed as the extension of [58] to systems with finite number of subsystems. Compared with those results, the method studied here shows the advantage as a unified framework for the analysis of stability problem. So there is no need to concern about the specific types of eigenvalues that are defined in the above papers. And some assumptions for the subsystems can be also avoided, which means that a wider range of switched systems can be investigated.

### 3.6 Conclusions

Starting from the idea of an ultimate flexible line-integral Lyapunov function, we have proposed the concept of phase function to characterize the existence condition of an appropriate Lyapunov function. Under this new concept, the problem of stability analysis for second-order switched system has been investigated. By considering and applying the inherent properties of phase function, necessary and sufficient condition for the stability of second-order switched systems under arbitrary switching has been obtained in a different approach. Compared with existing works, the stability condition obtained here shows advantages in terms of theoretical analysis and numerical computation.

# Chapter 4

## Extended results of the phase-based stability condition

*In existing research, it has been proven that the existence of CQLF for every three tuple of subsystems can ensure the stability<sup>1</sup> of the whole system. In this chapter we are interested to find out whether this can be improved by the phase-based condition.*

### 4.1 Introduction

In previous chapters, we discussed the stability problem of switched system based on the a presumed Lyapunov function. While specially for the second order switched system, mathematical methods like matrix analysis and convex set analysis [92, 93] can be applied to get analytical stability condition. In this direction, Shorten and Narendra [11] described equation  $\det\{A^T P + P A = 0\}$  of system matrix  $A$  and positive real matrix  $P$  as an ellipse in the 2-dimensional space, then solution of “ $P$ ” can be analyzed by set theory. By applying Helly’s theorem [92] they proven that the existence of a CQLF for the whole switched system is equivalent to the existence of a CQLF for every three-tuple of subsystems, while the analytical existence condition for the CQLF of three subsystems (in other words, the whole system) is still unknown. But on the other hand, by the analysis of eigenvalues, Shorten and Narendra have found the analytical explanation to the CQLF existence condition for a pair of Hurwitz system matrices  $A_1$  and  $A_2$ , which is, matrix pencils  $\alpha A_1 + (1 - \alpha)A_2$  and  $(1 - \alpha)A_1 + \alpha A_2$  are both Hurwitz for  $\alpha \in [0, 1]$ , or equivalently, matrices  $A_1 A_2$  and  $A_1 A_2^{-1}$  do not have real negative eigenvalues.

Following the above analytical explanation for CQLF existence condition of  $A_1$  and  $A_2$ , in this research we intend to improve the results in [11] by the phase-based condition in Chapter 3, to see whether the CQLF existence condition of every two-tuple of subsystems would be sufficient for the stability of the whole system. Instead of directly analyzing the LMI condition related with CQLF, we will start from the phase-based stability condition obtained in Chapter 3. Firstly, we will

discuss some typical properties of phase function. Based on these properties, the result in Chapter 3 will be extended to a much simpler sufficient condition with only one inequality criterion that is integral-free and thus easier to check. Secondly, such a new condition will be transformed into its equivalent algebraic form, which is expressed as the eigenvalue requirement of  $A_1 A_2$  and  $A_1 A_2^{-1}$ . Lastly, by considering the analytical explanation of CQLF existence condition in [11], we can verify that the CQLF existence condition of every pair of subsystems will be already sufficient to ensure stability of the whole system.

As an extension, we will also consider application of the main result in the special case of switched positive systems. This kind of switched systems are described by Metzler matrices [94, 95] and can be used to describe the dynamic processes such as epidemiology [96] and congestion control [97]. For this special case, we can find that the CQLF existence condition of every pair of subsystems will be both necessary and sufficient for stability of the whole system, as a result, alternative explanation for the conclusion in [98] can be obtained.

The remaining sections of this chapter are organized as follows. Section 4.2 illustrates the problem formulation of switched system stability analysis and preliminary about phase function. In Section 4.3, additional properties of phase function will be analyzed, and simplified phase-based stability condition and their transformations will be provided. In Section 4.4, we will discuss the special case of positive switched system. Finally in Section 4.5, a conclusion of this chapter will be drawn.

## 4.2 Problem formulation and preliminaries

### 4.2.1 Problem formulation

In this chapter again we consider a linear switched system of second-order, where system state  $x(t) \in \mathbb{R}^2$  and system matrix  $A_{\sigma(t)}$  can switch among a collection of constant matrices  $A_1, A_2, \dots, A_q$  in  $\mathbb{R}^{2 \times 2}$ . We introduce a set  $\mathcal{Q} \triangleq \{1, 2, \dots, q\}$  to describe the collection of indexes of subsystems. The system expression can be described as

$$\dot{x}(t) = A_{\sigma(t)}x(t), \quad \sigma(t) \in \mathcal{Q}. \quad (4.1)$$

To simplify the complex expressions, throughout this chapter we may neglect the input arguments of variables or functions, for example,  $A_{\sigma(t)}$  may be simplified as  $A_\sigma$ .

In this chapter, we consider the stability problem of system (4.1). A normal approach to check the stability of the equilibrium of switched system (4.1) is to find a CQLF for all the subsystems in (4.1). In literature, by applying Helly's theorem [92], Shorten and Narendra [11] have found the elegant result that the

existence of a CQLF for the whole switched system is equivalent to the existence of a CQLF for every three-tuple of subsystems. It means that, as long as we can find the individual CQLFs for every three-tuple of local subsystems, which are not necessarily same to each other, the equilibrium of the whole system will be stable.

Following such a conclusion, we are wondering whether the required number of subsystems for an individual CQLF can be further reduced from three to two. The answer to this question seems not clear since Helly's theorem is not applicable anymore in this case. But similar research has been done for some special class of second-order switched systems, namely the positive switched systems. Akar et al. [99] have verified that if all the subsystems of (4.1) are described by Hurwitz, Metzler matrices [94] and the diagonal entries of these matrices are  $-1$ , the existence of a diagonal CQLF for two-tuple of subsystems will ensure the stability of the whole system. Later in [98], Gurvits et al. further extended such a result by removing the restrictive assumption on the diagonal entries of the system matrices and CQLF.

It is interesting to know whether the above two-tuple based conclusion can be further extended to the general second-order switched systems. Around this question, we will consider the relation between CQLF existence condition of every pair of subsystems and the stability of the overall system. The method we choose is slightly different from [99] and [98] that focus directly on matrix and sets analysis. Instead, we will start the discussion based on the concept of phase function that has been proposed in Chapter 3.

### 4.2.2 Preliminaries about phase function

As it is explained in Chapter 3, the definition of phase function comes from the idea of describing the Lyapunov stability criteria as the mathematical conditions of subsystem phase angles. Denote a variable as the angle variation between vectors  $Ax$  and  $x$ . Specially if we simplify  $x$  as a unit vector  $\omega(\theta) \triangleq [\cos \theta \ \sin \theta]^T$ , such an angle variable will be a function of  $\theta$ . To start the analysis in this chapter, we firstly recall the phase function of a second order system matrix  $A$  which is defined in Equation (3.4) of Chapter 3.

$$\varphi(A, \theta) \triangleq \text{atan}(A\omega(\theta)) - \theta \pmod{2\pi}. \quad (4.2)$$

where  $\text{atan}(A\omega(\theta))$  is the phase angle of vector  $A\omega(\theta)$ , with  $\text{atan}(x)$  ( $x = [x_1, x_2]^T$ ) being defined in Equation (3.3) of Chapter 3. Exactly the expression of  $\text{atan}(x)$  can be recalled as below.

$$\text{atan}(x) \triangleq \begin{cases} \text{atan2}(x_2, x_1), & x_2 \geq 0; \\ \text{atan2}(x_2, x_1) + 2\pi, & x_2 < 0. \end{cases} \quad (4.3)$$

The graphical explanation and layout of phase function  $\varphi(A, x)$  can be found in Figure 4.1. Clearly, for the equilibrium of the switched system in (4.1) to be asymp-

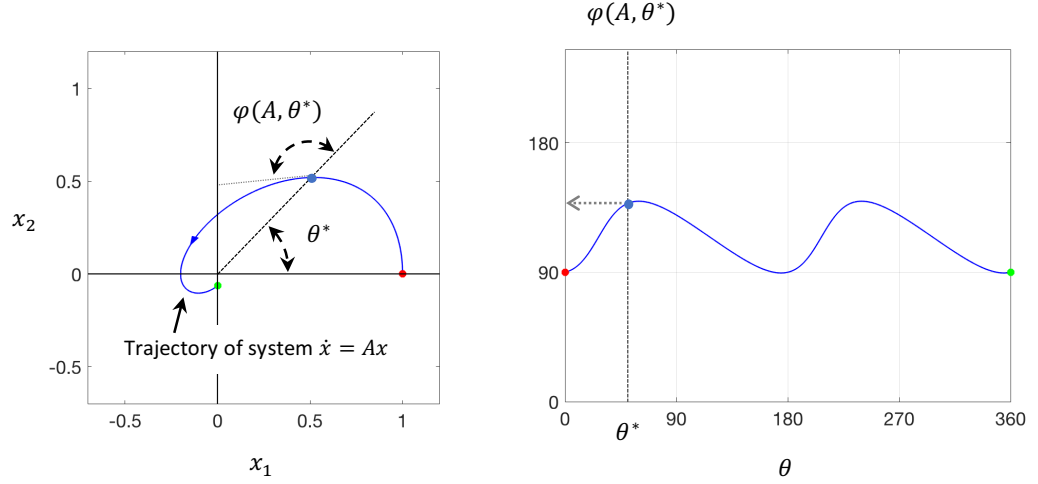


Figure 4.1: Definition of phase function  $\varphi(A, \theta)$  based on the trajectory of system  $\dot{x} = Ax$ . Right: Layout of phase function  $\varphi(A, \theta)$  with respect to  $\theta$ .

totically stable under arbitrary switching, a necessary condition is that all the subsystems should be stable. Hence it is natural to propose the same assumption as that in Chapter 3.

**Assumption 2.** *Matrices  $A_1, A_2, \dots, A_q$  are all Hurwitz matrices.*

For the phase function of second order system with Hurwitz matrix  $A$ , there are some special properties. To describe them, we need a general rotation matrix which is defined as

$$R(\theta) \triangleq \begin{bmatrix} \cos \theta & -\sin \theta \\ \sin \theta & \cos \theta \end{bmatrix}.$$

The properties about translational movement of a phase function can be described separately as vertical shift and horizontal shift. The one about vertical shift property can be expressed as

$$\varphi(R(\alpha)A, \theta) = \varphi(A, \theta) - \alpha, \quad (4.4)$$

where  $\alpha \in \mathbb{R}$  is scale of vertical shift. The one about horizontal shift property can be expressed as

$$\varphi(R^T(\alpha)AR(\alpha), \theta) = \varphi(A, \theta - \alpha), \quad (4.5)$$

where  $\alpha \in \mathbb{R}$  is scale of horizontal shift. Based on the definition of phase function  $\varphi(A, \theta)$  in (4.2), the proofs of (4.4) and (4.5) will be obtained, readers are referred to Lemma 3.1 of Chapter 3 for the detailed explanation of these proofs. With the

proposed concept of phase function and its properties, in the following part, we will further analyze the stability problem of second-order switched systems by using system phase function  $\varphi(A, \theta)$ .

## 4.3 Main results

In this part we will firstly review the result in Chapter 3. By analyzing the integral terms in the stability condition in Chapter 3, we then find a clue to simplify that stability condition based on some specific properties of phase function. Criterion in the newly obtained condition will be much easier to check. Secondly, to see the relation of the obtained new condition in regard with existing results in literature, we will transform the phase-based criterion into equivalent algebraic and LMI conditions. By the end of this part, relation between the stability of the whole system and existence condition of CQLF for every two-tuple of subsystems will be obtained. Illustrative examples will be provided to verify the results and show the improvement coming with the new stability condition.

### 4.3.1 Further analysis of the phase-based stability condition

In the previous chapter, the necessary and sufficient stability condition for second-order switched systems has been obtained. It is described by the maximum and minimum values of all the phase functions of  $A_1, A_2, \dots, A_q$ , which are defined as

$$\begin{aligned}\varphi_{\max}(\theta) &\triangleq \max \{ \varphi(A_1, \theta), \varphi(A_2, \theta), \dots, \varphi(A_q, \theta) \}, \\ \varphi_{\min}(\theta) &\triangleq \min \{ \varphi(A_1, \theta), \varphi(A_2, \theta), \dots, \varphi(A_q, \theta) \}.\end{aligned}$$

The obtained condition involves the constraint on the bias between  $\varphi_{\max}(\theta)$  and  $\varphi_{\min}(\theta)$  in (3.17), the positiveness of the integral of  $\cot \varphi_{\max}(\theta)$  in (3.18), and the negativeness of the integral of  $\cot \varphi_{\min}(\theta)$  in (3.19). The detailed conclusion can be summarized as Theorem 3.

Similar conclusions, which are obtained by system analysis in polar coordinate, can be found in [59, 60]. The result provided by Theorem 3 is expressed in the form of phase function. Generally the result in Theorem 3 is relatively simpler since there is no need to consider the distribution of system eigenvalues. To utilize this theorem, what we need are the numerical values of  $\varphi_{\max}(\theta)$  and  $\varphi_{\min}(\theta)$ . With these values, condition (3.17) is possible to check. A disadvantage of Theorem 3 is the integral conditions in (3.18) and (3.19). To improve the stability condition obtained in the framework of phase function, our initial concern is whether the relatively complex integral criteria (3.18) and (3.19) can be avoided in some special cases.

By comparison, we may find that conditions (3.18) and (3.19) are expressed in similar format, and to some extent, can be regarded as symmetric expressions. Our

intuitive thinking is whether these two conditions can be combined as a simplified one. To find the answer, we need to know the inherent relation between  $\varphi_{\max}(\theta)$  and  $\varphi_{\min}(\theta)$ . Actually,  $\varphi_{\max}(\theta)$  and  $\varphi_{\min}(\theta)$  might be described by irrelevant subsystems, for example,  $\varphi_{\max}(\theta) = \varphi(A_1, \theta)$  and  $\varphi_{\min}(\theta) = \varphi(A_2, \theta)$ , which gives no clue for inner relation. Then how about if  $A_1$  and  $A_2$  are the inverse matrices of each other, e.g.,  $A_1 A_2 = I$ ?

To investigate this special case, we start from the singular value decomposition  $A = U \Sigma V^T$ , where  $U$  and  $V$  are rotation matrices,  $\Sigma = \text{diag}\{\sigma_1, \sigma_2\}$  is a diagonal matrix. With this decomposition, the inverse matrix of  $A$  can be expressed as  $A^{-1} = V \Sigma^{-1} U^T$ . Since

$$\varphi(\Sigma, \theta) + \varphi(\Sigma^{-1}, \frac{\pi}{2} - \theta) \stackrel{2\pi}{=} \arctan\left(\frac{\sigma_1 \cos \theta}{\sigma_2 \sin \theta}\right) + \arctan\left(\frac{\sigma_2 \sin \theta}{\sigma_1 \cos \theta}\right) + \frac{\pi}{2} = \pi, \quad (4.6)$$

it is clear that  $\varphi(\Sigma, \theta)$  and  $\varphi(\Sigma^{-1}, \theta)$  have same layout as each other. Considering (4.4) and (4.5), we know that  $\varphi(A, \theta)$  and  $\varphi(A^{-1}, \theta)$  can be obtained by translational movement of  $\varphi(\Sigma, \theta)$  and  $\varphi(\Sigma^{-1}, \theta)$ , which means that  $\varphi(A, \theta)$  and  $\varphi(A^{-1}, \theta)$  also share the same layout. By further analysis we find the following relation between  $\varphi(A, \theta)$  and  $\varphi(A^{-1}, \theta)$ : For the given angles  $\theta$  and  $\alpha$  with constraint  $0 < \alpha < \pi$ ,

$$\text{if } \varphi(A, \theta) > \pi + \alpha, \text{ then } \varphi(A^{-1}, \theta - \alpha) < \pi - \alpha.$$

It means that, for the given  $\theta$  and  $\alpha$ , the values of  $\varphi(A, \theta)$  and  $\varphi(A^{-1}, \theta - \alpha)$  are symmetric about value  $\pi$ . The exact relation can be summarized as Lemma 6 with the newly defined angle sets  $\bar{\mathcal{S}}(A, \alpha)$  and  $\underline{\mathcal{S}}(A, \alpha)$ ,

$$\bar{\mathcal{S}}(A, \alpha) \triangleq \{\theta | \varphi(A, \theta) \geq \pi + \alpha\}, \quad \underline{\mathcal{S}}(A, \alpha) \triangleq \{\theta | \varphi(A, \theta) \leq \pi - \alpha\},$$

where  $\bar{\mathcal{S}}(A, \alpha)$  is the domain of  $\varphi(A, \theta)$  with value above  $\pi + \alpha$ , and  $\underline{\mathcal{S}}(A, \alpha)$  is the domain of  $\varphi(A, \theta)$  with value below  $\pi - \alpha$ . Proof of Lemma 6 can be found in the Appendix.

**Lemma 6.** *For a given Hurwitz matrix  $A$  and angular value  $0 < \alpha < \pi$ , the following relation between  $\bar{\mathcal{S}}(A, \alpha)$  and  $\underline{\mathcal{S}}(A, \alpha)$  holds*

$$\underline{\mathcal{S}}(A^{-1}, \alpha) = \{\theta | \theta = \theta^* - \alpha, \theta^* \in \bar{\mathcal{S}}(A, \alpha)\}. \quad (4.7)$$

By Lemma 6, we can find that the values of  $\underline{\mathcal{S}}(A^{-1}, \alpha)$  can be obtained by left shifting of the values of  $\bar{\mathcal{S}}(A, \alpha)$  with the distance  $\alpha$ . Denoting the Lebesgue measures [100] of a set  $\mathcal{S}$  as  $\mu_L(\mathcal{S})$ , then it follows that the Lebesgue measures of  $\underline{\mathcal{S}}(A^{-1}, \alpha)$  and  $\bar{\mathcal{S}}(A, \alpha)$  should be same. Mathematically this relation can be expressed as

$$\mu_L(\bar{\mathcal{S}}(A, \alpha)) = \mu_L(\underline{\mathcal{S}}(A^{-1}, \alpha)). \quad (4.8)$$

If  $\alpha$  is chosen to be the extreme values<sup>2</sup> of  $\varphi(A, \theta) - \pi$ , we will find the relation

$$\max \{ \varphi(A, \theta) \} - \pi = \pi - \min \{ \varphi(A^{-1}, \theta) \}, \quad (4.9)$$

$$\min \{ \varphi(A, \theta) \} - \pi = \pi - \max \{ \varphi(A^{-1}, \theta) \}. \quad (4.10)$$

With the equality properties in (4.8), (4.9) and (4.10), we may find the relation that, integrals of  $\varphi(A, \theta)$  and  $\varphi(A^{-1}, \theta)$  will compensate each other, which can be presented as

$$\int_0^{2\pi} \cot \varphi(A, \theta) d\theta + \int_0^{2\pi} \cot \varphi(A^{-1}, \theta) d\theta = 0. \quad (4.11)$$

The proof of (4.11) can be explained by following the same procedure as derivations in (B.12) and (B.13) which are provided in the Appendix B. To apply the special property in Lemma 6 and get the extended result of (4.11), we need to construct the maximum and minimum phase function values with not only subsystem matrices but also their inverses. Following this idea, we define the new maximum and minimum phase functions as

$$\hat{\varphi}_{\max}(\theta) \triangleq \max \{ \varphi(A_1, \theta), \varphi(A_1^{-1}, \theta), \dots, \varphi(A_q, \theta), \varphi(A_q^{-1}, \theta) \}, \quad (4.12)$$

$$\hat{\varphi}_{\min}(\theta) \triangleq \min \{ \varphi(A_1, \theta), \varphi(A_1^{-1}, \theta), \dots, \varphi(A_q, \theta), \varphi(A_q^{-1}, \theta) \}. \quad (4.13)$$

Based on the equality in (4.7), it can be further confirmed that the integrals of  $\cot \hat{\varphi}_{\max}(\theta)$  and  $\cot \hat{\varphi}_{\min}(\theta)$  from  $\theta = 0$  to  $\theta = 2\pi$  will also compensate each other. The exact description and prerequisite to use this property are summarized in Lemma 7.

**Lemma 7.** *Consider a group of  $q$  Hurwitz system matrices  $\{A_1, A_2, \dots, A_q\}$ . The following result always holds*

$$\int_0^{2\pi} \cot \hat{\varphi}_{\max}(\theta) d\theta + \int_0^{2\pi} \cot \hat{\varphi}_{\min}(\theta) d\theta = 0, \quad (4.14)$$

*if  $\hat{\varphi}_{\max}(\theta) \neq \hat{\varphi}_{\min}(\theta)$  for all  $\theta \in [0, 2\pi)$ .*

The proof of Lemma 7 is provided in the Appendix. To see clearly what the expression in (4.14) means, we provide a numerical case explanation in Example 3. By such a numerical case, we can also verify the relation similar to that in (4.9) and (4.10) and preview the layouts of  $\hat{\varphi}_{\max}(\theta)$  and  $\hat{\varphi}_{\min}(\theta)$ .

**Example 3.** *Consider a second-order system (4.1) with the following two subsystem*

---

<sup>2</sup>local maximum and minimum values



matrices  $A_1$  and  $A_2$  which are chosen as

$$A_1 = \begin{bmatrix} 0.3139 & -9.0215 \\ 4.5626 & -3.7008 \end{bmatrix} \quad A_2 = \begin{bmatrix} 1.8125 & -7.1869 \\ 3.4085 & -7.4462 \end{bmatrix}.$$

To see the relation between  $\varphi(A_i, \theta)$  and  $\varphi(A_i^{-1}, \theta)$ , ( $i = 1, 2$ ), and also the layouts of  $\hat{\varphi}_{\max}(\theta)$  and  $\hat{\varphi}_{\min}(\theta)$ , we now plot all of them in Figure 4.2. As it has been analyzed

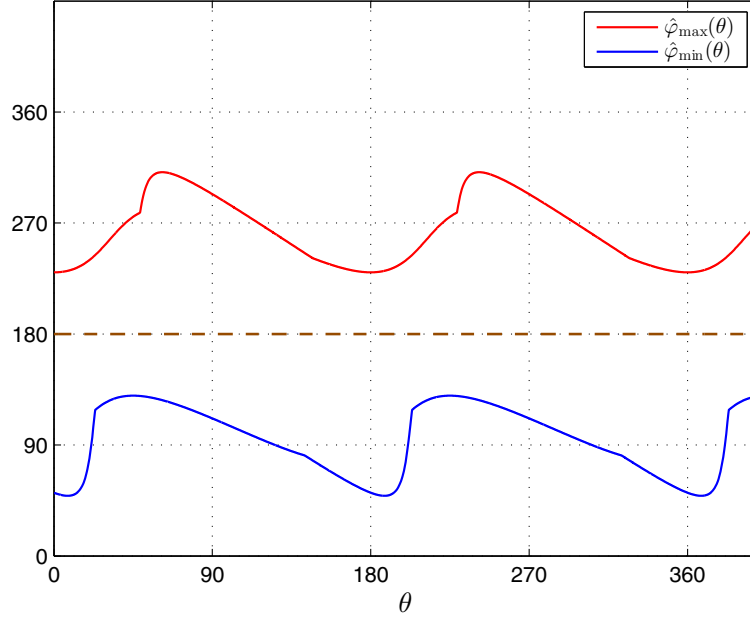


Figure 4.2: Layout of phase functions  $\hat{\varphi}_{\max}(\theta)$  and  $\hat{\varphi}_{\min}(\theta)$

in (4.6),  $\varphi(A_i, \theta)$  and  $\varphi(A_i^{-1}, \theta)$  are indeed the shifting translations of each other. However, as we can see, it is not so for  $\hat{\varphi}_{\max}(\theta)$  and  $\hat{\varphi}_{\min}(\theta)$ . But, same as (4.9) and (4.10), the maximum and minimum value relation will still hold if we replace  $\varphi(A, \theta)$  and  $\varphi(A^{-1}, \theta)$  with  $\hat{\varphi}_{\max}(\theta)$  and  $\hat{\varphi}_{\min}(\theta)$  respectively. Exactly we can find their values and relation as

$$\begin{aligned} \sup \{ \hat{\varphi}_{\max}(\theta) \} - \pi &= \pi - \inf \{ \hat{\varphi}_{\min}(\theta) \}, \text{ with value } 2.2018 \text{ rad}, \\ \inf \{ \hat{\varphi}_{\max}(\theta) \} - \pi &= \pi - \sup \{ \hat{\varphi}_{\min}(\theta) \}, \text{ with value } 0.7854 \text{ rad}, \end{aligned}$$

which are the extended version of (4.9) and (4.10). In addition, the property in (4.14) can be also verified as

$$\int_0^{2\pi} \cot \hat{\varphi}_{\max}(\theta) d\theta = - \int_0^{2\pi} \cot \hat{\varphi}_{\min}(\theta) d\theta = 59 \text{ rad}.$$

If we replace the phase functions  $\varphi_{\max}(\theta)$  and  $\varphi_{\min}(\theta)$  in Theorem 3 by  $\hat{\varphi}_{\max}(\theta)$  and  $\hat{\varphi}_{\min}(\theta)$  respectively, we will be able to avoid the integral conditions in (3.18) and (3.19) by the property in (4.14). As a result the original necessary and sufficient

condition will be reduced to a sufficient condition. The new result is summarized as Theorem 4 and its proof is provided right after the statement.

**Theorem 4.** *A sufficient condition for the asymptotic stability of the equilibrium of system (4.1) with arbitrary switching is that*

$$\hat{\varphi}_{\max}(\theta) - \hat{\varphi}_{\min}(\theta) < \pi, \quad \theta \in [0, 2\pi) \quad (4.15)$$

where  $\hat{\varphi}_{\max}(\theta)$  and  $\hat{\varphi}_{\min}(\theta)$  are defined in (4.12) and (4.13).

*Proof.* From (B.7) in the proof of Lemma 7 [in Appendix B], we know that

$$0 < \hat{\varphi}_{\min}(\theta) \leq \pi \leq \hat{\varphi}_{\max}(\theta) < 2\pi. \quad (4.16)$$

Firstly we consider the inequality case of (4.16),  $0 < \hat{\varphi}_{\min}(\theta) < \pi < \hat{\varphi}_{\max}(\theta) < 2\pi$ , where  $\hat{\varphi}_{\min}(\theta) \neq \pi \neq \hat{\varphi}_{\max}(\theta)$ . Starting from (4.15), one has

$$\hat{\varphi}_{\max}(\theta) - \frac{3\pi}{2} < \hat{\varphi}_{\min}(\theta) - \frac{\pi}{2}, \quad \theta \in [0, 2\pi). \quad (4.17)$$

The terms on both sides of inequality (4.17) fall within the interval  $(-\frac{\pi}{2}, \frac{\pi}{2})$ . Function  $\tan(\theta)$  is monotonically increasing in the concerned range  $(-\frac{\pi}{2}, \frac{\pi}{2})$ , thus inequality (4.17) can be extended as

$$\int_0^{2\pi} \tan(\hat{\varphi}_{\max}(\theta) - \frac{3\pi}{2}) d\theta < \int_0^{2\pi} \tan(\hat{\varphi}_{\min}(\theta) - \frac{\pi}{2}) d\theta.$$

Equivalently it means the validity of the following inequality,

$$\int_0^{2\pi} \cot \hat{\varphi}_{\max}(\theta) d\theta - \int_0^{2\pi} \cot \hat{\varphi}_{\min}(\theta) d\theta > 0.$$

Together with the property presented in (4.14), the above inequality ensures that

$$\int_0^{2\pi} \cot \hat{\varphi}_{\max}(\theta) d\theta > 0, \quad \int_0^{2\pi} \cot \hat{\varphi}_{\min}(\theta) d\theta < 0,$$

which are the strict inequality form of integral criteria shown in (3.18) and (3.19). It means that the system with subsystems matrices  $A_1, A_1^{-1}, A_2, A_2^{-1}, \dots, A_q$  and  $A_q^{-1}$  is asymptotically stable, thus the asymptotic stability of the equilibrium of system (4.1) is automatically ensured.

Secondly, we consider the case where the equality relation  $\hat{\varphi}_{\min}(\theta) = \pi$  or  $\hat{\varphi}_{\max}(\theta) = \pi$  holds in (4.16). Based on the relation  $\mathfrak{S}(A_i, 0) = \bar{\mathfrak{S}}(A_i^{-1}, 0)$  from Lemma 6, we can confirmed that “=” exists if and only if  $\hat{\varphi}_{\min}(\theta) = \pi = \hat{\varphi}_{\max}(\theta)$  at some certain points. In such case, there exists  $\theta^* \in [0, 2\pi)$  satisfying that  $\varphi(A_i, \theta^*) =$

$\varphi(A_i^{-1}, \theta^*) = \pi$  for all  $i = 1, 2, \dots, q$ . Based on the properties in Lemma 3, it can be also implied that all the matrices  $A_i$  ( $i = 1, 2, \dots, q$ ) share the common eigenvector  $\omega(\theta^*) = [\cos \theta^*, \sin \theta^*]^T$  with negative real eigenvalues, which means that the system state  $x$  of (4.1) will always converge to zero when  $\text{atan}(x) = \theta^*$ . Then the system equilibrium will also be asymptotically stable in this case. Proof of this theorem is thus completed.  $\square$

By using the property shown in Lemma 7, the stability condition in Theorem 3 has been simplified as that in Theorem 4. We can find that stability condition in Theorem 4 is simpler and it requires no integral criteria as those in (3.18) and (3.19). This is an advantage and makes this stability requirement easy to check. On the other hand, we need to note that, the stability condition provided in Theorem 3 is both necessary and sufficient. However, though being relatively simple, the condition in Theorem 4 is only sufficient but not necessary, which indicates the conservativeness of it. Then our next concern is how conservative the condition described by (4.15) is. Especially when it is compared with some existing LMI conditions, and whether it is still better than the CQLF existence requirement for every pair of subsystems. To make fair comparison from the theoretical point-of-view, we need to firstly transform the phase-based criterion in (4.15) into equivalent LMI criterion.

### 4.3.2 Transformation of the phase-based stability condition

We start this transformation with some further analysis of system matrices. The unit eigenvector of a matrix is an important medium to connect the matrix characteristics with the phase function obtained from such a matrix. Recalling the definition of phase function in (4.2), we may find the relation between the eigenvector of matrix  $A$  and the intersection point of  $\varphi(A, \theta)$  and  $\pi$ , which is summarized in Lemma 3. In addition, we can also find relations between eigenvectors of different multiplication combination of matrices  $A_1$  and  $A_2$ .

**Lemma 8.** *For the given matrices  $A_1$  and  $A_2$ , if  $\xi$  is an eigenvector of  $A_1 A_2^{-1}$  with eigenvalue  $\lambda$ , mathematically  $A_1 A_2^{-1} \xi = \lambda \xi$ , then the following results hold,*

1.  $(A_2^{-1} A_1)(A_2^{-1} \xi) = \lambda(A_2^{-1} \xi);$
2.  $(A_1^{-1} A_2)(A_2^{-1} \xi) = \lambda^{-1}(A_2^{-1} \xi);$
3.  $(A_2 A_1^{-1})\xi = \lambda^{-1}\xi.$

**Remark 6.** *By the results in Lemma 8, it can be implied that if  $A_1 A_2^{-1}$  has no negative eigenvalue, then other matrices combinations  $A_2^{-1} A_1$ ,  $A_1^{-1} A_2$ ,  $A_2 A_1^{-1}$  also have no negative eigenvalue, regardless of whether it is  $A_1$  or  $A_2$  that is expressed as an inverse matrix and regardless of the order of these two terms.*

To find the LMI version of Theorem 4, we need to break the analysis into several steps that will be supported by the equivalent algebraic statements. By Lemma 8 and discussion in Remark 6, inequality in (4.15) can be firstly interpreted as the eigenvalue criteria of products of subsystem matrices  $\{A_1, A_2, \dots, A_q\}$  and their inverses. Then the first step of our analysis goes like the result in Theorem 5.

**Theorem 5.** *A sufficient condition for the asymptotic stability of the equilibrium of system (4.1) with arbitrary switching is that*

$$A_i A_j \quad \text{and} \quad A_i A_j^{-1} \quad (4.18)$$

*have no negative real eigenvalue for all  $1 \leq i < j \leq q$ .*

*Proof.* We will firstly analyze the second term  $A_i A_j^{-1}$  in (4.18). Choose the state as  $x = \omega(\theta)$  and denote the phase angle of  $A_j x$  as  $\theta^* = \text{atan}(A_j x)$ . As it is mentioned in Assumption 2, the subsystem matrix  $A_j$  is Hurwitz, so this matrix is invertible. As a result, the phase angle value of state  $x$  can be obtained as  $\theta = \text{atan}(A_j^{-1} \omega(\theta^*))$ . With this relation, the difference between phase functions  $\varphi(A_i, \theta)$  and  $\varphi(A_j, \theta)$  can be calculated as

$$\varphi(A_i, \theta) - \varphi(A_j, \theta) \stackrel{2\pi}{=} \text{atan}(A_i A_j^{-1} \omega(\theta^*)) - \text{atan}(\omega(\theta^*)) = \varphi(A_i A_j^{-1}, \theta^*). \quad (4.19)$$

Considering the second item of Lemma 3, we know that the fact matrix combination  $A_i A_j^{-1}$  having no negative real eigenvalue indicates the following inequality

$$\varphi(A_i A_j^{-1}, \theta^*) \neq \pi, \quad 1 \leq i < j \leq q.$$

It means that  $\phi(A_i, \theta) - \phi(A_j, \theta) \neq \pi$ . As a result

$$-\pi < \varphi(A_i, \theta) - \varphi(A_j, \theta) < \pi, \quad i, j = 1, 2, \dots, q. \quad (4.20)$$

Similarly  $A_i A_j$  ( $1 \leq i < j \leq r$ ) having no negative real eigenvalue means that

$$-\pi < \varphi(A_i, \theta) - \varphi(A_j^{-1}, \theta) < \pi, \quad i, j = 1, 2, \dots, q. \quad (4.21)$$

What's more, as it is analyzed in Remark 6, we know that  $A_j^{-1} A_i^{-1} = (A_i A_j)^{-1}$  and  $A_j A_i^{-1} = (A_i A_j^{-1})^{-1}$ , and they have no negative real eigenvalue. Similarly  $A_i^{-1} A_j^{-1}$  and  $A_i^{-1} A_j$  have no negative eigenvalue. As a result, the following inequalities can be confirmed,

$$-\pi < \varphi(A_i^{-1}, x) - \varphi(A_j, x) < \pi, \quad i, j = 1, 2, \dots, q, \quad (4.22)$$

$$-\pi < \varphi(A_i^{-1}, x) - \varphi(A_j^{-1}, x) < \pi, \quad i, j = 1, 2, \dots, q. \quad (4.23)$$

Overall, the combination of (4.20)–(4.23) ensures that

$$\max_{i \in \mathcal{Q}} \{\varphi(A_i, x), \varphi(A_i^{-1}, x)\} - \min_{j \in \mathcal{Q}} \{\varphi(A_j, x), \varphi(A_j^{-1}, x)\} < \pi.$$

Equivalently we know that

$$\hat{\varphi}_{\max}(\theta) - \hat{\varphi}_{\min}(\theta) < \pi.$$

Considering the stability condition in Theorem 4, we know that the asymptotic stability of the equilibrium of system (4.1) with arbitrary switching is ensured. This lemma is thus proven.  $\square$

In the next step of the result transformation, we will discuss the relation between convex combination of matrices and the product combination of matrices. Such a result has been obtained in [54]. We now quote it as Lemma 9.

**Lemma 9.** [54] *A necessary and sufficient condition for  $A_1 A_2$  and  $A_1 A_2^{-1}$  to have no negative real eigenvalue is that the following convex combinations*

$$\alpha_1 A_1 + \alpha_2 A_2^{-1} \quad \text{and} \quad \alpha_1 A_1 + \alpha_2 A_2$$

*are non-singular for any  $0 \leq \alpha_1, \alpha_2 \leq 1$  and  $\alpha_1 + \alpha_2 = 1$ .*

With the proposed results in Lemmas 5 and 9, it will be easier for us to transform the phase function criteria in Theorem 4 to its equivalent LMI expression. In the following part, we will provide the equivalent LMI condition in Theorem 6 and discuss how the condition is obtained.

**Theorem 6.** *A sufficient condition for the stability of the equilibrium of system (4.1) with arbitrary switching signal is that, there exists a CQLF for every two-tuple of its subsystems. In other words, it can be also stated as, there exists a common positive definite matrix  $P \in \mathbb{R}^{2 \times 2}$  such that, for any indexes  $i, j$  satisfying  $1 \leq i < j \leq r$ , the following two inequalities are satisfied at the same time*

$$A_i^T P + P A_i < 0 \quad \text{and} \quad A_j^T P + P A_j < 0. \quad (4.24)$$

*Proof.* In the Theorem 3.1 of [11] it has been proven that a necessary and sufficient condition for convex combinations

$$\alpha_1 A_i + \alpha_2 A_j^{-1} \quad \text{and} \quad \alpha_1 A_i + \alpha_2 A_j$$

to be non-singular is that there exists a CQLF for  $A_i$  and  $A_j$ . Then according to Lemma 9, the existence of such a CQLF is also equivalent to that  $A_i A_j$  and

$A_i A_j^{-1}$  have no negative real eigenvalue. Further by Theorem 5, we know that the equilibrium of the given system (4.1) is stable under arbitrary switching if condition (4.24) is satisfied. Then proof of Theorem 6 is completed.  $\square$

The LMI stability condition obtained from [11] indicates that, to ensure the stability of the equilibrium of system (4.1), at least every three-tuple of its subsystem matrices share a CQLF. Based on the conclusion in Theorem 6, we can find that, by applying the phase function criterion in Theorem 4, the condition has been further relaxed as, every two-tuple of the subsystems share a CQLF. To see how effective the new condition in Theorem 6 is in reducing conservativeness, we will apply it to the following numerical example.

**Example 4.** Consider an example of second-order switched system with the following three subsystems

$$A_1 = \begin{bmatrix} -0.48 & -3.06 \\ 0.87 & -1.70 \end{bmatrix}, \quad A_2 = \begin{bmatrix} -2.27 & -2.37 \\ 1.56 & 0.09 \end{bmatrix},$$

and  $A_3 = R(b-a)\Lambda R(a)$  where  $\Lambda = \text{diag}\{-1, -3.5\}$ . To see the difference between stability conditions in [11] and Theorem 6, we now plot the feasible regions of  $(a, b)$  obtained by these two methods in the same figure. In the central part of Figure 4.3, we can clearly find that the feasible region obtained from [11] has been greatly extended by Theorem 6.

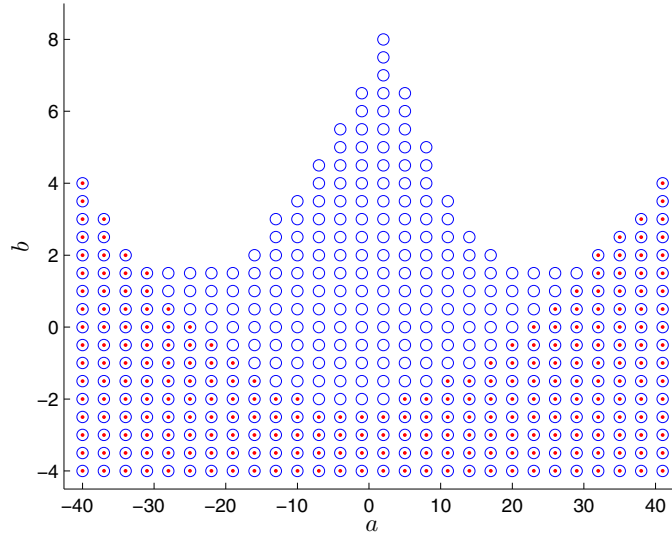


Figure 4.3: Feasible region of  $(a, b)$ : red dots for [11] (every three-tuple of subsystems share a CQLF), blue circles for Theorem 6 (every two-tuple of systems share a CQLF)

## 4.4 Special case: positive switched systems

Apart from the regular cases of a switched system, it is also possible to get some new results when the switched system is restricted to some special cases. If the off-diagonal entries of a matrix  $A$  are nonnegative, it can be called a Metzler matrix [94, 95]. An LTI system with such a Metzler matrix is known as positive linear system. In [98], it is shown that, for a second-order switched system whose subsystems are described by Hurwitz Metzler matrices, its equilibrium should be asymptotically stable if and only if every two-tuple of its subsystem matrices share a CQLF. Compared with the stability condition in Theorem 6, result in [98] shows the advantage that it is the necessary and sufficient condition. Then our next concern is whether we can get similar necessary and sufficient stability condition based on the result in Theorem 3, which can be expressed in the form of phase function.

Consider a second-order positive switched system

$$\dot{x}(t) = A_{\sigma(t)}x(t), \quad (4.25)$$

where  $A_{\sigma(t)}$  can switch among the given collection of Hurwitz Metzler matrices  $A_1, A_2, \dots, A_q$  in  $\mathbb{R}^{2 \times 2}$ . In this special case, the result in Theorem 3 will be greatly simplified while still retains the property as a necessary and sufficient condition. The new result can be summarized as Theorem 7.

**Theorem 7.** *Let  $A_1, A_2, \dots, A_q$  be Hurwitz and Metzler. A necessary and sufficient condition for the stability of the equilibrium of system (4.25) under arbitrary switching is that*

$$\varphi_{\max}(\theta) - \varphi_{\min}(\theta) < \pi, \quad \theta \in [0, 2\pi). \quad (4.26)$$

The main reason for the simplification to be possible is that, for switched system with Metzler subsystem matrices, the criterion  $\inf\{\varphi_{\max}(\theta)\} \leq \pi$  in (3.18) and criterion  $\sup\{\varphi_{\min}(\theta)\} \geq \pi$  in (3.19) can be automatically satisfied. The detailed analysis can be found in the following proof.

*Proof.* Denote the element on the  $j$ -th row and  $k$ -th column of  $A_i$  as  $a_{ijk}$ . Since  $A_i$  is Hurwitz, it holds that

$$\det(A_i) = a_{i11}a_{i22} - a_{i12}a_{i21} = \lambda_{i1}\lambda_{i2} > 0, \quad (4.27)$$

$$\text{tr}(A_i) = a_{i11} + a_{i22} = \lambda_{i1} + \lambda_{i2} < 0, \quad (4.28)$$

where  $\lambda_{i1}$  and  $\lambda_{i2}$  are the eigenvalues of matrix  $A_i$ . In addition,  $A_i$  is also a Metzler matrix, so  $a_{i12} \geq 0$ ,  $a_{i21} \geq 0$ , which means  $a_{i12}a_{i21} \geq 0$  and  $a_{i11}a_{i22} > 0$  can be ensured by (4.27). Also considering the inequality in (4.28), the following conclusion

can be confirmed,

$$a_{i11} < 0, \quad a_{i12} \geq 0, \quad a_{i21} \geq 0, \quad a_{i22} < 0. \quad (4.29)$$

By definition in (4.3) and applying the elements' positive or negative properties in (4.29), we can find

$$\frac{3\pi}{2} \leq \text{atan} \left( \frac{a_{i11}}{a_{i21}} \right) < 2\pi, \quad \frac{\pi}{2} < \text{atan} \left( \frac{a_{i12}}{a_{i22}} \right) \leq \pi,$$

which means that, for all subsystem matrices  $A_i$  ( $i = 1, 2, \dots, q$ ), their phase functions satisfy

$$\varphi(A_i, 0) = \text{atan} \left( \frac{a_{i11}}{a_{i21}} \right) > \pi, \quad \varphi(A_i, \frac{\pi}{2}) = \text{atan} \left( \frac{a_{i12}}{a_{i22}} \right) - \frac{\pi}{2} < \pi.$$

Obviously, for the maximum and minimum phase function values at  $\theta = 0$  and  $\theta = \frac{\pi}{2}$ , we can also get the following relation

$$\varphi_{\max}(\frac{\pi}{2}) < \pi < \varphi_{\min}(0),$$

which ensures that

$$\inf\{\varphi_{\max}(\theta)\} < \pi < \sup\{\varphi_{\min}(\theta)\}.$$

Based on the discussion presented in Theorem 3, it can be further confirmed that criteria in (3.18) and (3.19) are satisfied. So the equilibrium of system (4.25) is stable if criterion (4.26) can be ensured. The proof is then completed.  $\square$

Following the similar steps as the matrix algebraic analysis in Section 4.3, we can summarize all the equivalent results for the equilibrium of system (4.25) to be stable under arbitrary switching as the following corollary. Proof of the first three statements in it can be found in [98].

**Corollary 2.** *For the positive switched system in (4.25) the following statements are equivalent:*

1. *The equilibrium of system (4.25) is stable under arbitrary switching;*
2.  *$A_i A_j^{-1}$  has no negative real eigenvalue for all  $i, j = 1, 2, \dots, q$ ;*
3. *The convex combination  $\alpha_1 A_1 + \alpha_2 A_2$  is non-singular for all  $0 \leq \alpha_1, \alpha_2 \leq 1$ ,  $\alpha_1 + \alpha_2 = 1$ ;*
4.  *$\varphi_{\max}(\theta) - \varphi_{\min}(\theta) < \pi$  for all  $\theta \in [0, 2\pi)$ .*



## 4.5 Conclusions

Based on the analysis of some special properties of phase function we have extended the basic phase-based result to simpler stability criterion. Motivated by the concern of whether the CQLF existence condition for two-tuple of subsystems can ensure the stability of the whole system, we have transformed the phase-based result into equivalent algebraic criteria and also LMI condition. In such a way, connection has been found and it has been proven that the CQLF existence condition for every pair of subsystems is sufficient enough for the system stability. Improvement in regard with existing result has been verified in an illustrative example. Corresponding results on positive systems have also been provided.

# Chapter 5

## Membership dependent stability analysis of T-S fuzzy systems

*This chapter provides a new framework to inspect the conservativeness of membership-dependent stability conditions for T-S fuzzy systems. Under this framework, a graphic approach is proposed to reduce the variation of subsystems and obtain less conservative stability conditions.*

### 5.1 Introduction

In Chapter 3 our method to improve the system stability condition is based on the concept of phase function which is derived from the idea of an ultimate flexible line-integral Lyapunov function. In this chapter we change the focus of our analysis to the system itself. It means that we use the additional system information to improve the stability analysis results.

This system we considered in this chapter is a T-S fuzzy model. With this model, we can clearly see the how the system model will vary continuously among subsystems when the membership function changes. Here, the additional system information for us will be the membership function, and the corresponding method will be referred as membership-dependent. When it comes to the comparison of different membership-dependent methods, many existing researches, usually make analysis in the numerical approach [3, 86, 87]. Such an approach is simple and direct, and one can compare different methods based on the obtained feasible regions of preset system parameters. But the comparison results will be highly dependent on the specific example. And sometimes it is difficult to explain the inner relation of different methods.

To avoid those limitations and take one step further, in this chapter we will propose a new framework to inspect and compare the effectiveness of different membership-dependent methods. In addition, we will also provide an alternative approach to combine the membership information of T-S fuzzy systems into stability analysis.

The rest of this chapter is organized as follows. In Section 5.2, we will introduce the new framework of conservativeness analysis. In Section 5.3, the main results about extrema-based stability conditions are introduced. Comparisons of different methods in the new framework are provided in Section 5.4. Following the comparison, in Section 5.5, further discussion is provided to analyze the case of partly overlapping of polyhedrons in the membership space. In the final section, a conclusion is drawn.

## 5.2 Framework of conservativeness analysis

Following the preliminary result in Section 2.3, we consider the T-S fuzzy system

$$\dot{x} = \sum_{i=1}^p h_i(x) A_i x, \quad (5.1)$$

where  $x \in \mathbb{R}^n$  is the system state,  $p \in \mathbb{R}$  is the number of fuzzy rules,  $h_i(x) : \mathbb{R}^n \rightarrow \mathbb{R}$  is the membership function in the  $i$ -th rule,  $A_i \in \mathbb{R}^{n \times n}$  is the system matrix in the  $i$ -th rule. Our research focus in this part is the combination of membership information in the stability analysis, rather than the design of flexible Lyapunov function. To make it easier to follow, we choose  $V(x)$  as the commonly used quadratic Lyapunov function

$$V(x) = x^T P x,$$

where  $P \in \mathbb{R}^{n \times n}$  is a symmetric matrix satisfying  $P > 0$ . The time derivative of  $V(x)$  should be  $\dot{V}(x) = \sum_{i=1}^p h_i(x) x^T Q_i x$ , then a sufficient stability condition can be chosen as

$$\sum_{i=1}^p h_i(x) Q_i < 0 \quad (5.2)$$

for any  $x$  in the system state domain, where  $Q_i$  is defined in Section 2.3.1.2 as  $Q_i = A^T P_i + P_i A$ , ( $i = 1, 2, \dots, p$ ).

### 5.2.1 Unified space for membership functions

Generally, the layouts of membership functions  $h_1(x), h_2(x), \dots, h_p(x)$  are described in separate figures. In each separate figure the relation of  $h_i(x)$  ( $i = 1, 2, \dots, p$ ) with premise variable  $x$  is analyzed. A different idea is considering all functions  $h_1(x), h_2(x), \dots, h_p(x)$  as the elements of a unified vector [101],

$$h(x) \triangleq (h_1(x), h_2(x), \dots, h_p(x)).$$

The unified membership vector  $h(x)$  means the value distribution of

$$A(x) \triangleq \sum_{i=1}^p h_i(x) A_i$$

among matrices  $A_1, A_2, \dots, A_p$ . By definition the given membership functions satisfy the following conditions

$$\begin{cases} h_1(x) \geq 0, & h_2(x) \geq 0, & \dots, & h_p(x) \geq 0 \\ h_1(x) + h_2(x) + \dots + h_p(x) = 1. \end{cases} \quad (5.3)$$

Obviously, the trajectory of membership function  $h(x)$  can be described in a  $p$ -dimensional Euclidean space with Cartesian coordinates  $(h_1, h_2, \dots, h_p)$ . Choosing  $p = 2$  as an example, then by condition (5.3), we know that  $h(x)$  is distributed on the line

$$h_1(x) + h_2(x) = 1.$$

In addition, with condition (5.3), the trajectory of  $h(x)$  will be constrained in the first quadrant of the coordinate space. For the case of  $p = 3$ , the trajectory of  $h(x)$  is constrained in the regular triangle formed by vertices  $(1, 0, 0)$ ,  $(0, 1, 0)$ ,  $(0, 0, 1)$ , see Figure 5.1. Generally speaking, the number of degrees of freedom of  $h(x)$  should be smaller than  $p$ , which results from the condition in (5.3). The trajectory of  $h(x)$  plotted in Figure 5.1 has one degree of freedom. A simple example of  $h(x)$  with two degrees of freedom is  $h_1(x) = x_1$ ,  $h_2(x) = x_2$  and  $h_3(x) = 1 - h_1(x) - h_2(x)$ , with constraints  $0.14 \leq x_1 \leq 0.48$  and  $0.11 \leq x_2 \leq 0.47$ . This example is plotted in Figure 5.2.

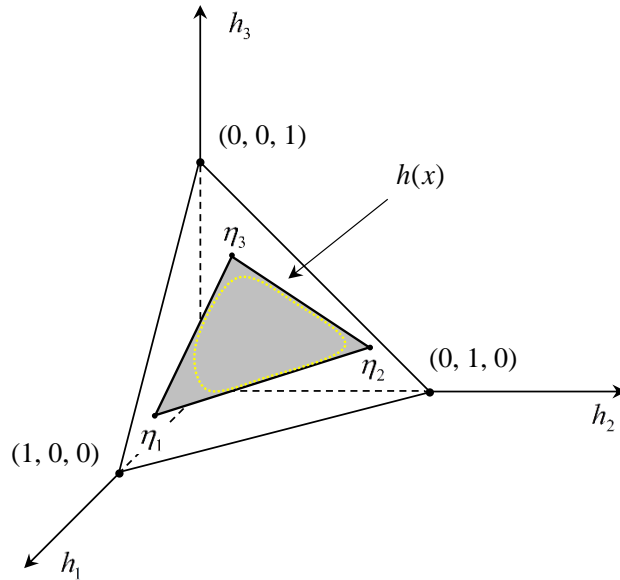


Figure 5.1:  $h(x)$  with one degree of freedom. The dotted line is the trajectory of  $h(x)$ .  $\eta_1, \eta_2, \eta_3$  are the vertices of a convex polyhedron enclosing  $h(x)$

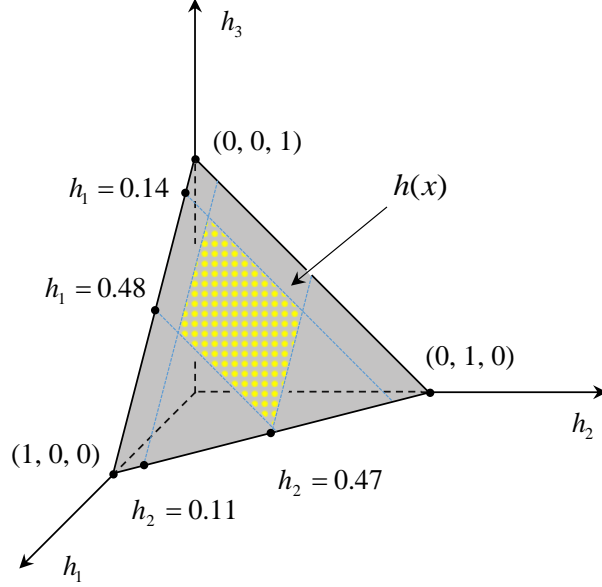


Figure 5.2:  $h(x)$  with two degrees of freedom. The dotted area is the layout  $h(x)$ .  $h(x)$  is constrained in the area  $0.14 \leq h_1(x) \leq 0.48$  and  $0.11 \leq h_2(x) \leq 0.47$  with  $h_3(x) = 1 - h_1(x) - h_2(x)$

Using the membership vector  $(h_1, h_2, \dots, h_p)$ , it will be easy to describe the exact value of  $A(x)$ . For example, the point  $(h_1^*, h_2^*, \dots, h_p^*)$  in the  $p$ -dimensional space represents the matrix  $\sum_{i=1}^p h_i^* A_i$ . It means that each point in the  $p$ -dimensional space is directly related with a certain system matrix. Specially, considering the case of  $p = 2$ , the point associated with the subsystem matrix  $A_1$  should be  $(1, 0)$  and the one associated with  $A_2$  should be  $(0, 1)$ .

**Remark 7.** *The idea of describing the membership functions  $h_i(x)$  ( $i = 1, 2, \dots, p$ ) as the elements of a joint vector  $h(x)$  is not new. If we also describe the parameters of LMIs stability condition as some points in this membership vector space, the convex polyhedron constructed from those points will indicate the conservativeness of the LMIs stability condition. So here we express this membership space as a framework of conservativeness analysis.*

### 5.2.2 Membership-dependent conditions as points in the membership space

To analyze the membership-dependent stability conditions, let us start with the following basic stability criterion for T-S fuzzy systems.

**Lemma 10.** *[102] If there exists a matrix  $P > 0$ , such that all the following inequalities hold*

$$Q_i < 0, \quad \forall i = 1, 2, \dots, p \quad (5.4)$$

where  $Q_i = A^T P_i + P_i A$ , then the equilibrium of system (5.1) is asymptotically stable.

We denote the standard basis of a  $p$ -dimensional Euclidean space as  $e_1, e_2, \dots, e_p$ . The result in Lemma 10 means that, if condition (5.4) is satisfied, the matrix represented by any point in the polyhedron formed by vertices  $e_i$ , ( $i = 1, 2, \dots, p$ ) should be stable<sup>1</sup>. Such a polyhedron can be viewed as the variation of subsystems. Matrix  $\sum_{i=1}^p h_i(x) A_i$  should be stable since  $h(x)$  is constrained in that polyhedron. Intuitively we want to know whether the conservativeness can be reduced by shrinking the area of polyhedron represented by  $e_1, e_2, \dots, e_p$ , for example, in 3-dimensional case, shrinking the triangle represented by  $(1, 0, 0)$ ,  $(0, 1, 0)$ ,  $(0, 0, 1)$  to the polygon represented by  $\eta_1, \eta_2, \eta_3$  in Figure 5.1.

To confirm that, we start from the simple case where  $p = 2$  and  $n = 1$ . Both  $A_1$  and  $A_2$  in this case should be numbers. From Figure 5.3, it is clear that the shrinking of line segment formed by points  $\eta_1 \triangleq (\eta_{11}, \eta_{12})$  and  $\eta_2 \triangleq (\eta_{21}, \eta_{22})$  means the enlargement of feasible area of  $(A_1, A_2)$ . For the general case, similar result can be ensured by the following lemma.

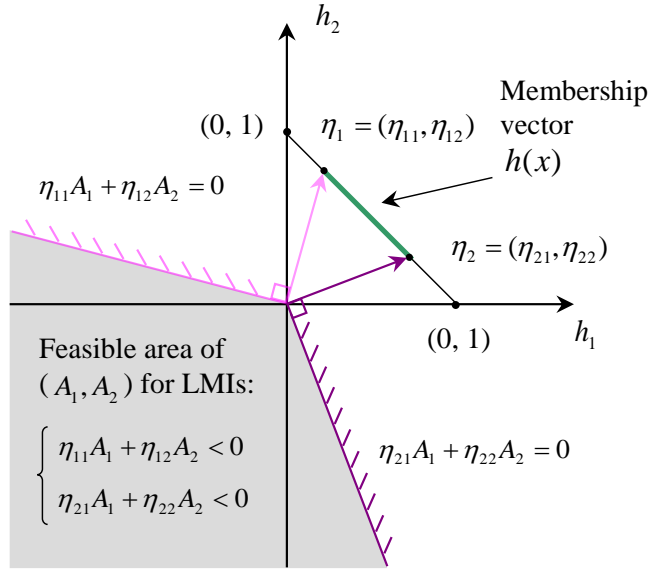


Figure 5.3: Feasible values of  $(A_1, A_2)$  in the case of  $p = 2$  and  $n = 1$ ,  $(A_1, A_2 \in \mathbb{R}^{1 \times 1})$ . Points  $\eta_1, \eta_2$  are the bounds of  $h(x)$

**Lemma 11.** [103] *If there exists a matrix  $P > 0$ , such that the following inequalities hold*

$$\sum_{j=1}^p \eta_{ij} (A_j^T P + P A_j) < 0, \quad \forall i = 1, 2, \dots, p$$

<sup>1</sup>The stability in this case is considered with respect to the equilibrium of the considered system matrix.

and all the values of point  $h(x) = (h_1(x), h_2(x), \dots, h_p(x))$  are contained in the convex polyhedron formed by points  $\eta_i = (\eta_{i1}, \eta_{i2}, \dots, \eta_{ip})$ , ( $0 \leq \eta_{ij} \leq 1$ , and  $\sum_{j=1}^p \eta_{ij} = 1$ ),  $i = 1, 2, \dots, p$ . Then the equilibrium of system (5.1) is asymptotically stable.

Now the idea is clear. The conservativeness of membership-dependent stability conditions can be analyzed by their corresponding convex polyhedrons in the coordinate of membership functions that describe the subsystem variation. We name the vertices of those polyhedrons as *checking points*, the coordinate components of which can be used to construct the LMIs together with the subsystem matrices. In this membership vector framework, the main task of conservativeness analysis is to find the equivalent checking points of the obtained LMIs, and compare the convex polyhedrons described by those checking points. If a smaller polyhedron is contained in a bigger polyhedron, then condition related with the smaller one should be less conservative. Besides, there might be the case that two polyhedrons share some overlapping area but are not completely contained in each other. In this case, it would be difficult to conclude which one is more conservative. Further analysis for this case will be discussed in Section 5.5.

In other words, the tighter bounds will lead to more relaxed stability analysis results. In the following sections, we will discuss how to find tighter bounds. Specially in the next section, we will propose an effective approach to construct the membership-dependent polyhedron simply based on the extrema of membership functions. This approach will be also extended to interval type-2 T-S fuzzy system. Later in Section 5.4, this alternative approach will be compared with the methods in Sections 2.3.1 and 2.3.2.

### 5.2.3 The extrema-based convex polyhedron construction method

Define the minimum and maximum values of  $h_i(x)$  as

$$h_{i \min} \triangleq \min_x \{h_i(x)\}, \quad h_{i \max} \triangleq \max_x \{h_i(x)\}$$

for all  $i = 1, 2, \dots, p$ .

In the following part, these extrema values will be used to construct a polyhedron that encloses the complete trajectory of membership function vector  $h(x)$ . Vertices of such a polyhedron can then be applied into stability analysis as checking points. The calculation algorithm of these vertices can be divided into two parts. In the first part, we need to redefine the subsystems based on the vertices obtained by the minimum value  $h_{i \min}$ , see Figure 5.4, where the vertex  $\eta_1 = (1 - h_{2 \min} - h_{3 \min}, h_{2 \min}, h_{3 \min})$  is the intersection point of surfaces  $h_2(x) = h_{2 \min}$ ,  $h_3(x) = h_{3 \min}$  and  $h_1(x) + h_2(x) + h_3(x) = 1$ . Vertices  $\eta_2$  and  $\eta_3$  are obtained in sim-

ilar ways. Here *redefine* means that vertices  $\eta_1, \eta_2, \eta_3$  are used as the replacement of vertices  $(1, 0, 0)$ ,  $(0, 1, 0)$  and  $(0, 0, 1)$ .

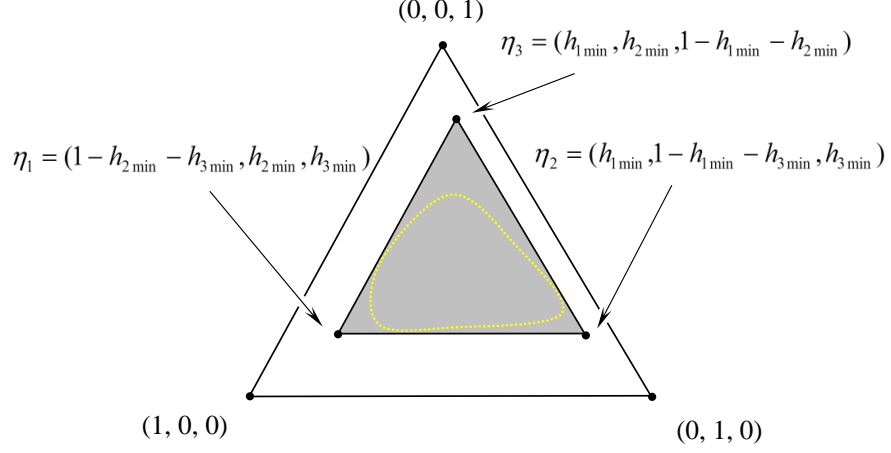


Figure 5.4: Convex polyhedron obtained by the minimum values of  $h_i(x)$ , with the dotted line being the trajectory of  $h(x)$

Then in the second part, we apply the maximum value  $h_{i\max}$  to further shrink the obtained polyhedron, see Figure 5.5, where the vertex  $\lambda_{11} = (h_{1\max}, 1 - h_{1\max} - h_{3\min}, h_{3\min})$  is the intersection point of surface  $h_1(x) = h_{1\max}$  and the edge between  $\eta_1$  and  $\eta_2$ . Vertex  $\lambda_{12}$  is the intersection point of surface  $h_1(x) = h_{1\max}$  and the edge between  $\eta_1$  and  $\eta_3$ . Vertices  $\lambda_{21}$ ,  $\lambda_{22}$ ,  $\lambda_{31}$  and  $\lambda_{32}$  can be obtained in similar ways. But there might be a special case that two of the six new vertices  $\lambda_{ij}$  ( $i = 1, 2, 3$ ,  $j = 1, 2$ ) become one. This special case will be discussed in the Step 4.2 of Algorithm 1.

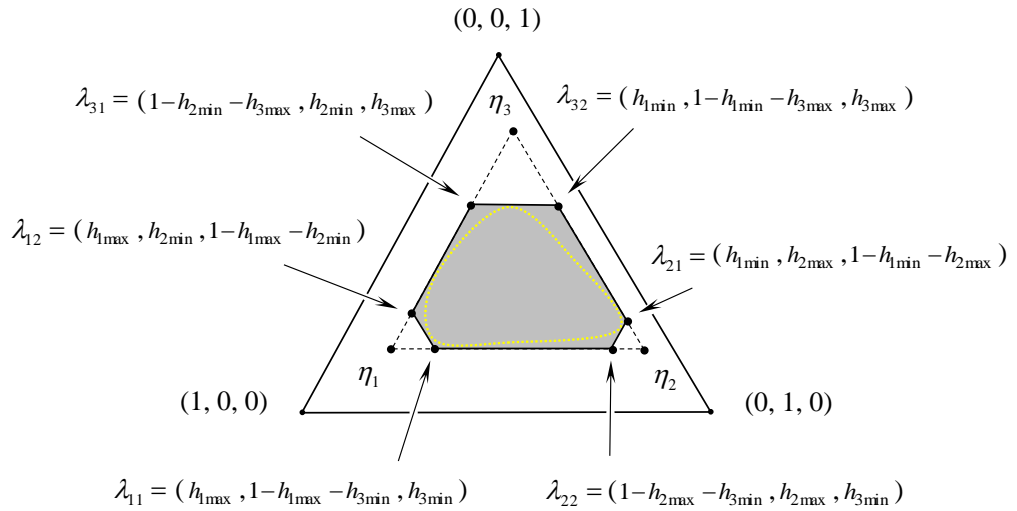


Figure 5.5: Convex polyhedron obtained by the extrema of  $h_i(x)$ , with the dotted line being the trajectory of  $h(x)$



The new subsystems related with the new vertices in Figure 5.4 should be

$$\bar{A}_q \triangleq \sum_{i=1}^p \eta_{qi} A_i = (1 - \sum_{i=1}^p h_{i \min}) A_q + \sum_{j=1}^p h_{j \min} A_j \quad (5.5)$$

for all  $q = 1, 2, \dots, p$ . Define the new membership functions as  $\bar{h}_i(x)$  ( $i = 1, 2, \dots, p$ ) and define the joint vector of these new functions as

$$\bar{h}(x) \triangleq (\bar{h}_1(x), \bar{h}_2(x), \dots, \bar{h}_p(x)).$$

From the definition in (5.5) and equation  $\sum_{i=1}^p \bar{h}_i(x) \bar{A}_i = \sum_{j=1}^p h_j(x) A_j$ , we can get the relation of  $\bar{h}(x)$  and  $h(x)$

$$(\delta I + \Gamma) \bar{h}^T(x) = h^T(x) \quad (5.6)$$

where  $\delta \triangleq 1 - \sum_{i=1}^p h_{i \min}$  and

$$\Gamma \triangleq \begin{bmatrix} h_{1 \min} & h_{1 \min} & h_{1 \min} & \cdots & h_{1 \min} \\ h_{2 \min} & h_{2 \min} & h_{2 \min} & \cdots & h_{2 \min} \\ h_{3 \min} & h_{3 \min} & h_{3 \min} & \cdots & h_{3 \min} \\ \vdots & \vdots & \vdots & \ddots & \vdots \\ h_{p \min} & h_{p \min} & h_{p \min} & \cdots & h_{p \min} \end{bmatrix}.$$

Note that for matrix  $\Gamma$ , it has the property  $\Gamma\Gamma = (1 - \delta)\Gamma$ , which means

$$(\delta I + \Gamma)(I - \Gamma) = \delta I + \Gamma - \delta\Gamma - (1 - \delta)\Gamma = \delta I.$$

In addition,  $\delta$  is a value satisfying  $0 < \delta \leq 1$ . Thus by derivation we can get the following equivalent expression of (5.6),

$$\bar{h}^T(x) = \frac{1}{\delta} (I - \Gamma) h^T(x). \quad (5.7)$$

From the relation in (5.7), the maximum value of  $\bar{h}_i(x)$  ( $i = 1, 2, \dots, p$ ) can be obtained as

$$\begin{aligned} \bar{h}_{i \max} &= \frac{1}{\delta} \max_x \left\{ h_i(x) - h_{i \min} \sum_{j=1}^p h_j(x) \right\} \\ &= \frac{1}{\delta} \max_x \{ h_i(x) - h_{i \min} \} \\ &= \frac{1}{\delta} (h_{i \max} - h_{i \min}). \end{aligned} \quad (5.8)$$

By the expression in (5.7), it can be found that the minimum value of  $\bar{h}_i(x)$  should be 0. Before the introduction of vertices calculation algorithm, we need to define two

new module functions that will make it easier to refer to the correct index. Assume that  $a$  and  $b$  are positive integers. Then define the new module functions  $[a]_b$  and  $(a)_b$  as

$$[a]_b \triangleq a \bmod b, \quad (a)_b \triangleq [a - 1]_b + 1.$$

It should be noted that the ranges of  $[a]_b$  and  $(a)_b$  are different, which are

$$0 \leq [a]_b \leq b - 1 \quad \text{and} \quad 1 \leq (a)_b \leq b.$$

With the above definitions, the vertices calculation method can be summarized as Algorithm 1 in the Appendix C. The following example will be a simple application of Algorithm 1.

**Example 5.** *To further explain Algorithm 1, we will go through all the steps based on a simple T-S fuzzy system with 3 rules. Assume that, in the first step, we get*

$$\begin{aligned} h_{1\min} &= 0.1, & h_{2\min} &= 0.12, & h_{3\min} &= 0.15 \\ h_{1\max} &= 0.5, & h_{2\max} &= 0.4, & h_{3\max} &= 0.5. \end{aligned}$$

*Directly we have  $\delta = 0.37$  (defined after Equation (5.6)). From (5.8), the maximum values of  $\bar{h}_i(x)$  ( $i = 1, 2, 3$ ) can be obtained as*

$$\bar{h}_{1\max} = 0.635, \quad \bar{h}_{2\max} = 0.444, \quad \bar{h}_{3\max} = 0.555.$$

*Following Steps 2 and 3, we summarize the relation of different variables in the following table, where variables in each line have the same value. To make it easier to be identified, the initial index 0 of each variable is marked in bold font.*

Table 5.1: Relation of the intermediate variables in Algorithm 1

	$\alpha_{1i}$	$\alpha_{2i}$	$\alpha_{3i}$	$\beta_{11i}$	$\beta_{12i}$	$\beta_{21i}$	$\beta_{22i}$	$\beta_{31i}$	$\beta_{32i}$
$\bar{h}_{1\max}$	$\alpha_{1\mathbf{0}}$	$\alpha_{22}$	$\alpha_{31}$	$\beta_{11\mathbf{0}}$	$\beta_{12\mathbf{0}}$	$\beta_{212}$	$\beta_{221}$	$\beta_{311}$	$\beta_{322}$
$\bar{h}_{2\max}$	$\alpha_{11}$	$\alpha_{2\mathbf{0}}$	$\alpha_{32}$	$\beta_{111}$	$\beta_{122}$	$\beta_{21\mathbf{0}}$	$\beta_{22\mathbf{0}}$	$\beta_{312}$	$\beta_{321}$
$\bar{h}_{3\max}$	$\alpha_{12}$	$\alpha_{21}$	$\alpha_{3\mathbf{0}}$	$\beta_{112}$	$\beta_{121}$	$\beta_{211}$	$\beta_{222}$	$\beta_{31\mathbf{0}}$	$\beta_{32\mathbf{0}}$

*It is obvious that  $\bar{h}_{1\max} + \bar{h}_{2\max} > 1$ ,  $\bar{h}_{2\max} + \bar{h}_{3\max} < 1$  and  $\bar{h}_{3\max} + \bar{h}_{1\max} > 1$ . According to Step 4, we need to make the following modification*

$$\begin{aligned} \beta_{111} &= 1 - \beta_{11\mathbf{0}} = 0.365, & \beta_{112} &= 0; & \beta_{121} &= 1 - \beta_{12\mathbf{0}} = 0.365, & \beta_{122} &= 0 \\ \beta_{212} &= 1 - \beta_{21\mathbf{0}} - \beta_{211} = 0.001; & & & \beta_{221} &= 1 - \beta_{22\mathbf{0}} = 0.556, & \beta_{222} &= 0 \\ \beta_{311} &= 1 - \beta_{31\mathbf{0}} = 0.445, & \beta_{312} &= 0; & \beta_{322} &= 1 - \beta_{32\mathbf{0}} - \beta_{321} = 0.001 \end{aligned}$$

*and the rest of  $\beta_{qmk}$  ( $q = 1, 2, 3$ ,  $m = 1, 2$ ,  $k = 0, 1, 2$ ) are unchanged. A flow*

chart of Steps 1–4 in Algorithm 1 can be described as Figure 5.6. In Steps 5–6, the subscripts of parameter  $\beta_{qmk}$  will be rearranged to get the coordinate parameters of checking points. We give it the new names  $\gamma_{qmk}$  and  $\tilde{\lambda}_{qmk}$  in each step to indicate the difference. These two steps can be viewed as the reverse process of Step 3.

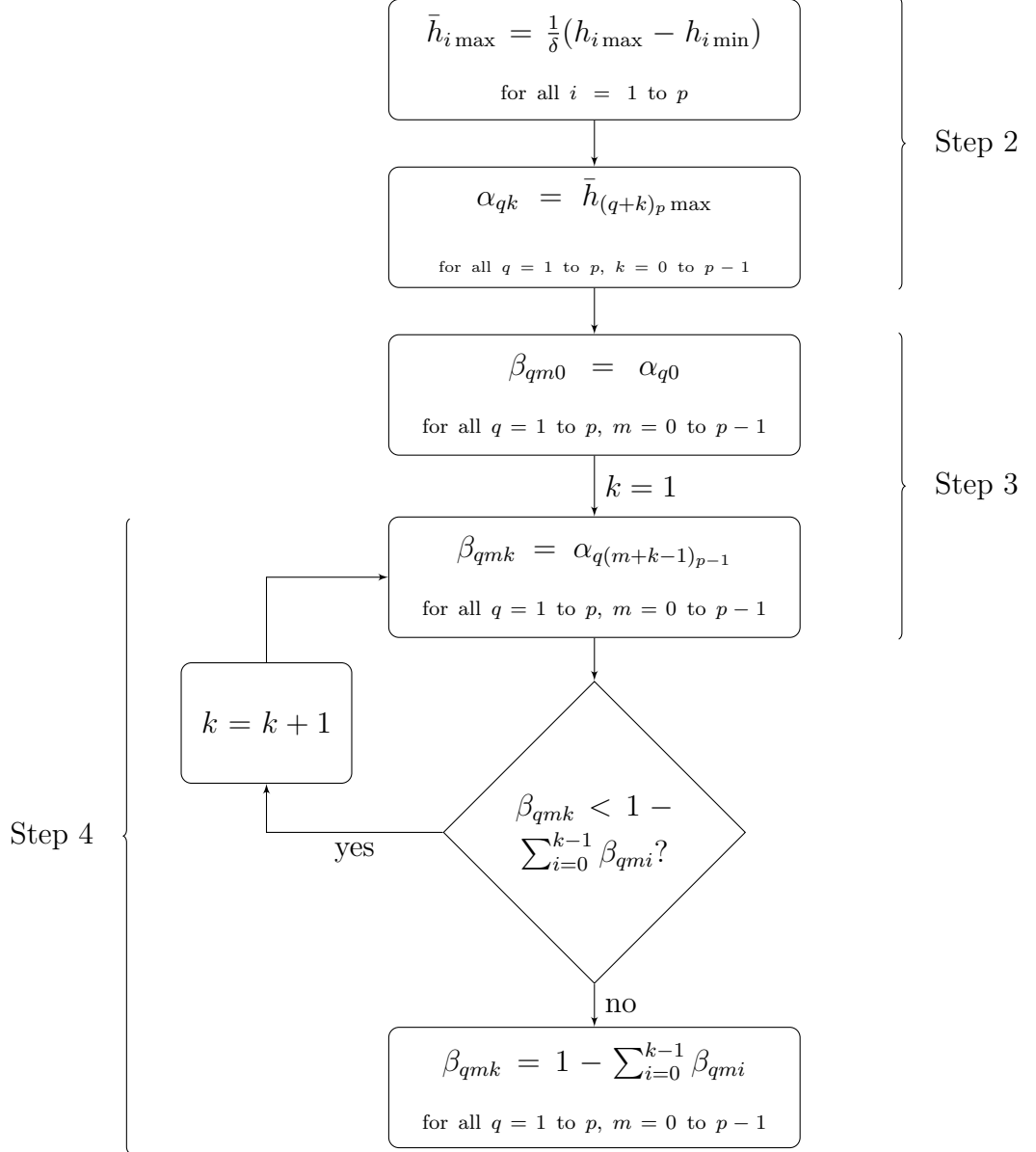


Figure 5.6: Flow chart of Steps 2–4 in Algorithm 1, explaining the calculation of  $\alpha_{qk}$  and  $\beta_{qmk}$

Denote  $\tilde{\lambda}_{qm} \triangleq (\tilde{\lambda}_{qm1}, \tilde{\lambda}_{qm2}, \tilde{\lambda}_{qm3})$  for  $q = 1, 2, 3$ ,  $m = 1, 2$ . With Steps 5 and 6, locations of the 6 checking points in the resized coordinate should be

$$\begin{aligned} \tilde{\lambda}_{11} &= (\beta_{110}, \beta_{111}, \beta_{112}); & \tilde{\lambda}_{12} &= (\beta_{120}, \beta_{121}, \beta_{122}) \\ \tilde{\lambda}_{21} &= (\beta_{212}, \beta_{210}, \beta_{211}); & \tilde{\lambda}_{22} &= (\beta_{221}, \beta_{220}, \beta_{222}) \end{aligned}$$

$$\tilde{\lambda}_{31} = (\beta_{311}, \beta_{312}, \beta_{310}); \quad \tilde{\lambda}_{32} = (\beta_{322}, \beta_{321}, \beta_{320}).$$

By expression (C.3) in Step 7 which can be viewed as the inverse process of Step 2, the 6 checking points in the original coordinate should be

$$\begin{aligned} \lambda_{11} &= (0.500, 0.350, 0.150); & \lambda_{12} &= (0.500, 0.120, 0.380) \\ \lambda_{21} &= (0.101, 0.400, 0.500); & \lambda_{22} &= (0.450, 0.400, 0.150) \\ \lambda_{31} &= (0.380, 0.120, 0.500); & \lambda_{32} &= (0.101, 0.400, 0.500). \end{aligned}$$

In the above calculation  $\bar{h}_{2\max} + \bar{h}_{3\max} < 1$  means that two checking points in Figure 5.5 come together. Thus we have  $\lambda_{21} = \lambda_{32}$  in the above results.

#### 5.2.4 Extension to the case of interval type-2 T-S fuzzy systems

For interval type-2 T-S fuzzy systems [104–108], the possible position of  $h_i(x)$  is restricted between the upper- and lower-membership functions  $h_i^L(x)$  and  $h_i^U(x)$ , that is

$$0 \leq h_i^L(x) \leq h_i(x) \leq h_i^U(x) \leq 1.$$

Then by integration from  $i = 1$  to  $i = p$ , we know that

$$0 \leq \sum_{i=1}^p h_i^L(x) \leq 1 \leq \sum_{i=1}^p h_i^U(x) \leq p.$$

It means that point  $(h_1^L(x), h_2^L(x), \dots, h_p^L(x))$  is located below the flat surface

$$h_1(x) + h_2(x) + \dots + h_p(x) = 1 \tag{5.9}$$

and point  $(h_1^U(x), h_2^U(x), \dots, h_p^U(x))$  is located above the flat surface in (5.9). As it is depicted in Figure 5.7, for any state  $x = x^*$ , the possible value of  $h(x^*)$  is restricted in the hypercube formed by vertices

$$(h_1^L(x^*), h_2^L(x^*), \dots, h_p^L(x^*)) \quad \text{and} \quad (h_1^U(x^*), h_2^U(x^*), \dots, h_p^U(x^*)).$$

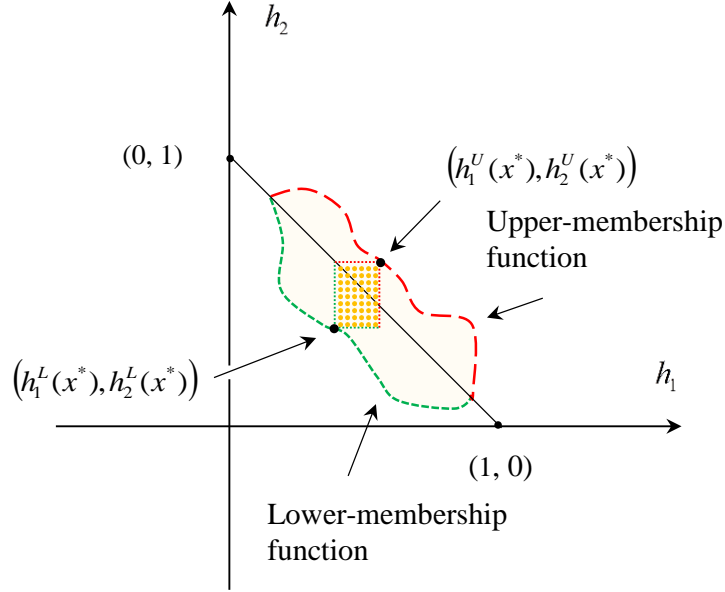


Figure 5.7: Possible distribution of an interval type-2 membership function with one degree of freedom, yellow dotted area is the hypercube formed by  $(h_1^L(x^*), h_2^L(x^*))$  and  $(h_1^U(x^*), h_2^U(x^*))$ .

It is obvious that, for any positive scalar  $\gamma$ , the LMI condition constructed by checking point  $(\gamma h_1, \gamma h_2, \dots, \gamma h_p)$  should be same as that by  $(h_1, h_2, \dots, h_p)$ . Thus by projecting all the possible values of  $h(x^*)$  onto surface  $\sum_{i=1}^p h_i(x) = 1$ , similar algorithm for interval type-2 T-S fuzzy system can be also obtained. For a specific point  $x^*$ , the projection of all possible  $h(x^*)$  should be enclosed by the projection of hypercube formed by vertices

$$(h_1^L(x^*), h_2^L(x^*), \dots, h_p^L(x^*)) \quad \text{and} \quad (h_1^U(x^*), h_2^U(x^*), \dots, h_p^U(x^*)).$$

Denote  $\hat{h}_{i,0}(x) \triangleq h_i^L(x)$  and  $\hat{h}_{i,1}(x) \triangleq h_i^U(x)$  for  $i = 1, 2, \dots, p$ . The vertices of such a hypercube will be

$$(\hat{h}_{1,\tau_1}(x^*), \hat{h}_{2,\tau_2}(x^*), \dots, \hat{h}_{i,\tau_i}(x^*), \dots, \hat{h}_{p,\tau_p}(x^*))$$

where  $\tau_1, \tau_2, \dots, \tau_i, \dots, \tau_p = 0, 1$ . Their projection on flat surface  $\sum_{i=1}^p h_i(x) = 1$  should be

$$(h_{1,j}(x^*), h_{2,j}(x^*), \dots, h_{i,j}(x^*), \dots, h_{p,j}(x^*))$$

where  $j = 1, 2, 3, \dots, 2^p$ , and for  $j = \sum_{i=1}^p \tau_i \times 2^{i-1} + 1$  we have

$$h_{i,j}(x) \triangleq \frac{\hat{h}_{i,\tau_i}(x)}{\hat{h}_{1,\tau_1}(x) + \dots + \hat{h}_{i,\tau_i}(x) + \dots + \hat{h}_{p,\tau_p}(x)}.$$

Based on the projected membership function, the vertices calculation method can be summarized as Algorithm 2 in the appendix.

### 5.3 Extrema-based stability conditions

Based on the obtained vertices, now the stability condition can be presented as:

**Theorem 8.** *If there exists a matrix  $P > 0$ , such that the following inequality holds*

$$\sum_{k=1}^p \lambda_{qm_k} (A_k^T P + P A_k) < 0 \quad (5.10)$$

*for all  $q = 1, 2, \dots, p$  and  $m = 1, 2, \dots, p - 1$ , where  $\lambda_{qm_k}$  is obtained from the Algorithm 1, and  $(\lambda_{qm_1}, \lambda_{qm_2}, \dots, \lambda_{qm_p})$  is the obtained checking point. Then the equilibrium of system (5.1) is asymptotically stable.*

**Remark 8.** *By the proposed method, we can directly construct the final stability LMI conditions by the parameters  $\lambda_{qm_k}$  which are obtained from the membership functions. As a result, conservativeness can be reduced by considering the membership information and, at the same time, we can keep the final conditions concise.*

In this case, only the extrema information in membership functions is applied to the stability analysis. Of course, we can find a smaller convex polyhedron [101] (smaller means the small convex polyhedron is contained in the current one) to obtain even less conservative vertices. But this would involve some complex linear-programming-related methods [109]. Those methods are usually not very effective for systems with  $p \geq 3$ , if so, the computational burden will increase sharply with respect to  $p$ .

**Remark 9.** *If a small convex polyhedron is completely enclosed in a bigger one, then we can reach the conclusion that, the stability condition related with the small polyhedron is less conservative. For the case of partially overlapping, we cannot say which method is better. But improved result can be obtained by considering the overlapping area as a new polyhedron. Further discussion on this topic can be found in Section 5.5.*

An alternative approach is to divide the original domain of membership function into  $d$  ( $d \in \mathbb{N}$ ) sub-regions. For each sub-region  $R_\tau(x)$  ( $\tau = 1, 2, \dots, d$ ), we use the above algorithms to find the local convex polyhedrons. Since the local membership function is part of the original one, all the local polyhedrons formed by the local extrema values should be included in the global polyhedron, which means the reduction of subsystem variation and conservativeness. In this way, the computational burden for complex polyhedron will be avoided, and we can simply choose a larger  $d$  to achieve less conservative analysis. We now summarize the extended stability analysis method in the following theorem.

**Theorem 9.** *If there exists a matrix  $P > 0$ , such that the following inequality holds*

$$\sum_{k=1}^p \lambda_{(\tau)qmk} (A_k^T P + P A_k) < 0 \quad (5.11)$$

for all  $\tau = 1, 2, \dots, d$ ,  $q = 1, 2, \dots, p$ , and  $m = 1, 2, \dots, p-1$ , where  $\lambda_{(\tau)qmk}$  ( $\tau = 1, 2, \dots, r$ ) is obtained from Algorithm 1 with the amendment that

$$h_{i\min} = \min_{x \in R_\tau(x)} \{h_i(x)\}, \quad h_{i\max} = \max_{x \in R_\tau(x)} \{h_i(x)\}.$$

Then the equilibrium of system (5.1) is asymptotically stable.

Clearly, Theorem 8 is a special case of Theorem 9 with  $d = 1$ . Specially in the following section where the premise variable of  $h(x)$  in the Example 6 is one-dimensional, we can simply choose the sub-regions  $R_\tau(x)$  based on the sample points of piecewise linear approximation method. This will greatly facilitate our comparison.

## 5.4 Comparison of different membership-dependent methods

In this section, we will compare the method introduced in this chapter with existing membership-dependent methods: piecewise linear approximation method in [4] and bound-dependent method in [5] and [87]. Both theoretical and numerical analysis will be provided. We will firstly go back to the methods reviewed in Section 2.3, and find the corresponding checking points of them.

### 5.4.1 Get the checking points for existing membership dependent methods

#### 5.4.1.1 Piecewise linear approximation method in [4]

Firstly we recall the preliminary result in Condition (2.18) of Section 2.3.1, which is

$$\begin{cases} r_i \geq h_i(x_1) - \hat{h}_i(x_1), & \forall i = 1, 2, \dots, p \\ Q_i + M \geq 0, & \forall i = 1, 2, \dots, p \\ \sum_{i=1}^p h_i(x_1^{(\tau)}) Q_i < - \sum_{i=1}^p r_i (Q_i + M) \end{cases} \quad (5.12)$$

for all  $\tau = 1, 2, \dots, d, d+1$ , where  $r_i$  ( $i = 1, 2, \dots, p$ ) is a scalar and  $M$  is a symmetric matrix of appropriate dimension.

To compare the stability condition in (5.12) with that of Theorem 9, we assume that these two methods share the same sub-regions. Thus they have the same number of sub-regions  $d$ , and the sample points  $x_1^{(\tau)}$  ( $\tau = 1, 2, \dots, d$ ) of them are same as each other. Without loss of generality, we set  $p = 3$ . Then a necessary condition of (5.12) is

$$\begin{cases} r_i \geq h_i(x_1) - \hat{h}_i(x_1), & \forall i = 1, 2, \dots, p \\ \sum_{i=1}^3 h_i(x_1^{(\tau)}) Q_i < -r_2(Q_2 - Q_1) - r_3(Q_3 - Q_1) \\ \sum_{i=1}^3 h_i(x_1^{(\tau)}) Q_i < -r_1(Q_1 - Q_2) - r_3(Q_3 - Q_2) \\ \sum_{i=1}^3 h_i(x_1^{(\tau)}) Q_i < -r_1(Q_1 - Q_3) - r_2(Q_2 - Q_3) \end{cases}$$

for all  $\tau = 1, 2, \dots, d+1$ . Equivalently it means that

$$\begin{cases} r_i \geq h_i(x_1) - \hat{h}_i(x_1), & \forall i = 1, 2, \dots, p \\ (h_1(x_1^{(\tau)}) - r_2 - r_3)Q_1 + (h_2(x_1^{(\tau)}) + r_2)Q_2 + (h_3(x_1^{(\tau)}) + r_3)Q_3 < 0 \\ (h_1(x_1^{(\tau)}) + r_1)Q_1 + (h_2(x_1^{(\tau)}) - r_1 - r_3)Q_2 + (h_3(x_1^{(\tau)}) + r_3)Q_3 < 0 \\ (h_1(x_1^{(\tau)}) + r_1)Q_1 + (h_2(x_1^{(\tau)}) + r_2)Q_2 + (h_3(x_1^{(\tau)}) - r_1 - r_2)Q_3 < 0 \end{cases}$$

for all  $\tau = 1, 2, \dots, d+1$ . So the equivalent stability checking points are

$$\begin{cases} (h_1(x_1^{(\tau)}) - r_2 - r_3, h_2(x_1^{(\tau)}) + r_2, h_3(x_1^{(\tau)}) + r_3) \\ (h_1(x_1^{(\tau)}) + r_1, h_2(x_1^{(\tau)}) - r_1 - r_3, h_3(x_1^{(\tau)}) + r_3) \\ (h_1(x_1^{(\tau)}) + r_1, h_2(x_1^{(\tau)}) + r_2, h_3(x_1^{(\tau)}) - r_1 - r_2) \end{cases} \quad (5.13)$$

for all  $\tau = 1, 2, \dots, d+1$ , where

$$r_i = \max_{x_1} (h_i(x_1) - \hat{h}_i(x_1)), \quad \forall i = 1, 2, 3.$$

For systems with high dimensional premise variables, the sample points for membership approximation are selected as  $x^{(\tau)}$  ( $\tau = 1, 2, \dots, d+1$ ). Then equivalent checking points can be similarly obtained as

$$(h_1(x^{(\tau)}) + r_1, h_2(x^{(\tau)}) + r_2, \dots, h_i(x^{(\tau)}) + r_i - \sum_{j=1}^p r_j, \dots, h_p(x^{(\tau)}) + r_p) \quad (5.14)$$

for all  $j = 1, 2, \dots, p$  and  $\tau = 1, 2, \dots, d+1$ , where

$$r_i = \max_x (h_i(x) - \hat{h}_i(x)), \quad \forall i = 1, 2, \dots, p.$$



#### 5.4.1.2 Membership-bound-dependent method in [5]

Similarly, we firstly recall the preliminary sufficient condition (2.19) of Section 2.3.2, which is

$$\begin{cases} \beta_i \geq h_i(x) \\ N_i \geq 0 \\ Q_i - N_i + \sum_{j=1}^p \beta_j N_j < 0 \end{cases} \quad (5.15)$$

for all  $i = 1, 2, \dots, p$ . Now let us come to the stability condition (5.15) which is obtained by the bound-dependent method in Section 2.3.2. The condition in (5.15) can be equivalently expressed as

$$\begin{cases} N_i \geq 0, \quad \forall i = 1, 2, \dots, p \\ Q_i - N_i + \sum_{j=1}^p h_{j \max} N_j < 0, \quad \forall i = 1, 2, \dots, p. \end{cases} \quad (5.16)$$

As a special case, we set  $p = 2$ . It is obvious that  $1 - h_{i \max} \geq 0$  for  $i = 1, 2$ . Then by taking the weighted sum of inequalities in (5.16), one can get the following necessary condition of (5.16),

$$\begin{cases} N_1 \geq 0, \quad N_2 \geq 0 \\ (1 - h_{1 \max})(Q_2 - N_2 + h_{1 \max} N_1 + h_{2 \max} N_2) \\ \quad + h_{1 \max}(Q_1 - N_1 + h_{1 \max} N_1 + h_{2 \max} N_2) < 0 \\ (1 - h_{2 \max})(Q_1 - N_1 + h_{1 \max} N_1 + h_{2 \max} N_2) \\ \quad + h_{2 \max}(Q_2 - N_2 + h_{1 \max} N_1 + h_{2 \max} N_2) < 0 \end{cases}$$

which means

$$\begin{cases} N_1 \geq 0, \quad N_2 \geq 0 \\ (1 - h_{2 \max})Q_1 + h_{2 \max}Q_2 < (1 - h_{1 \max} - h_{2 \max})N_1 \\ h_{1 \max}Q_1 + (1 - h_{1 \max})Q_2 < (1 - h_{1 \max} - h_{2 \max})N_2. \end{cases}$$

Clearly we can see that, in this case, condition (5.15) is a sufficient condition of Theorem 9 with  $d = 1$ , which means more conservativeness.

Since we are not sure whether  $1 - \sum_{i=1}^p h_{i \max} + h_{j \max}$ ,  $j = 1, 2, \dots, p$  are positive or not, the above derivation cannot be extended to the case  $p \geq 3$ . Hopefully,  $(1 - \sum_{i=1}^p h_{i \min} + h_{j \min})$  ( $j = 1, 2, \dots, p$ ) should be always positive, thus we can make that generalized extension for the lower-bound-based version (where  $h_{j \min}$  is

used). In this case, the LMIs in (5.16) will be replaced by

$$\begin{cases} N_i \geq 0, & \forall i = 1, 2, \dots, p \\ Q_i + N_i - \sum_{j=1}^p h_{j \min} N_j < 0, & \forall i = 1, 2, \dots, p \end{cases}$$

Following the same derivation as case  $p = 2$  of the upper-bound-based version, we can obtain the following necessary condition

$$\begin{cases} N_i \geq 0, & \forall i = 1, 2, \dots, p \\ \sum_{i=1}^p h_{i \min} Q_i + (1 - \sum_{i=1}^p h_{i \min}) Q_j < (\sum_{i=1}^p h_{i \min} - 1) N_j \end{cases} \quad (5.17)$$

for all  $j = 1, 2, \dots, p$ . Since  $\sum_{i=1}^p h_{i \min} - 1 \leq 0$ , a necessary condition of (5.17) will be

$$\sum_{i=1}^p h_{i \min} Q_i + (1 - \sum_{i=1}^p h_{i \min}) Q_j < 0$$

for all  $j = 1, 2, \dots, p$ . The corresponding checking points are

$$\begin{cases} (h_{1 \min}, h_{2 \min}, \dots, h_{(p-1) \min}, 1 + h_{p \min} - \sum_{i=1}^p h_{i \min}) \\ (h_{1 \min}, h_{2 \min}, \dots, 1 + h_{(p-1) \min} - \sum_{i=1}^p h_{i \min}, h_{p \min}) \\ \dots \\ (1 + h_{1 \min} - \sum_{i=1}^p h_{i \min}, h_{2 \min}, \dots, h_{(p-1) \min}, h_{p \min}). \end{cases} \quad (5.18)$$

#### 5.4.2 Numerical test for the checking points of different methods

To see clearly the relations of checking points of different methods, we will plot and compare them in a unified membership space in the following example.

**Example 6.** *The comparisons will be based on the following system whose membership function trajectory is a round circle in the 3-dimensional space (the yellow round trajectory in Figure 5.8):*

$$\dot{x} = \sum_{i=1}^3 h_i(x) A_i x$$

where

$$h_1(x) = \frac{1}{3} + \frac{0.7}{\sqrt{36}} \cos x_1 - \frac{0.7}{\sqrt{12}} \sin x_1,$$

$$h_2(x) = \frac{1}{3} + \frac{0.7}{\sqrt{36}} \cos x_1 + \frac{0.7}{\sqrt{12}} \sin x_1,$$

$$h_3(x) = \frac{1}{3} - \frac{0.7}{\sqrt{9}} \cos x_1,$$

and

$$A_1 = \begin{bmatrix} -1 & 2 \\ 0 & -1 \end{bmatrix}, \quad A_2 = \begin{bmatrix} -1 & 0.3 \\ b & -1 \end{bmatrix}, \quad A_3 = \begin{bmatrix} -1 & 0 \\ a & -1 \end{bmatrix}.$$

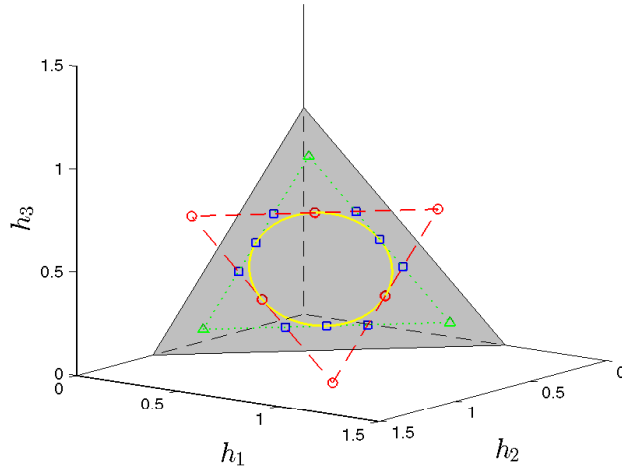


Figure 5.8: Checking points of different methods (piecewise linear approximation method [4] with  $d = 3$ : red circle points; bound-dependent method [5]: green triangle points; Theorem 9 with  $d = 3$ : blue square points).

The vertices obtained from (5.13) with  $d = 3$  (where  $x_1^{(1)} = 0$ ,  $x_1^{(2)} = \frac{2\pi}{3}$ ,  $x_1^{(3)} = \frac{4\pi}{3}$ ) are plotted as the red circle points in Figure 5.8. The vertices obtained from (5.18) are plotted as the green triangle points in Figure 5.8. For the method mentioned in Theorem 9, we choose  $d = 3$  and sub-regions are divided based on the sample points in piecewise linear approximation method, which are

$$R_1(x) = \{x | x_1^{(1)} \leq x_1 < x_1^{(2)}\}$$

$$R_2(x) = \{x | x_1^{(2)} \leq x_1 < x_1^{(3)}\}$$

$$R_3(x) = \{x | x_1^{(3)} \leq x_1 < x_1^{(1)}\}.$$

The obtained checking points are plotted as blue square points. Clearly, we can find that the convex polytope constructed by the square points is contained in both that of circle points and that of triangle points. It means that the method described in Theorem 9 is superior in the aspect of conservativeness. To further confirm the above conservativeness relation, let us compare the feasible regions of  $(a, b)$  obtained by different methods. The results are described in Figure 5.9. It is obvious that the method introduced in Theorem 9 has larger feasible region.

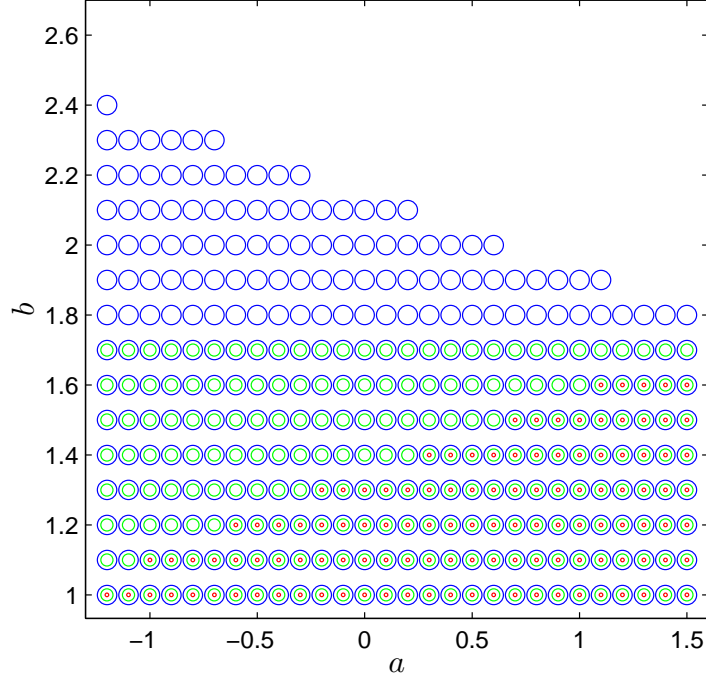


Figure 5.9: Feasible regions of different methods (piecewise linear approximation method [4] with  $d = 3$ : red dots; bound-dependent method [5]: small green circles; Theorem 9 with  $d = 3$ : big blue circles).

*From the numerical point of view, the method in Theorem 9 would require lower computational burden since there is no additional matrix variable involved in the final LMIs. Another merit of Theorem 9 is that there is no need to concern about the dimension of premise variable. In addition, it can be easily extended to interval type-2 T-S fuzzy systems (see Figure 5.7). In this sense, one can reach the conclusion that Theorem 9 can be applied to the analysis of a wider range of fuzzy systems, and the results will be less conservative and require less computational burden.*

## 5.5 Further discussion

In the above comparison analysis, we only discussed the case where one polyhedron is fully enclosed in another. In that case, one can reach the conclusion that, stability conditions related with smaller polyhedron should be less conservative. For the case that two polyhedrons share some overlapping parts but are not completely contained in each other, global conservativeness comparison result cannot be obtained. But in such a case, we can get less conservative stability condition by combining the two methods together. The idea is that, polyhedron area without overlapping means that such an area is not necessary for stability checking. Thus, theoretically, we can shrink the enclosing polyhedron to the overlapped area of several ones.

Denote  $\mathcal{P}_i$  as the equivalent convex polyhedron of the  $i$ -th method ( $i = 1, 2, \dots, l$ ). This idea will be based on the following set theory.

**Lemma 12.** [110] *If  $h(x)$  is fully contained in all the convex polyhedrons  $\mathcal{P}_i$  ( $i = 1, 2, \dots, l$ ), then  $h(x)$  is fully contained in their overlapping area  $\mathcal{P} \triangleq \mathcal{P}_1 \cap \mathcal{P}_2 \cap \dots \cap \mathcal{P}_l$ .*

Denote the  $d$  vertices of  $\mathcal{P}$  as  $\eta_j = (\eta_{j1}, \eta_{j2}, \dots, \eta_{jp})$  ( $j = 1, 2, \dots, d$ ). Then the stability condition can be expressed in the following theorem.

**Theorem 10.** *The equilibrium of system (5.1) is asymptotically stable if there exists a matrix  $P > 0$  such that the following condition is satisfied*

$$\sum_{k=1}^p \eta_{jk} (A_k^T P + P A_k) < 0$$

for all  $j = 1, 2, \dots, d$ , where  $\eta_j = (\eta_{j1}, \eta_{j2}, \dots, \eta_{jp})$ ,  $j = 1, 2, \dots, d$ , are the vertices of overlapping area  $\mathcal{P}$ .

Denote the membership-dependent LMI condition related with  $j$ -th method ( $j = 1, 2, \dots, l$ ) as

$$P < 0 \quad \text{and} \quad L_j(Q_1, Q_2, \dots, Q_p) < 0,$$

where  $Q_i = P A_i + A_i^T P$  for  $i = 1, 2, \dots, p$ , and  $L_i(Q_1, Q_2, \dots, Q_p) < 0$  represents the LMIs constructed by using the vertices of  $\mathcal{P}_i$  as checking points, see expression (5.10). Alternatively, we can get the direct combination of multiple methods.

**Theorem 11.** *The equilibrium of system (5.1) is asymptotically stable if the following condition is satisfied*

$$\begin{cases} P > 0, \\ L_1 < 0 \text{ or } L_2 < 0 \text{ or } \dots \text{ or } L_l < 0. \end{cases}$$

where  $L_i$  is the abbreviation of  $L_i(Q_1, Q_2, \dots, Q_p)$  which is associated with polyhedron  $\mathcal{P}_i$ .

For a given fuzzy system with uncertain parameter (the one like Example 4), the feasible solution of uncertain parameter obtained by Theorem 11 should be the union of feasible solutions obtained by methods 1 to  $l$ . Theoretically the method in Theorem 10 will be less conservative than the simple combination result in Theorem 11. To verify such a conclusion, we start with the one-dimensional system. For the given subsystems  $A_i \in \mathbb{R}^{1 \times 1}$  ( $i = 1, 2, \dots, p$ ), expression

$$h_1(x)A_1 + h_2(x)A_2 + \dots + h_p(x)A_p = 0 \tag{5.19}$$

should be a surface perpendicular to vector  $(A_1, A_2, \dots, A_p)$  and passing through the origin point. Since  $A_i$  is one-dimensional, the allowable subsystem variation

determined by (5.2) can be expressed as (5.19). The validity of condition  $P > 0$  and  $L_i < 0$  is equivalent to say that  $\mathcal{P}_i$  is located on one side of surface (5.19) (the side satisfying  $\sum_{i=1}^p h_i(x)A_i < 0$ ). On the other hand, the invalidity of condition  $P > 0$  and  $L_i < 0$  means that  $\mathcal{P}_i$  is partly located in the area  $\sum_{i=1}^p h_i(x)A_i \geq 0$ .

In the case that, all  $\mathcal{P}_i$  ( $i = 1, 2, \dots, l$ ) have intersection with surface (5.19),  $\mathcal{P}$  can still be on only one side of surface (5.19), see Figure 5.10. It means that when Theorem 11 is not satisfied, the condition in Theorem 10 may still be achieved. This verifies the reduced conservativeness of Theorem 10. The main difficulty in applying Theorem 10 lies in the algorithm to find the vertices of  $\mathcal{P}$  based on the vertices of  $\mathcal{P}_i$  ( $i = 1, 2, \dots, l$ ).

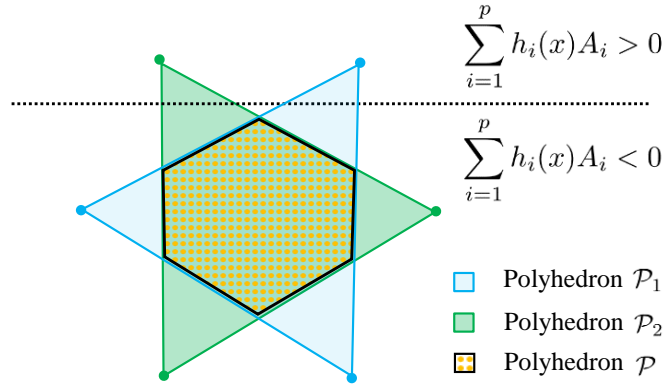


Figure 5.10: Both polyhedrons  $\mathcal{P}_1$  and  $\mathcal{P}_2$  have intersection with surface (5.19), but their overlapping area  $\mathcal{P}$  is on only one side of surface (5.19). Here  $A_i \in \mathbb{R}^{1 \times 1}$  for all  $i = 1, 2, \dots, p$

## 5.6 Conclusions

By considering the membership functions in a unified space, we can construct the final LMI conditions based on the vertices of a convex polyhedron enclosing the membership trajectory, and conservativeness can be reduced by shrinking the range of such a polyhedron. Following this idea, the extrema values of membership functions have been used to construct a tighter polyhedron to reduce conservativeness. Compared with existing methods, this method shows advantage of less conservativeness, simplicity, and there is no need to concern about the number of degrees of freedom of membership functions. Moreover, it has been extended to the stability analysis of interval type-2 T-S fuzzy systems. Conversely, by deriving the checking points of existing LMIs, this membership vector framework can be also used to inspect the conservativeness of membership-dependent stability conditions.

# Chapter 6

## Fuzzy model based stability analysis of the metamorphic robotic palm

*In this chapter the stability problem of a metamorphic palm control system will be investigated based on the T-S fuzzy model. By applying the membership-dependent stability condition in Chapter 5, a wider range of stable palm dynamic performance will be ensured.*

### 6.1 Introduction

As the end-effector of a robot, a robotic hand is a critical component between the robot and environment. In terms of application fields, robotic hands have two typical categories, grippers [41] and dexterous hands [42]. As a trade-off of these two design approaches, a metamorphic robotic hand [43, 44] with a reconfigurable palm was developed by taking advantages of intelligent mechanisms. The palm design was originally inspired by origami with a mechanism equivalent method [46] to relate the panels and crisis to links and joints, respectively. This new structure retains robustness property of grippers and, at same time, can generate delicate motion as a dexterous hand [47].

Kinematically the flexibility of such a hand can be greatly improved by the novel reconfigurable palm mechanism [44]. But when it comes to the problem of dynamic manipulation, additional dynamics coming with the reconfigurable palm should be a major concern. Since the palm is where fingers are mounted, the stability of palm position control system should be crucial for the whole device. Conventional scheme is generally treating the palm as the load of joint actuators [111] and ignore the complex dynamic coming with the palm. However, the technical requirement for joint actuators would be unnecessarily increased if we want to tolerated the wide range of palm dynamics. An efficient way to avoid this should be the stability analysis of palm dynamics.

As it is shown in Figure 6.1, the reconfigurable palm is a closed-chain mechanism [112] with highly nonlinear dynamics. Direct stability analysis for the nonlinear palm control system should not be easy, an alternative idea is to describe the system by multi-model methodology [113]. Among the existing methods, T-S fuzzy model [29] which has been considered in Chapter 5 is proven to be an effective approach. Such a model is described by fuzzy IF-THEN rules which represents local linear input-output relations of a nonlinear system [102]. In this way, the local dynamics can be expressed by a group of local linear models, and the overall model can be achieved by fuzzy “blending” of the obtained linear models. As a result, stability analysis of the original nonlinear model can be achieved based on the analysis of local linear models.

Motivated by the above discussion, in this chapter, we investigate the stability problem of the metamorphic palm control system by the T-S fuzzy modeling method. Firstly, dynamic model of the metamorphic palm will be obtained based on the Euler-Lagrange theory and geometric constraints. Then a geometry dependent controller will be applied to compensate the major nonlinearity of model and keep the closed-loop system simple. Finally stability problem will be solved based on the T-S fuzzy model of palm control system.

Compared with existing work, our contributions to the modeling of this metamorphic palm can be summarized in the following two points:

1. The existing research considered a lot about the kinematic model of this metamorphic palm, while we will move one step further to consider the dynamic modeling of this robotic palm.
2. In addition, we will represent the closed-loop palm dynamic system by a T-S fuzzy model, which is the first time for the analysis of this robotic palm.

## 6.2 Kinematic analysis and dynamic modeling of the metamorphic palm

Before the stability analysis of the palm control system, dynamic model of the metamorphic palm is need. The modeling process of this palm will be based on the Euler-Lagrangian dynamics. Firstly we need to find the kinetic and potential energy of the metamorphic palm based on the kinematic analysis of it.

To start, we need to go back to the physical model of the palm. Mechanically, the palm itself can be divided into two serial chains at joint  $C$ , see Figure 6.1. The first chain contains spherical links 2 and 3. The second chain contains spherical links 4 and 5. The set of all link indexes can be defined as

$$\mathcal{S}_1 \triangleq \{2, 3, 4, 5\}.$$



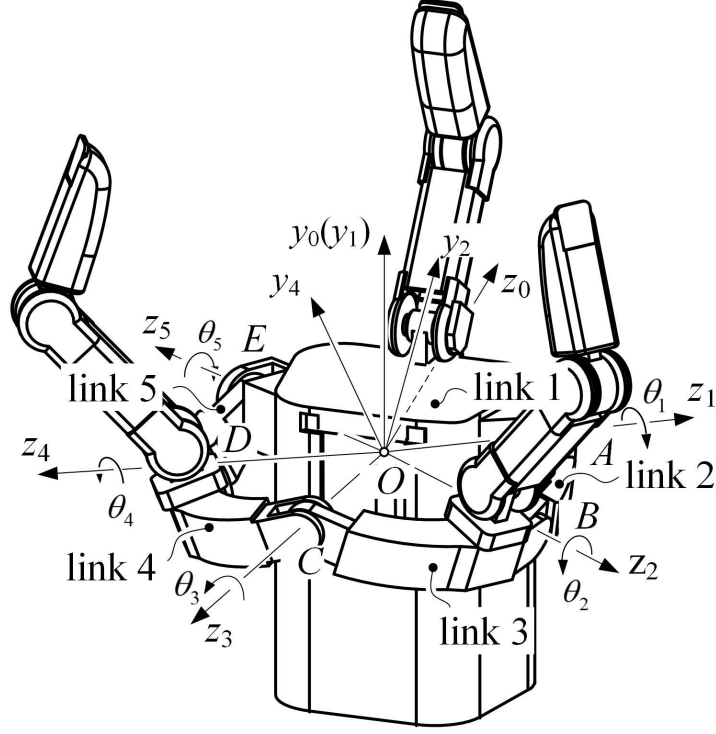


Figure 6.1: Parameters and frames of the metamorphic hand with a reconfigurable palm [12]

Before the detailed analysis, we introduce the following notation symbols for the metamorphic palm and also some related definitions to facilitate our analysis.

Table 6.1: Parameter definitions of the metamorphic palm

Category	Definition
$m_i$	The mass of link $i$ ( $i \in \mathcal{S}_1$ )
$I_i^j$	The inertia tensor of link $i$ about the center of mass in frame $j$ ( $i, j \in \mathcal{S}_1$ )
$I_i$	The inertia tensor of link $i$ about the center of mass in the global frame ( $i \in \mathcal{S}_1$ )
$r_i^j$	Position of the center of mass of link $i$ in the body attached frame ( $i, j \in \mathcal{S}_1$ )
$r_i$	Position of the center of mass of link $i$ in the global frame ( $i \in \mathcal{S}_1$ )
$v_i$	Linear velocity of the center of mass of link $i$ in the global frame ( $i \in \mathcal{S}_1$ )
$\omega_i$	Angular velocity of the center of mass of link $i$ in the global frame ( $i \in \mathcal{S}_1$ )

Category	Definition
$\alpha_i$	Arc angle length of link $i$ ( $i \in \mathcal{S}_1$ )
$\theta_i$	Joint angle from the extension of link $i$ to link $i+1$ for $i = 1, 2, 3, 4$ , and from the extension of link $i$ to link $i-4$ for $i = 5$

The values of parameters  $m_i$ ,  $I_i^j$ ,  $r_i^j$  and  $\alpha_i$  ( $i, j \in \mathcal{S}_1$ ) are provided in Appendix D. The mechanical design can be found in [12]. Define the skew matrix of a vector  $u = [u_x, u_y, u_z]^T$  as

$$S(u) \triangleq \begin{bmatrix} 0 & -u_z & u_y \\ u_z & 0 & -u_x \\ -u_y & u_x & 0 \end{bmatrix}.$$

And define a rotation matrix for a rotation by an angle of  $\theta$  about an axis in the direction of  $u$  as  $R(u, \theta)$ , mathematically this rotation matrix can be represented by  $S(u)$  in the following way

$$R(u, \theta) = \cos \theta \cdot I + \sin \theta \cdot S(u) + (1 - \cos \theta) \cdot u \otimes u$$

where  $\otimes$  is the tensor product. To describe the location in a 3-dimensional space, we define unit vectors  $\mathbf{i} = [1, 0, 0]^T$ ,  $\mathbf{j} = [0, 1, 0]^T$ ,  $\mathbf{k} = [0, 0, 1]^T$  and the following unified vector of joint angles

$$q \triangleq \begin{bmatrix} \theta_1 & \theta_5 & \theta_2 & \theta_4 \end{bmatrix}^T.$$

Following the standard expression as [114], we define the rotation from frame  $i$  to  $j$  as  $R_i^j$ , ( $i, j = 1, 2, 3, 4, 5$ ). If a matrix  $M$  or vector  $v$  depends on  $q$  then it will be expressed as  $M(q)$  or  $v(q)$ , respectively. Based on these notations and definitions, we can now make the kinematic analysis of the palm.

### 6.2.1 Kinematics analysis of the partial reconfigurable palm

Since we assume that the closed chain of the palm can be divided into two open chains at joint  $C$ , the kinematics of these two chains can be considered as independent. As a result, we can analyze their global kinematic properties individually. We start with the open serial chain on the right hand side of the palm. The position of center of mass of link 2 in the global frame should be

$$r_2(q) = R_2^0(q)r_2^2$$

where  $R_2^0(q) = R_1^0 R(z_1, \theta_1) R(y_1, -\alpha_2)$  and  $R_1^0 = R(y_0, -\frac{1}{2}\alpha_1)$ . From [114], linear velocity of center of mass of link 2 in the global frame can be obtained as

$$v_2(q) = S(r_A)r_2(q)\dot{\theta}_1$$

where  $r_A = R_1^0 \mathbf{k}$ . For the angular velocity, we have

$$\omega_2(q) = r_A \dot{\theta}_1.$$

Now we move forward to link 3 which is the subsequent link connected to link 2. The position of center of mass of link 3 in the global frame should be

$$r_3(q) = R_2^0(q)R_3^2(q)r_3^3$$

where  $R_3^2(q) = R(z_2, \theta_2)R(y_2, -\alpha_3)$ . Then the linear velocity of center of mass of link 3 in the global frame will be

$$v_3(q) = S(r_A)r_3(q)\dot{\theta}_1 + S(r_B(q))r_3(q)\dot{\theta}_2$$

where  $r_B(q) = R_2^0(q)\mathbf{k}$ . Similarly the angular velocity of  $\omega_{3c}$  can be also obtained in the following way

$$\omega_3(q) = r_A \dot{\theta}_1 + r_B(q)\dot{\theta}_2.$$

By the same method, we can get the link kinematic expressions for the left open serial chain. To summarize, we have the following kinematic expressions

$$v_i(q) = J_{v_i}(q)\dot{q}, \quad \omega_i(q) = J_{\omega_i}(q)\dot{q}, \quad \forall i \in \mathcal{S}_1$$

where

$$\begin{aligned} J_{v_2}(q) &= \begin{bmatrix} S(r_A)r_2(q) & 0 & 0 & 0 \end{bmatrix}, \quad J_{\omega_2}(q) = \begin{bmatrix} r_A & 0 & 0 & 0 \end{bmatrix}, \\ J_{v_3}(q) &= \begin{bmatrix} S(r_A)r_3(q) & 0 & S(r_B(q))r_3(q) & 0 \end{bmatrix}, \\ J_{\omega_3}(q) &= \begin{bmatrix} r_A & 0 & r_B(q) & 0 \end{bmatrix}, \quad J_{\omega_4}(q) = \begin{bmatrix} 0 & -r_D(q) & 0 & -r_E \end{bmatrix} \\ J_{v_4}(q) &= \begin{bmatrix} 0 & -S(r_D(q))r_4(q) & 0 & -S(r_E)r_4(q) \end{bmatrix}, \\ J_{v_5}(q) &= \begin{bmatrix} 0 & 0 & 0 & -S(r_E)r_5(q) \end{bmatrix}, \quad J_{\omega_5}(q) = \begin{bmatrix} 0 & 0 & 0 & -r_E \end{bmatrix} \end{aligned}$$

and

$$\begin{aligned} r_E &= R_1^0 R(y_1, \alpha_1) \mathbf{k}, \quad r_D = R_5^0(q) R(y_5, \alpha_5) \mathbf{k}, \\ r_5(q) &= R_5^0(q)r_5^5, \quad R_5^0(q) = R_1^0 R(y_0, \alpha_1) R(z_0, -\theta_5), \\ r_4(q) &= R_5^0(q)R_4^5(q)r_4^4, \quad R_4^5(q) = R(y_5, \alpha_5) R(z_5, -\theta_4). \end{aligned}$$

With the above kinematic expression, it will be easier for us to describe the dynamic model of the reconfigurable palm.

### 6.2.2 Lagrangian method based dynamic modeling of the partial reconfigurable palm

The commonly used modeling approach for complex mechanical device is the Lagrangian method. To apply this method, our first step is to find the kinetic and potential energy of the palm. The kinetic energy is associated with translational, rotational motion, inertia tensor and mass of each link. The inertia tensors  $I_i^i$  ( $i \in \mathcal{S}_1$ ) expressed in the body attached frames are constant and they can be exported from the hand model CAD design in SolidWorks [115]. Their exact values can be found in Appendix D. To find their expression in the global frame we need the transformation  $I_i(q) = R_i^0(q)I_i^i R_i^0(q)^T$ , ( $i \in \mathcal{S}_1$ ). Overall the kinetic energy is associated with the rotational and translational velocities and can be expressed as

$$\mathcal{K}(q) = \frac{1}{2} \dot{q}^T \mathcal{D}(q) \dot{q} \quad (6.1)$$

where

$$\mathcal{D}(q) = \sum_{i \in \mathcal{S}_1} (m_i J_{v_i}(q)^T J_{v_i}(q) + J_{\omega_i}(q)^T I_i(q) J_{\omega_i}(q)).$$

The potential energy of all links is associated with the center of gravity of each link and can be calculated as

$$\mathcal{P}(q) = \sum_{i \in \mathcal{S}_1} m_i g^T r_i(q)$$

where  $g = [0, 0, 9.81]^T$ . Then from [112], the Euler-Lagrangian dynamic equation can be presented as

$$\mathcal{D}(q) \ddot{q} + \mathcal{C}(q, \dot{q}) \dot{q} + \mathbf{g}(q) = \alpha_q(q)^T \lambda \quad (6.2)$$

where  $\lambda$  is the vector of Lagrange multipliers,  $\alpha_q(q)$  is the parameter obtained from close-chain constraints,  $\alpha_q(q)^T \lambda$  represents the constraints generalized force vector.  $\mathbf{g}(q)$  is the term related with gravity that can be exactly expressed as

$$\mathbf{g}(q) = \left( \frac{\partial \mathcal{P}(q)}{\partial q} \right)^T = \sum_{i \in \mathcal{S}_1} m_i J_{v_i}(q)^T g.$$

The element on the  $k$ -th row and  $j$ -column of matrix  $\mathcal{C}(q, \dot{q})$  should be

$$c_{kj}(q) = \sum_{i \in \mathcal{S}_1} c_{ijk}(q) \dot{q}_i. \quad (6.3)$$

Define the  $i$ -th row and  $j$ -th column element of matrix  $\mathcal{D}(q)$  as  $d_{ij}(q)$ , then the *Christoffel symbol*  $c_{ijk}(q)$  in (6.3) can be described as

$$c_{ijk}(q) = \frac{1}{2} \left( \frac{\partial d_{kj}(q)}{\partial q_i} + \frac{\partial d_{ki}(q)}{\partial q_j} - \frac{\partial d_{ij}(q)}{\partial q_k} \right). \quad (6.4)$$

### 6.2.3 Geometrical constraints based palm kinematics analysis

In the above analysis we divided the links of the palm into two independent chains and considered their dynamics separately. But actually, their dynamics are still restricted by the closed-chain constraint that can be used to get the actual palm dynamics. The closed-chain constraint of the palm is that the right partial chain and left partial chain are connected at point  $C$ . This relation can be expressed as the following mathematical equation

$$r_{Cr}(q) - r_{Cl}(q) = 0 \quad (6.5)$$

where  $r_{Cr}(q)$  is the position of  $C$  calculated from the right serial chain,  $r_{Cl}(q)$  is the position of  $C$  calculated from the left serial chain, and can be obtained as

$$r_{Cr}(q) = R_2^0(q)R_3^2(q)\mathbf{k}r, \quad r_{Cl}(q) = R_5^0(q)R_4^5(q)R(y_5, \alpha_4)\mathbf{k}r$$

with  $r = 4.75 \times 10^{-2}$  m being the radius of the palm sphere. In fact, because of the physical constraints from the hand wrist (base link 1), the point  $C$  is only allowed to move within the front half sphere of the palm, where  $z < 0$ . Thus we can simply require that  $r_{Cr}(q)$  and  $r_{Cl}(q)$  have the same projection on the  $x - y$  plane. The above constraints can be reduced to

$$\alpha(q) = [I_{2 \times 2} \quad 0_{2 \times 1}] \cdot (r_{Cr}(q) - r_{Cl}(q)) = 0.$$

Calculating the derivative of  $\alpha(q)$  with respect to time  $t$ , we have

$$\alpha_q(q)\dot{q} = [I_{2 \times 2} \quad 0_{2 \times 1}] J_C(q)\dot{q}$$

where

$$\alpha_q(q) \triangleq \frac{\partial \alpha(q)}{\partial q}, \quad J_C(q) \triangleq \begin{bmatrix} [S(r_A)r_{Cr}(q)]^T \\ [S(r_E)r_{Cl}(q)]^T \\ [S(r_B^0(q))r_{Cr}(q)]^T \\ [S(r_D^0(q))r_{Cl}(q)]^T \end{bmatrix}^T.$$

Actually in the palm spherical linkage, angles  $\theta_3$  and  $\theta_4$  of the passive joints are not independent, which means the palm structure can be determined simply by angles  $\theta_1$

and  $\theta_2$  at the two active joints. Consequently, the degree of freedom of the dynamic model can be reduced.

To achieve that, we define the independent generalized coordinate as  $p = \beta(q) = [I_{2 \times 2} \ 0_{2 \times 2}] q$ . For a specific point in the independent coordinate  $p$ , there is a unique mapping point  $q = \sigma(p)$  from the dependent coordinate  $q$  [116], among which we define

$$\gamma(q) \triangleq \begin{bmatrix} \alpha(q) \\ \beta(q) \end{bmatrix}, \quad \gamma_q(q) \triangleq \frac{\partial \gamma(q)}{\partial q}.$$

Based on the definitions of  $\alpha(q)$  and  $\beta(q)$ ,  $\gamma_q(q)$  can be further expressed as

$$\gamma_q(q) = \begin{bmatrix} [I_{2 \times 2} \ 0_{2 \times 1}] J_C(q) \\ [I_{2 \times 2} \ 0_{2 \times 2}] \end{bmatrix}.$$

Following the same method as [112], we can get the mapping relation between  $\dot{q}$  and  $\dot{p}$  as

$$\dot{q} = \rho(q)\dot{p} \tag{6.6}$$

where

$$\rho(q) = \gamma_q^{-1}(q) \begin{bmatrix} 0_{2 \times 2} \\ I_{2 \times 2} \end{bmatrix} = \begin{bmatrix} 1 & 0 \\ 0 & 1 \\ \rho_{13}(q) & \rho_{14}(q) \\ \rho_{23}(q) & \rho_{24}(q) \end{bmatrix}.$$

#### 6.2.4 Dynamic modeling of the reconfigurable palm

The mapping  $q = \sigma(p)$ , from  $p$  to  $q$ , can be obtained by the spherical cosine law. Readers can refer to [116] for the detailed analysis. By the mapping relations  $q = \sigma(p)$  and  $\dot{q} = \rho(q)\dot{p}$ , in this section, we will explain how to find the expression of reduced dynamic model in the independent coordinate  $p$ . By taking the derivative of (6.6), we can get the angular acceleration of  $q$  as

$$\ddot{q} = \dot{\rho}(q, \dot{q})\dot{p} + \rho(q)\ddot{p}$$

where

$$\dot{\rho}(q, \dot{q}) = \sum_{i=1}^4 \frac{\partial \rho(q)}{\partial q_i} \dot{q}_i = \sum_{i=1}^4 \sum_{j=1}^2 \frac{\partial \rho(q)}{\partial q_i} \rho_{ij}(q) \dot{p}_j.$$

Now the dynamic equation in (6.2) can be reduced to the following expression of  $p$ ,

$$\mathbf{D}(p)\ddot{p} + \mathbf{C}(p, \dot{p})\dot{p} + \mathbf{g}(p) = \mathbf{u} \quad (6.7)$$

with

$$\begin{cases} \mathbf{D}(p) &= \rho(q)^T \mathcal{D}(q) \rho(q) \\ \mathbf{C}(p, \dot{p}) &= \rho(q)^T \mathcal{C}(q, \dot{q}) \rho(q) + \rho(q)^T \mathcal{D}(q) \dot{\rho}(q, \dot{q}) \\ \mathbf{g}(p) &= \rho(q)^T \mathbf{g}(q) \\ \dot{q} &= \rho(q) \dot{p}, \quad q = \sigma(p) \end{cases} \quad (6.8)$$

In the following sections, we will investigate the stability problem of the closed-loop palm control system. This can be achieved in two steps:

1. Construct a feedback controller to get the expression of closed-loop palm control system;
2. Choose a specific joint position as the system equilibrium point and analyze the stability problem in this case.

## 6.3 Geometry variation based controller design of the metamorphic palm

In this part, we consider the controller design problem. The controller structure will be chosen in such a way, firstly to keep the closed-loop system simple and also make it easier to tune the dynamic performance. Feasible range of the controller parameters will be analyzed in Section 6.4. The feedback control methodology will be based on the following assumption.

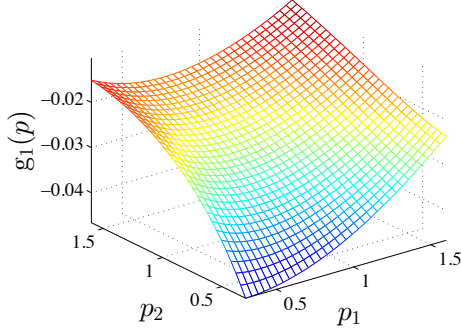
**Assumption 3.** *The real-time values of  $p$  and  $\dot{p}$  can be precisely obtained.*

### 6.3.1 Controller design based on inertia and gravity compensation

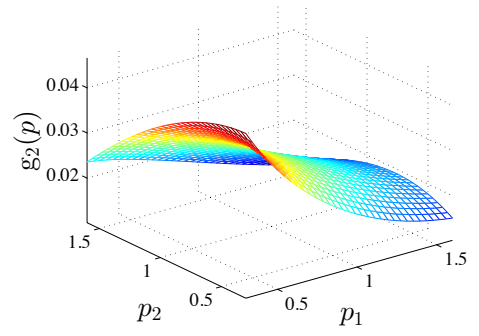
The control input can be designed as a function of  $p$  and  $\dot{p}$ . Firstly we need torque to compensate the influence of gravity. Corresponding input would be  $\mathbf{u}_1(p) = \mathbf{g}(p)$ . Based on the technical parameters of the hand model, we can find the layouts of  $\mathbf{g}(p)$  and  $\mathbf{g}(p)$  with respect to the joint state  $p$ . Exactly, parameter values in  $\mathbf{g}(p) = [\mathbf{g}_1(p), \mathbf{g}_2(p)]^T$  are presented in Figure 6.2.

Moreover, additional input  $\mathbf{u}_2(p, \dot{p})$  is needed to ensure the system stability and reach the required performance. The relation can be expressed as

$$\mathbf{D}(p)\ddot{p} + \mathbf{C}(p, \dot{p})\dot{p} = \mathbf{u}_2(p, \dot{p}). \quad (6.9)$$



(a) Relationship between gravity parameter  $g_1(p)$  and joint state  $p$



(b) Relationship between gravity parameter  $g_2(p)$  and joint state  $p$

Figure 6.2: Relationship between parameters gravity vector  $g(p)$  and joint state  $p$

All the elements of the inertial matrix  $D(p)$  are state-dependent,

$$D(p) = \begin{bmatrix} d_{11}(p) & d_{12}(p) \\ d_{21}(p) & d_{22}(p) \end{bmatrix}.$$

From (6.8) we know that  $D(p)$  is symmetric, which means  $d_{21}(p) = d_{12}(p)$ . In Figure 6.3, we can find the relation of the elements  $d_{11}(p)$ ,  $d_{12}(p)$  and  $d_{22}(p)$  of  $D(p)$  with  $p$ . In addition, the following relation holds

$$\dot{p}^T D(p) \dot{p} = \dot{p}^T \rho(q)^T \mathcal{D}(q) \rho(q) \dot{p} = \dot{q}^T \mathcal{D}(q) \dot{q} = 2\mathcal{K}(q)$$

where  $\mathcal{K}(q)$  is defined in (6.1). It means that  $\frac{1}{2}\dot{p}^T D(p) \dot{p}$  is the kinetic energy of the palm, which is generally positive and can be zero iff  $\dot{p} = 0$ . Thus it can be confirmed that  $D(p) > 0$ . As a result (6.9) can be transformed to

$$\ddot{p} + D(p)^{-1} C(p, \dot{p}) \dot{p} = \bar{u}_2(p, \dot{p})$$

where  $\bar{u}_2(p, \dot{p}) \triangleq D(p)^{-1} u_2(p, \dot{p})$ .

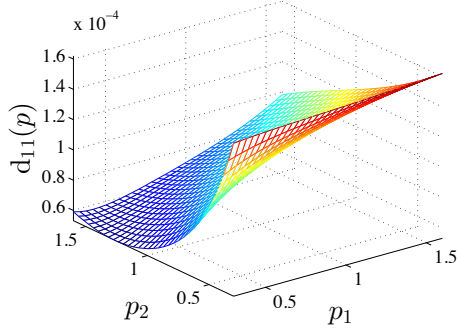
To analyze the system dynamic performance in the system state space, we define the system state as

$$x = [x_1, x_2, x_3, x_4]^T = [\dot{p}_1, \dot{p}_2, p_1 - p_1^*, p_2 - p_2^*]^T$$

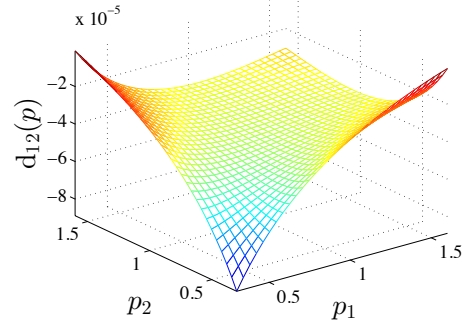
where  $p_1^*$  and  $p_2^*$  are the required positions of  $\theta_1$  and  $\theta_5$ . Equivalently  $\bar{u}_2(p, \dot{p})$  can be also expressed as  $\bar{u}_2(x)$ .

Dynamics expressed by  $C(p, \dot{p}) \dot{p}$  are combination of *centrifugal forces* and *Coriolis forces*. Both of them depend on the velocity term  $\dot{p}$ . For the problem of palm position control, the dynamic speed  $|\dot{p}|$  is generally low. Also, from (6.8), (6.3) and (6.4), we can see that the expression of  $C(p, \dot{p})$  involves derivatives of both  $d_{ij}(q)$  and  $\rho(q)$ . Thus the computation of real-time value of  $C(p, \dot{p})$  should be much more complex

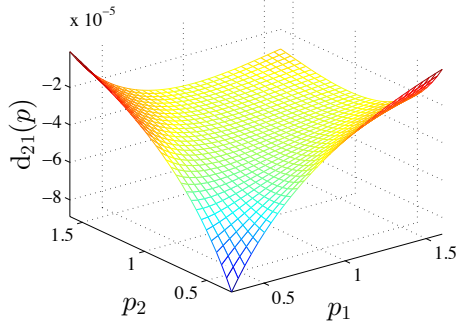




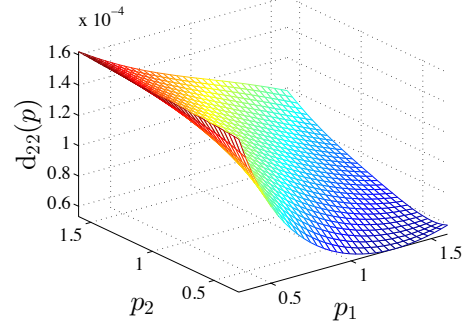
(a) Relation between parameter  $d_{11}(p)$  and joint state  $p$



(b) Relation between parameter  $d_{12}(p)$  and joint state  $p$



(c) Relation between parameter  $d_{21}(p)$  and joint state  $p$



(d) Relation between parameter  $d_{22}(p)$  and joint state  $p$

Figure 6.3: Relation between the parameters in inertia matrix  $D(p)$  and joint state  $p$

and time-consuming than that of  $D(p)$ . In this sense, we may neglect the influence of  $C(p, \dot{p})\dot{p}$  in the dynamic performance analysis and treat it as system uncertainty  $\Delta A(x)x$ . Then the system equation should be

$$\dot{x} = Ax + \Delta A(x)x + B\bar{u}_2(x) \quad (6.10)$$

where

$$A = \begin{bmatrix} 0_{2 \times 2} & 0_{2 \times 2} \\ E_{2 \times 2} & 0_{2 \times 2} \end{bmatrix}, \quad B = \begin{bmatrix} E_{2 \times 2} \\ 0_{2 \times 2} \end{bmatrix},$$

$$\Delta A(x) = \begin{bmatrix} D(p)^{-1}C(p, \dot{p}) & 0_{2 \times 2} \\ 0_{2 \times 2} & 0_{2 \times 2} \end{bmatrix}.$$

To keep it simple, now we choose  $\bar{u}_2(x)$  as the linear function of  $x$ , which can be designed in the following form

$$\bar{u}_2(x) = Kx = \begin{bmatrix} k_{11} & 0 & k_{12} & 0 \\ 0 & k_{21} & 0 & k_{22} \end{bmatrix} x.$$

The overall control scheme  $\mathbf{u}(p, \dot{p})$  that we mentioned in dynamic equation (6.7) can be summarized as

$$\mathbf{u}(p, \dot{p}) = \mathbf{u}_1(p) + \mathbf{u}_2(x) = \mathbf{g}(p) + \mathbf{D}(p)^{-1} \mathbf{K}x. \quad (6.11)$$

### 6.3.2 Dynamic performance analysis

The state matrix for closed-loop system without uncertainty  $\Delta \mathbf{A}(x)$  should be

$$\hat{\mathbf{A}} = \mathbf{A} + \mathbf{B}\mathbf{K}. \quad (6.12)$$

The corresponding characteristic equation would be

$$\det(s\mathbf{E} - \hat{\mathbf{A}}) = (s^2 - \mathbf{k}_{11}s - \mathbf{k}_{12})(s^2 - \mathbf{k}_{21}s - \mathbf{k}_{22}). \quad (6.13)$$

The first factor is associated with the performance of  $\theta_1(t)$ , the second factor is associated with performance of  $\theta_5(t)$ . In some sense, this kind of controller can be also regarded as the modified Proportional-Differential (PD) controller. In other words,  $\mathbf{k}_{11}$  and  $\mathbf{k}_{12}$  are the differential and proportional parameters associated with  $\theta_1(t)$ , and  $\mathbf{k}_{21}$  and  $\mathbf{k}_{22}$  are the differential and proportional parameters associated with  $\theta_5(t)$ . In this way, the controllers associated with  $\theta_1(t)$  and  $\theta_5(t)$  have been decoupled from each other and can be designed independently. In this specific case, the palm structure in Figure 6.1 is symmetric, thus we can simply choose  $\mathbf{k}_{11} = \mathbf{k}_{21} = \mathbf{k}_1$  and  $\mathbf{k}_{12} = \mathbf{k}_{22} = \mathbf{k}_2$  to ensure the same dynamic performance of  $\theta_1(t)$  and  $\theta_5(t)$ .

## 6.4 Fuzzy model based stability analysis

Stability is a basic requirement for any system to work normally, specially for the metamorphic palm which is the operation base of fingers. As a result, the influence of term  $\mathbf{C}(p, \dot{p})\dot{p}$  on system stability cannot be neglected. It means that, within the working space of  $p$  and  $\dot{p}$ , the designed feedback gain  $\mathbf{K}$  in (6.12) should also ensure the system stability for any  $\mathbf{C}(p, \dot{p})\dot{p}$ . In this part, we will analyze the feasible range of  $\mathbf{K}$  based on the stability condition obtained from the fuzzy model. We start from the system state space expression of the palm control system. By (6.10) and (6.12), we have

$$\dot{x} = (\hat{\mathbf{A}} + \Delta \mathbf{A}(x))x \quad (6.14)$$

where

$$\hat{\mathbf{A}} = \begin{bmatrix} \mathbf{k}_1 \mathbf{E}_2 & \mathbf{k}_2 \mathbf{E}_2 \\ \mathbf{E}_2 & \mathbf{0}_{2 \times 2} \end{bmatrix}, \quad \Delta \mathbf{A}(x) = \begin{bmatrix} \mathbf{M}(x) & \mathbf{0}_{2 \times 2} \\ \mathbf{0}_{2 \times 2} & \mathbf{0}_{2 \times 2} \end{bmatrix}$$

and

$$\mathbf{M}(x) = \mathbf{D}(p)^{-1} \mathbf{C}(p, \dot{p}) = \begin{bmatrix} \mathbf{m}_{11}(x) & \mathbf{m}_{12}(x) \\ \mathbf{m}_{21}(x) & \mathbf{m}_{22}(x) \end{bmatrix}.$$

According to the mechanical constraint and working requirement, we consider the stability problem of palm control system in task domain  $\mathcal{S}$ , which is defined as

$$\mathcal{S} \triangleq \{p, \dot{p} \mid 0.3 < p_1, -p_2 < 1.5, |\dot{p}_1| < 10, |\dot{p}_2| < 10\}.$$

Generally it is difficult to consider the palm stability problem based on its original nonlinear model in (6.14). One alternative approach is to replace the state dependent matrix  $\Delta \mathbf{A}(x)$  by the T-S fuzzy combination of finite number of constant matrices. To clearly explain the modeling details, we consider the concept of sector nonlinearity in [102] to manually find its equivalent T-S fuzzy model. The state-dependent parameters  $\mathbf{m}_{ij}(x)$  (the  $i, j$  elements of  $\mathbf{M}(x)$ ,  $i, j = 1, 2$ ) are all highly nonlinear functions of  $x_1, x_2, x_3, x_4$ . For each element  $\mathbf{m}_{ij}(x)$  ( $i, j = 1, 2$ ) of  $\mathbf{M}(x)$ , we can find its maximum and minimum values

$$\mathbf{m}_{ij1} = \max_{x \in \mathcal{S}} \mathbf{m}_{ij}(x), \quad \mathbf{m}_{ij2} = \min_{x \in \mathcal{S}} \mathbf{m}_{ij}(x).$$

Their exact values can be calculated based on expression (6.3) and the palm technical details.

Table 6.3: Maximum and minimum values of the parameters  $\mathbf{m}_{ij}(x)$ ,  $i, j = 1, 2$

	$\mathbf{m}_{11k}$	$\mathbf{m}_{12k}$	$\mathbf{m}_{21k}$	$\mathbf{m}_{22k}$
$k = 1$	13.24	35.68	27.27	25.84
$k = 2$	-13.24	-35.68	-27.27	-25.84

The variable  $\mathbf{m}_{ij}(x)$  can be expressed as a linear combination of its extrema values, that is

$$\mathbf{m}_{ij}(x) = h_{ij1}(x) \mathbf{m}_{ij1} + h_{ij2}(x) \mathbf{m}_{ij2}$$

where

$$h_{ij1}(x) = \frac{\mathbf{m}_{ij}(x) - \mathbf{m}_{ij2}}{\mathbf{m}_{ij1} - \mathbf{m}_{ij2}}, \quad h_{ij2}(x) = \frac{\mathbf{m}_{ij1} - \mathbf{m}_{ij}(x)}{\mathbf{m}_{ij1} - \mathbf{m}_{ij2}}.$$

In this way,  $M(x)$  can be presented as

$$M(x) = \sum_{i=1}^2 \sum_{j=1}^2 \sum_{k=1}^2 \sum_{l=1}^2 h_{11i}(x)h_{12j}(x)h_{21k}(x)h_{22l}(x) \cdot M_{ijkl}$$

with  $M_{ijkl} = \begin{bmatrix} m_{11i} & m_{12j} \\ m_{21k} & m_{22l} \end{bmatrix}$ . Define the new membership functions and subsystems as

$$\tilde{h}_m(x) \triangleq h_{11i}(x)h_{12j}(x)h_{21k}(x)h_{22l}(x),$$

$$\tilde{A}_m \triangleq \hat{A} + \begin{bmatrix} M_{ijkl} & 0_{2 \times 2} \\ 0_{2 \times 2} & 0_{2 \times 2} \end{bmatrix} \quad (6.15)$$

with  $m = 8i + 4j + 2k + l - 15$  for all  $i, j, k, l = 1, 2$ . It follows that  $\hat{A} + \Delta A(x) = \sum_{i=1}^{16} \tilde{h}_i(x)\tilde{A}_i$ , and the T-S fuzzy model of (6.14) becomes  $\dot{x} = \sum_{i=1}^{16} \tilde{h}_i(x)\tilde{A}_i x$ .

Now the stability analysis methods in [102] and Chapter 5 can be used to solve the stability problem. In the following part we will adopt the stability condition in Chapter 5 to reduce the conservativeness of stability analysis. In this way, a larger feasible area of  $(k_1, k_2)$  can be ensured, and wider range of dynamics will be allowed. For comparison, we will start with commonly used basic stability condition in [102] which can be expressed in the following lemma.

**Lemma 13.** [102] *If there exists a matrix  $P > 0$ , such that all the following inequalities hold*

$$\tilde{A}_i^T P + P \tilde{A}_i < 0, \quad \forall i = 1, 2, \dots, 16, \quad (6.16)$$

*then the equilibrium of system (6.5) is asymptotically stable.*

The palm *stability region* is defined as the range of  $(k_1, k_2)$  that ensures the stability of palm control system in (6.14). This region can be estimated by the stability condition in Lemma 13. Changing the values of  $k_1$  and  $k_2$ , with the obtained matrices  $\tilde{A}_m$  ( $m = 1, 2, \dots, 16$ ), if condition (6.16) in Lemma 13 is satisfied, then the set  $(k_1, k_2)$  should be contained in the stability region. By Matlab LMI toolbox, we can find the estimated stability region as

$$\{k_1, k_2 \mid k_1 < -51.4, k_2 < 0\}. \quad (6.17)$$

The basic stability analysis method in Lemma 13 is membership-independent, undoubtedly it should be relatively conservative. To reduce the conservativeness of stability analysis, we adopt the following membership-dependent method from Theorem 8 in Chapter 5.

**Corollary 3.** *If there exists a matrix  $P > 0$ , such that the following inequality holds*

$$\sum_{k=1}^{16} \lambda_{ijk} (\tilde{A}_k^T P + P \tilde{A}_k) < 0 \quad (6.18)$$

*for all  $i = 1, 2, \dots, 16$  and  $j = 1, 2, \dots, 15$ . Then the equilibrium of system (6.5) is asymptotically stable.*

In Corollary 6.4,  $\lambda_{ijk}$  is a parameter obtained by *Algorithm 1* in Chapter 5. With this theorem, the 16 LMIs in Lemma 13 will be replaced by 240 ( $16 \times 15$ ) new LMIs, and conservativeness will be greatly reduced. To get the value of  $\lambda_{ijk}$ , all the maximum and minimum values of  $\tilde{h}_i(x)$  ( $i = 1, 2, \dots, 16$ ) should be known. Based on the technical design of this metamorphic palm, one can numerically find the maximum and minimum values of  $\tilde{h}_i(x)$  for all  $x \in \mathcal{S}$ , see Figure 6.4. Following the calculation in *Algorithm 1* of Chapter 5, we can get the parameters  $\lambda_{ijk}$  for all  $i = 1, 2, \dots, 16$ ,  $j = 1, 2, \dots, 15$  and  $k = 1, 2, \dots, 16$ . By condition (6.18) in Corollary 6.4, the estimated stability region of  $(k_1, k_2)$  can be further improved to

$$\{k_1, k_2 \mid k_1 < -27.0, k_2 < 0\}. \quad (6.19)$$

In this way, the feasible range of  $k_1$  and  $k_2$  has been enlarged, and we will get more freedom to tune the dynamic performances.

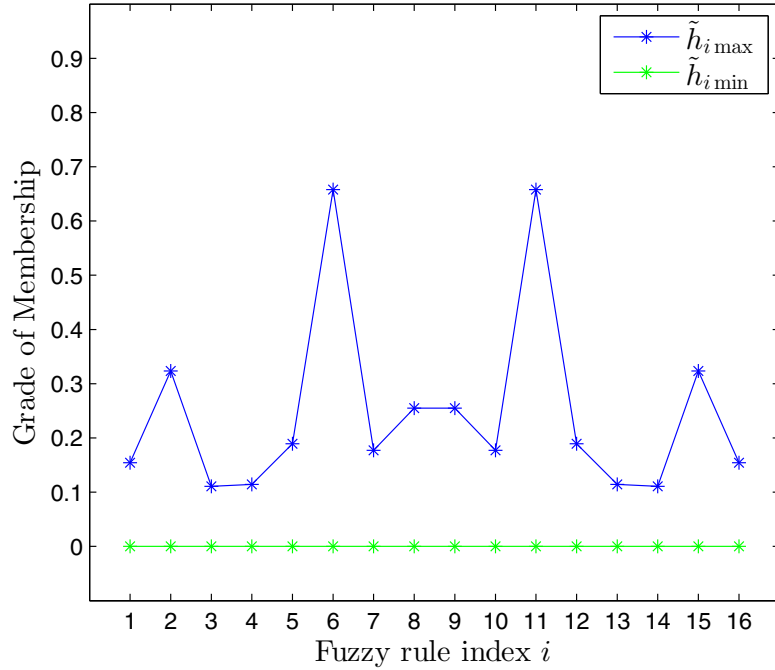


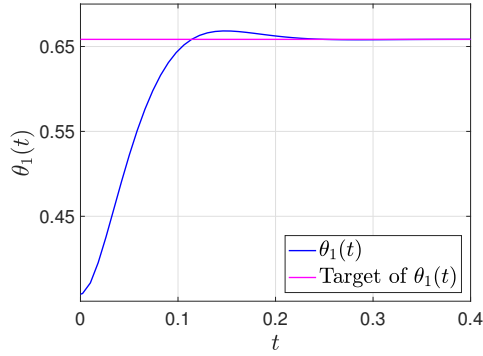
Figure 6.4: Maximum and minimum values of  $h_i(x)$ ,  $i = 1, 2, \dots, 16$

Within the feasible range (6.19), we set the parameters  $k_1$  and  $k_2$  based on the time-domain dynamic performance criteria in [111]. Choose the desired settling time

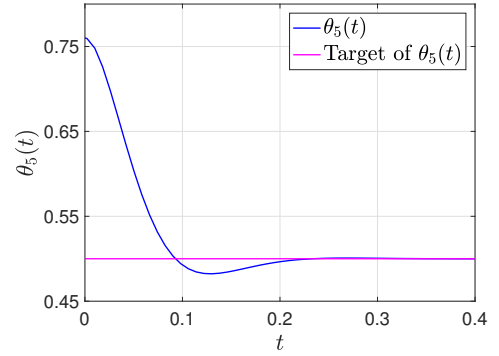
as  $t_s = 0.15s$  and overshoot as  $\sigma\% = 4\%$ . By the relation discussed in [111],  $k_1$  and  $k_2$  can be obtained as

$$k_1 = \frac{7}{-t_s} = -46.67, \quad k_2 = \frac{k_1^2(\pi^2 + (\ln \sigma\%)^2)}{-(2 \ln \sigma\%)^2} = -1063.06.$$

In this specific case,  $(k_1, k_2)$  is out of region (6.17) but still contained in (6.19), which verifies the improvement of method in Corollary 6.4. By the SimMechanics<sup>TM</sup> toolbox, we can get the dynamic simulation of this palm. The angles of active joints at points  $A$  and  $E$  are plotted in Figure 6.5. It is clear that the palm system is asymptotically stable, which verifies the less conservativeness of the new stability analysis method. In addition, the actual settling time and overshoot are almost same as parameters we set. It means that the dynamic analysis in Section 6.3.2 is quite reasonable.

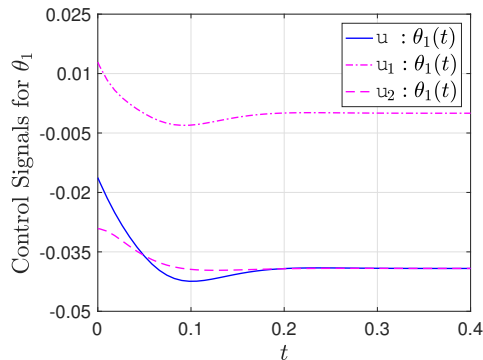


(a) Dynamic trajectory of joint angle  $\theta_1(t)$  under the given control parameters  $k_1$  and  $k_2$

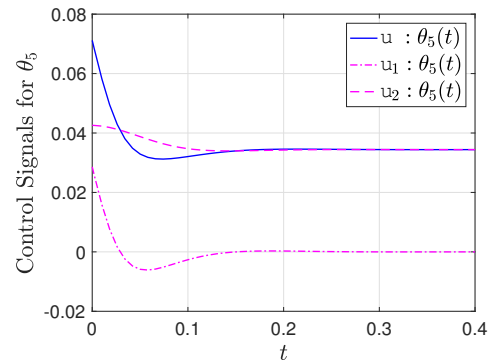


(b) Dynamic trajectory of joint angle  $\theta_5(t)$  under the given control parameters  $k_1$  and  $k_2$

Figure 6.5: Dynamic trajectories of joint angles  $\theta_1(t)$  and  $\theta_5(t)$  under the given control parameters  $k_1$  and  $k_2$



(a) Control inputs  $u(x)$ ,  $u_1(x)$  and  $u_2(x)$  for joint angle  $\theta_1(t)$



(b) Control inputs  $u(x)$ ,  $u_1(x)$  and  $u_2(x)$  for joint angle  $\theta_5(t)$

Figure 6.6: Control inputs  $u(x)$ ,  $u_1(x)$  and  $u_2(x)$  under the given control parameters  $k_1$  and  $k_2$

Similarly, we can also get the trajectories on control inputs  $u(x)$ ,  $u_1(x)$  and  $u_1(x)$  on joints  $\theta_1(t)$  and  $\theta_5(t)$ , see Figure 6.6. The simulation considered here is the ideal case where no restriction is applied on the control signals. But in the practical case, the torque actuators may have their maximum power limit because of input saturation. This will be one limitation of the control scheme in (6.11) for real applications. Another practical limitation of this theoretical framework is the ignorance of uncertainties in the system parameters, which should be considered in real applications.

## 6.5 Conclusions

The dynamic model of the metamorphic palm has been obtained based on the Lagrange-Euler dynamics and geometric constraints. A palm-geometry based controller has been adopted to compensate the model nonlinearity related with the joint positions. By describing the closed-loop system dynamics with a T-S fuzzy model, membership-dependent analysis method has been applied to get the less conservative stability condition. As a result, wider range of control parameters can be used to achieve better dynamic performance.

# Chapter 7

## Conclusions and future work

*This final chapter concludes the research in this thesis, summarizes the work and contributions of earlier chapters, elaborates the limitations and gives suggestion for future research.*

### 7.1 Main findings

In this thesis, we have investigated the fundamental problem of stability for dynamic models with multiple subsystems. Because of the nonlinear property of the considered model, a general way to investigate the stability problem would be the Lyapunov method, i.e. if there is a common appropriate Lyapunov function for the considered model then the equilibrium point of such a model can be considered as stable.

Our main findings in this research start with the analysis of the above statement. In such a statement, we can find two subjects: Lyapunov function and the considered system model. So there will be two approaches to investigate. We can either work on the Lyapunov function by making it more flexible to wider range of model variation, or we can work on the considered model by minimizing its subsystem variation to facilitate the search of appropriate Lyapunov functions.

The first approach has been investigated in this thesis as the stability problem of switched system under arbitrary switching. In this direction, most existing methods investigate the system stability property by actually constructing a highly flexible (usually complicated) Lyapunov function and testing its feasibility. But in this thesis, we have found that such a complicated and conservative approach can be avoided by focusing on a specific (but general) point of the level surface of the Lyapunov function and by analyzing the necessary and sufficient condition for the existence of a proper Lyapunov function, in the micro-space around that point.

The second approach has been treated as the membership-dependent stability analysis of T-S fuzzy systems. For this approach, instead of analyzing the piecewise approximation or boundary information of membership functions separately, we have analyzed them together in a joint membership space as a whole picture. In



this way, we have found that the conservativeness in membership-dependent stability conditions can be reduced by minimizing the variation of subsystems described in such a membership space, and the tighter convex boundary of the subsystem variation can be obtained by the maximum and minimum values of membership functions.

## 7.2 Original contributions to knowledge

Based on the main findings and their following up research, we have obtained some novel results regarding the stability problems of switched systems and T-S fuzzy systems. According to the points we mention in Section 1.4, our main contributions to knowledge can be summarized and fully justified as below:

1. In Chapter 3, the concept of Phase Function has been proposed. Based on this new concept, we have obtained the necessary and sufficient stability condition of switched systems, which is simple and computational efficient. Corresponding result has been published in [117].
2. In Chapter 4, we have verified that the existence of CQLF for every two tuples of subsystems (instead of three tuples as it is mentioned in the literature) can ensure stability of the whole switched system.
3. In Chapter 5, an efficient algorithm has been designed to find the less conservative membership dependent stability condition for T-S fuzzy systems. And the obtained result has been published in [103] and [118].
4. In Chapter 6, the closed loop dynamic system of a robotic palm has been represented as a T-S fuzzy model, and the membership dependent stability analysis method has been applied to ensure the wider range of configuration of such a robotic palm. The research in this chapter has been published in the IFAC conference as [45].

## 7.3 Limitations of the work

Meanwhile, there are also limitations for the work investigated in this thesis. They can be elaborated as below:

1. The methods in Chapters 3 and 4 are applicable only to second-order switched systems. The equivalent definition of Phase Function for higher order switched systems has yet to be considered.
2. In the membership-dependent research in Chapter 5, when different polyhedrons share some overlapping parts but are not completely contained in each

other, theoretically we can shrink the enclosing polyhedron to the overlapped area of several ones. But we have not obtained the practical calculation algorithm to do so.

3. For the application research in Chapter 6, we have not considered the practical issues of input saturation and parameter uncertainties in the control scheme.

## 7.4 Suggestion for future research

With the strengths and limitations considered, there would be mainly three directions for the potential future research. Two of them are related with the follow-up research of Chapter 3 and Chapter 5, e. g. the concept of phase function for higher order system and reducing subsystem variation by the information in switching signal. Another one will be the potential combination of the core ideas in these two chapters.

*First direction:* As we have mentioned before, compared with existing literatures, the results we have obtained in Chapter 3 show advantages in terms of theoretical analysis and numerical computation, but the consider system is still only second-order. In the future, we would like to find the similar concept of phase function for higher order models and investigate the stability problem with that concept.

*Second direction:* The research to minimize graphical description of subsystem variation has been treated as the membership-dependent stability analysis of T-S fuzzy system in Chapter 5, but it has not been discussed for the model of switched systems. In the future we would like to investigate how the information of switching signal can be applied to minimize the subsystem variation of switched system and make it easier for the construction of appropriate Lyapunov function.

*Third direction:* Chapters 3 and 5 presented ideas from different aspects to consider the problem of stability analysis. Both of them are intended to make the analysis clear and reduce the conservativeness of obtained results. We would like to see whether these research ideas can be combined to get even better results, and whether the complexity of such a combination would be acceptable in the practical case.

# Appendices

# Appendix A

## Proofs in Chapter 3

### A.1 Proof of Proposition 2

*Proof.* Based on the given phase function  $\varphi_p^*(\theta)$  of  $p(x)$ , we can design the Lyapunov function as

$$V(x) = \|x\|_2 \exp(\rho(x)), \quad (\text{A.1})$$

where  $\rho(x) = \int_0^{\text{atan}(x)} \tan \varphi_p^*(\phi) d\phi$ . Clearly,  $\rho(x)$  is only related with  $\text{atan}(x)$  and irrelevant to the value of  $\|x\|_2$ . Also,  $\exp(\rho(x)) > 0$  for any  $x$  satisfying (3.12). Thus if we increase the value of  $\|x\|_2$  along a constant angle  $\theta = \text{atan}(x)$ ,  $V(x)$  will increase proportionally. So the designed  $V(x)$  in (A.1) is radially unbounded. For  $x = \|x\|_2 \omega(\text{atan}(x))$ , we can find the equivalent expression

$$\begin{aligned} V(x) &= \|x\|_2 \exp(\rho(x)) \\ &= \|x\|_2 \cos \phi_p^*(x) \frac{\exp(\rho(x))}{\cos \phi_p^*(x)} \\ &= \|x\|_2 \left( \cos(\phi_p^*(x) + \text{atan}(x)) \cos(\text{atan}(x)) \right. \\ &\quad \left. + \sin(\phi_p^*(x) + \text{atan}(x)) \sin(\text{atan}(x)) \right) \frac{\exp(\rho(x))}{\cos \phi_p^*(x)} \\ &= x^T \omega(\phi_p^*(x) + \text{atan}(x)) \frac{\exp(\rho(x))}{\cos \phi_p^*(x)} \\ &= p(x) \cdot x, \end{aligned} \quad (\text{A.2})$$

where

$$p(x) \triangleq \omega(\phi_p^*(x) + \text{atan}(x)) \frac{\exp(\rho(x))}{\cos \phi_p^*(x)}. \quad (\text{A.3})$$

Note that  $\frac{\partial p_1(x)}{\partial x_2} = \frac{\partial p_2(x)}{\partial x_1}$ , we can further obtain the line-integral expression of  $V(x)$ ,

$$V(x) = \int_0^x p(x) dx. \quad (\text{A.4})$$

By condition (3.12), we have  $\cos \phi_p^*(x) > 0$ , so  $V(x) = \|p(x)\|_2 \|x\|_2 \cos \phi_p^*(x)$  is ensured to be positive-definite, which ensures condition (b) in Section 3.2. From (A.3) we know that  $p(x) = [p_1(x) \ p_2(x)]^T$  will not change with respect to  $\|x\|_2$ , thus

$$\begin{aligned} \frac{dp_1(x)}{d\theta} &= -\sin(\phi_p^*(x) + \theta) \frac{\exp(\rho(x))}{\cos \phi_p^*(x)} \left( \frac{d\phi_p^*(x)}{d\theta} + 1 \right) \\ &\quad + \cos(\phi_p^*(x) + \theta) \frac{\exp(\rho(x))}{\cos \phi_p^*(x)} \tan \phi_p^*(x) \\ &\quad + \cos(\phi_p^*(x) + \theta) \frac{\exp(\rho(x))}{\cos^2 \phi_p^*(x)} \sin \phi_p^*(x) \frac{d\phi_p^*(x)}{d\theta} \\ &= -\sin(\phi_p^*(x) + \theta) \frac{\exp(\rho(x))}{\cos \phi_p^*(x)} \left( \frac{d\phi_p^*(x)}{d\theta} + 1 \right) \\ &\quad + \cos(\phi_p^*(x) + \theta) \frac{\exp(\rho(x))}{\cos \phi_p^*(x)} \tan \phi_p^*(x) \left( \frac{d\phi_p^*(x)}{d\theta} + 1 \right) \\ &= -\sin \theta \frac{\exp(\rho(x))}{\cos^2 \phi_p^*(x)} \left( \frac{d\phi_p^*(x)}{d\theta} + 1 \right), \end{aligned}$$

similarly

$$\frac{dp_2(x)}{d\theta} = \cos \theta \frac{\exp(\rho(x))}{\cos^2 \phi_p^*(x)} \left( \frac{d\phi_p^*(x)}{d\theta} + 1 \right).$$

Overall we have

$$\dot{p}(x) = \frac{\dot{\theta} \exp(\rho(x))}{\cos^2 \phi_p^*(x)} \left( \frac{d\phi_p^*(x)}{d\theta} + 1 \right) \begin{bmatrix} -\sin \theta \\ \cos \theta \end{bmatrix}. \quad (\text{A.5})$$

Consequently, the time derivative of  $V(x)$  can be obtained as

$$\dot{V}(x) = p(x) \cdot f_\sigma(x) + \dot{p}(x) \cdot x = p(x) \cdot f_\sigma(x). \quad (\text{A.6})$$

From (A.6) it can be found that  $V(x)$  is continuously differentiable, then condition (a) in Section 2 is ensured. From (A.1) we can know that the radial unbounded condition (c) is also satisfied. So  $V(x)$  is an appropriate line-integral Lyapunov function candidate. From (3.11) and (A.6), we know that  $\dot{V}(x) = \|p(x)\|_2 \|f_\sigma(x)\|_2 \cos(\phi_p^*(x) - \phi_\sigma(x)) \leq 0$  for any  $x$ . Thus the equilibrium of system (3.1) is ensured to be stable under arbitrary switching. Moreover, the strict form of (3.11) ensures  $\dot{V}(x) < 0$ , in which case the asymptotic stability of the equilibrium of system (3.1) under arbitrary switching is guaranteed. The proof is then completed.  $\square$

## A.2 Proof of Lemma 4

In the proof of Lemma 4, we need the following result in (A.7) to know the derivative of function  $\text{atan}(A\omega(\theta))$  with respect to  $\theta$ .

**Lemma 14.** *For any  $A \in \mathbb{R}^{2 \times 2}$  with  $\det(A) > 0$ , the following equation holds*

$$\frac{\partial \text{atan}(A\omega(\theta))}{\partial \theta} = \frac{\det(A)}{\|A\omega(\theta)\|_2^2}. \quad (\text{A.7})$$

*Proof.* Define  $a_{ij}$  ( $i, j = 1, 2$ ) as the  $i$ -th row and  $j$ -th column element of  $A$  and  $[a_1(\theta), a_2(\theta)]^T \triangleq A\omega(\theta)$ . By calculation we get

$$\begin{aligned} \frac{\partial (a_2(\theta)/a_1(\theta))}{\partial \theta} &= \frac{(-a_{i21} \sin \theta + a_{i22} \cos \theta)a_1(\theta)}{a_1^2(\theta)} \\ &\quad - \frac{a_2(\theta)(-a_{i11} \sin \theta + a_{i12} \cos \theta)}{a_1^2(\theta)} \\ &= \frac{a_{11}a_{22} - a_{12}a_{21}}{a_1^2(\theta)} = \frac{\det(A)}{a_1^2(\theta)}. \end{aligned}$$

It follows that

$$\frac{\partial \text{atan}(A\omega(\theta))}{\partial \theta} = \frac{a_1^2(\theta)}{a_1^2(\theta) + a_2^2(\theta)} \frac{\det(A)}{a_1^2(\theta)} = \frac{\det(A)}{\|A\omega(\theta)\|_2^2}.$$

Thus the proof is completed.  $\square$

The **Proof of Lemma 4** will be summarized in the following part.

*Proof.* We construct the proof by a counter-example. In this example, we will find a chattering sequence  $\sigma(t)$ , along which, the system state  $x(t)$  will diverge to infinity. The design process will be divided into three steps. In the first step we will find the sector region for the chattering; in the second step, we will prove that the chattering trajectory will magnify outward to the boundless direction. Finally in the third step, we will confirm the chatter signal  $\sigma(t)$  to achieve such a chattering effect.

**[Step 1.** Find the region  $\theta \in [\theta^*, \theta^* + \varepsilon_2]$  satisfying  $\varphi_{\max}(\theta) - \varphi_{\min}(\theta) > \pi + \varepsilon_1]$

Note that both  $\varphi_{\max}(\theta)$  and  $\varphi_{\min}(\theta)$  are continuous functions. Thus the negation of (3.14) implies that there exist  $\theta^* \in [0, 2\pi)$  and  $\varepsilon_1 > 0$  satisfying

$$\varphi_{\max}(\theta^*) - \varphi_{\min}(\theta^*) = 2\varepsilon_1 + \pi. \quad (\text{A.8})$$

Matrices  $A_i$  ( $i \in \mathcal{Q}$ ) are all Hurwitz matrices, which ensure that, for any  $\theta \in [0, 2\pi)$ ,  $\|A_i\omega(\theta)\|_2^2 > 0$  and  $\det(A_i) > 0$ . Recalling the result in (A.7), one gets the partial

derivative expression of  $\varphi(A_i, \theta)$ ,

$$\frac{\partial \varphi(A_i, \theta)}{\partial \theta} = -1 + \frac{\det(A_i)}{\|A_i \omega(\theta)\|_2^2}.$$

It means that

$$-1 < \frac{\partial \varphi(A_i, \theta)}{\partial \theta} \leq \eta - 1, \quad i \in \mathcal{Q}, \quad (\text{A.9})$$

where  $\eta \triangleq \max_{i \in \mathcal{Q}} \left\{ \frac{\det(A_i)}{\inf_{\theta} \{\|A_i \omega(\theta)\|_2^2\}} \right\}$ . Further, we have

$$-\eta < \frac{\partial \varphi(A_i, \theta)}{\partial \theta} - \frac{\partial \varphi(A_j, \theta)}{\partial \theta} < \eta, \quad \forall \theta \in [0, 2\pi)$$

for all  $i, j \in \mathcal{Q}$ . Choose a real number  $\varepsilon_2 = \frac{\varepsilon_1}{\eta} > 0$ . Then considering (A.8) and based on the mean value theorem, for any  $\theta \in [\theta^*, \theta^* + \varepsilon_2]$ , we have

$$\begin{aligned} \varphi_{\max}(\theta) - \varphi_{\min}(\theta) &= \max_{i, j \in \mathcal{Q}} \{ \varphi(A_i, \theta) - \varphi(A_j, \theta) \} \\ &> \max_{i, j \in \mathcal{Q}} \{ \varphi(A_i, \theta^*) - \varphi(A_j, \theta^*) - \eta(\theta - \theta^*) \} \\ &\geq \varphi_{\max}(\theta^*) - \varphi_{\min}(\theta^*) - \varepsilon_2 \eta \\ &= \pi + \varepsilon_1. \end{aligned} \quad (\text{A.10})$$

**[Step 2.** Prove that  $\cot \varphi_{\min}(\theta) - \cot \varphi_{\max}(\theta) \geq \varepsilon_1$  for all  $\theta \in [\theta^*, \theta^* + \varepsilon_2]$ ]

From part 3.7 in Lemma 3, one may find that, the Hurwitz property of  $A_i$  ( $i \in \mathcal{Q}$ ) ensures  $0 < \varphi(A_i, \theta) < 2\pi$ , consequently  $0 < \varphi_{\min}(\theta) \leq \varphi_{\max}(\theta) < 2\pi$ . Combined with (A.10), the above inequality leads to

$$0 < \varphi_{\min}(\theta) < \pi - \varepsilon_1, \quad \pi + \varepsilon_1 < \varphi_{\max}(\theta) < 2\pi.$$

Also note that  $\cot \phi$  is a monotonically decreasing function for  $\phi \in (0, \pi)$ . Thus from (A.10), it follows that

$$\cot \varphi_{\min}(\theta) > \cot(\varphi_{\max}(\theta) - \pi - \varepsilon_1) = \cot(\varphi_{\max}(\theta) - \varepsilon_1), \quad (\text{A.11})$$

for all  $\theta \in [\theta^*, \theta^* + \varepsilon_2]$ . Further applying mean value theorem, we know that, for any  $\theta \in [\theta^*, \theta^* + \varepsilon_2]$  there exists  $\tilde{\varphi} \in [\varphi_{\max}(\theta) - \varepsilon_1, \varphi_{\max}(\theta)]$  satisfying

$$\cot(\varphi_{\max}(\theta) - \varepsilon_1) = \cot \varphi_{\max}(\theta) + \varepsilon_1 \csc^2 \tilde{\varphi}. \quad (\text{A.12})$$

Note that  $\csc^2 \tilde{\varphi} \geq 1$ , thus combining (A.11) and (A.12) we get

$$\cot \varphi_{\min}(\theta) - \cot \varphi_{\max}(\theta) \geq \varepsilon_1. \quad (\text{A.13})$$

**[Step 3.** Design the switching signal  $\sigma(t)$  such that  $x(t)$  chatters to infinity in sector  $[\theta^*, \theta^* + \varepsilon_2]$

From Equation (4) in ([57]) and using (3.10) for  $A_\sigma \omega(\theta)$ , we obtain

$$\dot{\theta} = \gamma^T(\theta) A_\sigma \omega(\theta) = \|A_\sigma \omega(\theta)\|_2 \sin \varphi_\sigma(\theta), \quad (\text{A.14})$$

$$\frac{1}{r} \dot{r} = \omega^T(\theta) A_\sigma \omega(\theta) = \|A_\sigma \omega(\theta)\|_2 \cos \varphi_\sigma(\theta), \quad (\text{A.15})$$

where  $\gamma(\theta) \triangleq [-\sin \theta \quad \cos \theta]^T$ ,  $\dot{\theta} \triangleq \frac{d\theta}{dt}$  and  $\dot{r} \triangleq \frac{dr}{dt}$ , so that we conclude

$$\frac{1}{r} \dot{r} = \cot \varphi_\sigma(\theta) \dot{\theta}. \quad (\text{A.16})$$

From (A.14) we know that, if  $\sigma(t)$  changes among  $\mathcal{Q}$  such that  $\varphi_\sigma(\theta) = \varphi_{\max}(\theta) > \pi + \varepsilon_1$ , then  $\dot{\theta} < 0$ . On the contrary, if  $\varphi_\sigma(\theta) = \varphi_{\min}(\theta) < \pi - \varepsilon_1$  then  $\dot{\theta} > 0$ . Set the initial state as  $x(0) = r(0)\omega(\theta^*)$ , where  $r(0) > 0$ . And choose the switching signal in the following manner: if  $\theta = \theta^*$  we choose the signal  $\sigma(t)$  such that  $\varphi_\sigma(\theta) = \varphi_{\min}(\theta)$  for all  $\theta(x) \in [\theta^*, \theta^* + \varepsilon_2]$ ; if  $\theta = \theta^* + \varepsilon_2$  we choose the signal  $\sigma(t)$  such that  $\varphi_\sigma(\theta) = \varphi_{\max}(\theta)$  for all  $\theta(x) \in [\theta^*, \theta^* + \varepsilon_2]$ . Denote the sequential switching times at  $\theta = \theta^*$  as  $t_0, t_2, t_4, \dots, t_{2m}, \dots$  and the sequential switching times at  $\theta = \theta^* + \varepsilon_2$  as  $t_1, t_3, t_5, \dots, t_{2m+1}, \dots$  where  $m \in \mathbb{N}_0$ ,  $t_0 = 0$  and  $t_i < t_{i+1}$  for all  $i \in \mathbb{N}_0$ . Now, integrating (A.16) from  $t_0$  to  $t_{2m}$  and considering the relation in (A.13), we then arrive at

$$\begin{aligned} \ln r(t_{2m}) - \ln r(t_0) &= \int_{t_0}^{t_{2m}} \cot \varphi_\sigma(\theta) \dot{\theta} dt \\ &= \sum_{i=0}^{m-1} \left( \int_{t_{2i}}^{t_{2i+1}} \cot \varphi_{\min}(\theta) \dot{\theta} dt + \int_{t_{2i+1}}^{t_{2i+2}} \cot \varphi_{\max}(\theta) \dot{\theta} dt \right) \\ &= \sum_{i=0}^{m-1} \left( \int_{\theta^*}^{\theta^* + \varepsilon_2} \cot \varphi_{\min}(\theta) d\theta + \int_{\theta^* + \varepsilon_2}^{\theta^*} \cot \varphi_{\max}(\theta) d\theta \right) \\ &= m \int_{\theta^*}^{\theta^* + \varepsilon_2} (\cot \varphi_{\min}(\theta) - \cot \varphi_{\max}(\theta)) d\theta \\ &> m \varepsilon_1 \varepsilon_2. \end{aligned}$$

It means that  $r(t_{2m}) > r(0) \exp(m \varepsilon_1 \varepsilon_2)$ . Apparently as  $t_{2m}$  goes to infinity,  $r(t_{2m})$  increases to infinity. So, under the specially constructed switching law, the equilibrium of system (3.1) is unstable. The necessity of (3.14) is then proven.  $\square$

### A.3 Proof of Theorem 3

Before the proof of Theorem 3, we need to explain why the *if* conditions in criteria (3.18) and (3.19) are needed. Clearly, if  $\inf\{\varphi_{\max}(\theta)\} \leq \pi$ , there may exist the case



that  $\varphi_{\max}(\theta) = \pi$  for some  $\theta$ , then the function  $\cot \varphi_{\max}(\theta)$  is not properly defined. It will be impossible for us to design the integral condition of  $\cot \varphi_{\max}(\theta)$  similar to that in (3.13). In this case we can construct another modified function  $\varphi_{\max \epsilon}(\theta)$  which is always bigger than  $\pi$  and satisfying  $\pi < \varphi_{\max \epsilon}(\theta) < 2\pi$ ,

$$\varphi_{\max \epsilon}(\theta) \triangleq \max \{ \varphi_{\max}(\theta), \pi + \epsilon \}, \quad (\text{A.17})$$

where  $\epsilon$  is a small positive value satisfying  $0 < \epsilon < \pi$ . Specially, if we choose  $\epsilon$  as

$$\epsilon \triangleq \frac{1}{10} \min \left\{ 2\pi - \sup \{ \varphi_{\max}(\theta) \}, \inf \{ \varphi_{\min}(\theta) \} \right\}, \quad (\text{A.18})$$

we can find that the integration of  $\cot \varphi_{\max \epsilon}(\theta)$  from 0 to  $2\pi$  will never be negative. This property can be summarized as Lemma 15.

**Lemma 15.** *If  $\inf \{ \varphi_{\max}(\theta) \} \leq \pi$ , then the integration of  $\cot \varphi_{\max \epsilon}(\theta)$  should always be equal to or greater than 0, mathematically it can be expressed as*

$$\int_0^{2\pi} \cot \varphi_{\max \epsilon}(\theta) d\theta \geq 0, \quad (\text{A.19})$$

where  $\varphi_{\max \epsilon}(\theta)$  is defined in (A.17) and  $\epsilon$  is a scalar obtained from (A.18).

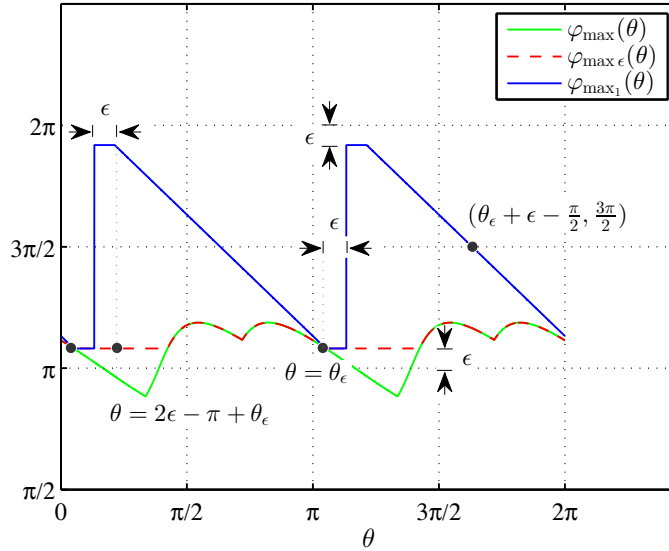


Figure A.1: Layouts of functions  $\varphi_{\max}(\theta)$ ,  $\varphi_{\max \epsilon}(\theta)$  and  $\varphi_{\max_1}(\theta)$

*Proof.* To prove that  $\int_0^{2\pi} \cot \varphi_{\max \epsilon}(\theta) d\theta \geq 0$ , we need to construct an assistant periodical function  $\varphi_{\max_1}(\theta) = \varphi_{\max_1}(\theta + \pi)$  which is not smaller than  $\varphi_{\max \epsilon}(\theta)$  and satisfying

$$\int_0^{2\pi} \cot \varphi_{\max_1}(\theta) d\theta = 0. \quad (\text{A.20})$$

Assume that  $\theta_\epsilon \in [0, \pi)$  is one intersection point of  $\varphi_{\max}(\theta)$  and horizontal line  $\pi + \epsilon$ , then  $\varphi_{\max_1}(\theta)$  can be constructed as a symmetric function around point  $(\theta_\epsilon + \epsilon - \frac{\pi}{2}, \frac{3\pi}{2})$ ,

$$\varphi_{\max_1}(\theta) \triangleq \begin{cases} 2\pi - \epsilon, & \theta - \theta_\epsilon \in (\epsilon - \pi, 2\epsilon - \pi]; \\ \pi + \epsilon - (\theta - \theta_\epsilon), & \theta - \theta_\epsilon \in (2\epsilon - \pi, 0]; \\ \pi + \epsilon, & \theta - \theta_\epsilon \in (0, \epsilon]. \end{cases}$$

Apparently (A.20) is satisfied since  $\varphi_{\max_1}(\theta)$  is symmetric around point  $(\theta_\epsilon + \epsilon - \frac{\pi}{2}, \frac{3\pi}{2})$ . From (A.9) we know that for any  $\theta \in (2\epsilon - \pi + \theta_\epsilon, \theta_\epsilon]$ , it holds that

$$\varphi_{\max}(\theta) \leq \varphi_{\max}(\theta_\epsilon) - (\theta - \theta_\epsilon) = \varphi_{\max_1}(\theta). \quad (\text{A.21})$$

Actually (A.21) can be satisfied for any  $\theta$ , thus

$$\int_0^{2\pi} \cot \varphi_{\max \epsilon}(\theta) d\theta \geq \int_0^{2\pi} \cot \varphi_{\max_1}(\theta) d\theta = 0. \quad (\text{A.22})$$

The proof is completed.  $\square$

We now provide the **proof of Theorem 3** in the following part. For convenience, firstly we recall of content of it here.

**Theorem 3.** *A necessary and sufficient condition for the stability of the equilibrium of system (3.1) under arbitrary switching is that*

$$\sup\{\varphi_{\max}(\theta) - \varphi_{\min}(\theta)\} \leq \pi, \quad (3.17)$$

and

$$\inf\{\varphi_{\max}(\theta)\} \leq \pi \quad \text{or} \quad \int_0^{2\pi} \cot \varphi_{\max}(\theta) d\theta \geq 0, \quad \text{if } \inf\{\varphi_{\max}(\theta)\} > \pi, \quad (3.18)$$

$$\sup\{\varphi_{\min}(\theta)\} \geq \pi \quad \text{or} \quad \int_0^{2\pi} \cot \varphi_{\min}(\theta) d\theta \leq 0, \quad \text{if } \sup\{\varphi_{\min}(\theta)\} < \pi. \quad (3.19)$$

Moreover, the equilibrium of system (3.1) is asymptotically stable if all the involved inequalities are satisfied as strict ones.

*Proof. (Sufficiency)*

The proof of sufficiency will be divided into three steps. In the first step, we will construct new phase functions  $\hat{\varphi}_{\max}(\theta)$  and  $\hat{\varphi}_{\min}(\theta)$  which can avoid the *if* conditions in criteria (3.18) and (3.19). In the second step, we will find the appropriate phase function  $\varphi_p^*(\theta)$  of Lyapunov function which is located between  $\hat{\varphi}_{\max}(\theta)$  and  $\hat{\varphi}_{\min}(\theta)$ , and criterion  $\int_0^{2\pi} \tan \varphi_p^*(\theta) d\theta = 0$  in Proposition 2. In the third step, the case of asymptotic stability will be discussed.

**[Step 1.** Construct new functions  $\hat{\varphi}_{\max}(\theta)$  and  $\hat{\varphi}_{\min}(\theta)$  such that  $\cot \hat{\varphi}_{\min}(\theta)$  and  $\cot \hat{\varphi}_{\max}(\theta)$  are well defined and satisfying  $\int_0^{2\pi} \cot \hat{\varphi}_{\min}(\theta) d\theta \leq 0 \leq \int_0^{2\pi} \cot \hat{\varphi}_{\max}(\theta) d\theta$ ].

Define  $\varphi_{\min \epsilon}(\theta)$  as

$$\varphi_{\min \epsilon}(\theta) \triangleq \min \{ \varphi_{\min}(\theta), \pi - \epsilon \},$$

where  $\epsilon$  is defined in (A.18). Following the proof of Lemma 15, we know that, if  $\sup \{ \varphi_{\min}(\theta) \} \geq \pi$ , then

$$\int_0^{2\pi} \cot \varphi_{\min \epsilon}(\theta) d\theta \leq 0. \quad (\text{A.23})$$

Define the following new functions to cover both cases of the *if* conditions in (3.18) and (3.19)

$$\hat{\varphi}_{\max}(\theta) \triangleq \begin{cases} \varphi_{\max \epsilon}(\theta), & \inf \{ \varphi_{\max}(\theta) \} \leq \pi; \\ \varphi_{\max}(\theta), & \inf \{ \varphi_{\max}(\theta) \} > \pi, \end{cases} \quad (\text{A.24})$$

$$\hat{\varphi}_{\min}(\theta) \triangleq \begin{cases} \varphi_{\min \epsilon}(\theta), & \sup \{ \varphi_{\min}(\theta) \} \geq \pi; \\ \varphi_{\min}(\theta), & \sup \{ \varphi_{\min}(\theta) \} < \pi. \end{cases} \quad (\text{A.25})$$

By (A.19) and (3.18) we can assert that

$$\int_0^{2\pi} \cot \hat{\varphi}_{\max}(\theta) d\theta \geq 0. \quad (\text{A.26})$$

Similarly by (3.19) and (A.23), for any  $\varphi_{\min}(\theta)$ , one has

$$\int_0^{2\pi} \cot \hat{\varphi}_{\min}(\theta) d\theta \leq 0. \quad (\text{A.27})$$

Moreover, the definitions in (A.24) and (A.25) also ensure that

$$0 < \hat{\varphi}_{\min}(\theta) < \pi < \hat{\varphi}_{\max}(\theta) < 2\pi, \quad (\text{A.28})$$

and

$$\hat{\varphi}_{\min}(\theta) < \varphi_{\sigma}(\theta) < \hat{\varphi}_{\max}(\theta). \quad (\text{A.29})$$

**[Step 2.** Construct the desired phase function  $\varphi_p^*(\theta)$  based on the weighted sum of  $\hat{\varphi}_{\max}(\theta)$  and  $\hat{\varphi}_{\min}(\theta)$ ]

Construct the new variable  $\hat{\varphi}(\theta, \alpha)$  which is a continuous function of  $\theta$  and  $\alpha \in$

$[0, 1]$ ,

$$\hat{\varphi}(\theta, \alpha) \triangleq \alpha \cdot (\hat{\varphi}_{\max}(\theta) - \frac{3\pi}{2}) + (1 - \alpha) \cdot (\hat{\varphi}_{\min}(\theta) - \frac{\pi}{2}). \quad (\text{A.30})$$

Based on (A.26) and (A.27), we know  $\hat{\varphi}(\theta, \alpha)$  possesses the property that

$$\int_0^{2\pi} \tan \hat{\varphi}(\theta, 0) d\theta \geq 0, \quad \int_0^{2\pi} \tan \hat{\varphi}(\theta, 1) d\theta \leq 0.$$

The function  $\int_0^{2\pi} \tan \hat{\varphi}(\theta, \alpha) d\theta$  is continuous with respect to  $\alpha \in [0, 1]$ . Based on the intermediate value theorem, we know that there exists an  $\tilde{\alpha} \in [0, 1]$  satisfying

$$\int_0^{2\pi} \tan \hat{\varphi}(\theta, \tilde{\alpha}) d\theta = 0. \quad (\text{A.31})$$

Thus criterion (3.13) is satisfied. Recalling the definition in (A.18), we may find the relation

$$\varphi_{\min}(\theta) \geq 10\epsilon, \quad \varphi_{\max}(\theta) \leq 2\pi - 10\epsilon.$$

Then the following inequalities will also be ensured,

$$\begin{aligned} \varphi_{\max}(\theta) - (\pi - \epsilon) &\leq \pi - 9\epsilon \leq \pi, \\ (\pi + \epsilon) - \varphi_{\min}(\theta) &\leq \pi - 9\epsilon \leq \pi, \\ (\pi + \epsilon) - (\pi - \epsilon) &\leq 2\epsilon \leq \pi. \end{aligned}$$

Together with the condition in (3.17), we know that  $\hat{\varphi}_{\max}(\theta) - \hat{\varphi}_{\min}(\theta) \leq \pi$ , which equivalently means

$$\hat{\varphi}_{\max}(\theta) - \frac{3\pi}{2} \leq \hat{\varphi}_{\min}(\theta) - \frac{\pi}{2}. \quad (\text{A.32})$$

The definition in (A.30) ensures that  $\hat{\varphi}(\theta, \tilde{\alpha})$  has value between  $\hat{\varphi}_{\max}(\theta) - \frac{3\pi}{2}$  and  $\hat{\varphi}_{\min}(\theta) - \frac{\pi}{2}$ ,

$$\hat{\varphi}_{\max}(\theta) - \frac{3\pi}{2} \leq \hat{\varphi}(\theta, \tilde{\alpha}) \leq \hat{\varphi}_{\min}(\theta) - \frac{\pi}{2}. \quad (\text{A.33})$$

So together with (A.29), inequality (A.33) indicates that criterion (3.11) can be satisfied,

$$\varphi_{\sigma}(\theta) - \frac{3\pi}{2} \leq \hat{\varphi}(\theta, \tilde{\alpha}) \leq \varphi_{\sigma}(\theta) - \frac{\pi}{2}. \quad (\text{A.34})$$

Considering (A.28) and (A.33), we know that criterion (3.12) is also ensured,

$$-\frac{\pi}{2} < \hat{\varphi}(\theta, \tilde{\alpha}) < \frac{\pi}{2}. \quad (\text{A.35})$$

Combined with criterion (A.31), the criteria (A.34) and (A.35) imply that  $\hat{\varphi}(\theta, \tilde{\alpha})$  can be regarded as the desired phase function  $\varphi_p^*(\theta)$  which guarantees the stability of the equilibrium of system (3.1). Based on the statement in Proposition 2, the sufficiency of (3.17)–(3.19) for stability is thus proven.

**[Step 3.** Proof of asymptotic stability in the case of strict inequalities]

Moreover, if all the involved inequalities are satisfied as strict ones, parameter  $\tilde{\alpha}$  in (A.31) will be restricted by  $0 < \tilde{\alpha} < 1$  and the constraint in (A.32) will be strengthened as strict inequality. Therefore, (A.33) becomes strict inequality, and so is (A.34). By Proposition 2, the equilibrium of system (3.1) can be guaranteed to be asymptotically stable if all the involved inequalities are satisfied as strict ones.

**(Necessity)**

Lemma 4 ensures the necessity of (3.17). The remaining work is the proof of the necessity of (3.18) and (3.19). We finish this part by a pseudo-proposition of (3.18) which can be stated as

$$\inf\{\varphi_{\max}(\theta)\} > \pi \quad \text{and} \quad \int_0^{2\pi} \cot \varphi_{\max}(\theta) d\theta > 0. \quad (\text{A.36})$$

From (A.14), if the switching sequence  $\sigma(t)$  is chosen to ensure  $\varphi_\sigma(\theta) = \varphi_{\max}(\theta)$ , then  $\dot{\theta} < 0$  can be guaranteed by the first inequality in (A.36). Denote the initial state as  $x(0) = r(0)\omega(\theta_0)$  where  $r(0) > 0$ , and the time sequence at  $\theta = \theta_0$  as  $t_0, t_1, t_2, \dots, t_m, \dots$  where  $m \in \mathbb{N}_0$ ,  $t_0 = 0$  and  $t_i < t_{i+1}$  for all  $i \in \mathbb{N}_0$ . Based on the polar coordinate model, we get  $r(t_m) = r(0)\exp(m\varepsilon)$ , where  $\varepsilon = \int_0^{2\pi} \cot \varphi_{\max}(\theta) d\theta > 0$ . It means that  $r(t_m)$  goes to infinity as  $t_m$  increases and then the equilibrium of system (3.1) under the designed switching strategy is unstable. Similarly, without condition (3.19) the equilibrium of system (3.1) is unstable under the switching sequence  $\sigma(t)$  that satisfies  $\varphi_\sigma(\theta) = \varphi_{\min}(\theta)$ . The proof of necessity is then completed.  $\square$

# Appendix B

## Proofs in Chapter 4

### B.1 Proof of Lemma 6

*Proof.* Considering the properties of  $\varphi(A, \theta)$  in (4.4), one has

$$\begin{aligned}\underline{\mathcal{S}}(A^{-1}, \alpha) &= \{\theta | \varphi(A^{-1}, \theta) = \pi - \alpha_1, \alpha_1 \geq \alpha\} \\ &= \{\theta | \varphi(R(-\alpha_1)A^{-1}, \theta) = \pi, \alpha_1 \geq \alpha\}.\end{aligned}$$

The equation  $\varphi(R(-\alpha_1)A^{-1}, \theta) = \pi$  means that  $\omega(\theta)$  is an eigenvector of matrix  $R(-\alpha_1)A^{-1}$ . So  $\omega(\theta)$  should also be an eigenvector of its inverse matrix  $AR(\alpha_1)$ , as a result

$$\underline{\mathcal{S}}(A^{-1}, \alpha) = \{\theta | \varphi(AR(\alpha_1), \theta) = \pi, \alpha_1 \geq \alpha\}.$$

Also considering the relation in (4.4) and (4.5), we can get

$$\begin{aligned}\underline{\mathcal{S}}(A^{-1}, \alpha) &= \{\theta | \varphi(R(\alpha_1)A, \theta + \alpha_1) = \pi, \alpha_1 \geq \alpha\} \\ &= \{\theta | \varphi(A, \theta + \alpha_1) = \pi + \alpha_1, \alpha_1 \geq \alpha\}.\end{aligned}$$

To check whether the value of  $\alpha_1$  can be replaced with  $\alpha$  based on relation  $\alpha_1 \geq \alpha$ , we define the new set  $\bar{\mathcal{S}}^*(A, \alpha)$  in (B.1) and compare its relation with  $\underline{\mathcal{S}}(A^{-1}, \alpha)$ . The definition goes like this

$$\bar{\mathcal{S}}^*(A, \alpha) \triangleq \{\theta | \varphi(A, \theta + \alpha) \geq \pi + \alpha\}. \quad (\text{B.1})$$

For any  $\bar{\theta} \in \underline{\mathcal{S}}(A^{-1}, \alpha)$ , there exist the corresponding  $\alpha_1 \geq \alpha$  and  $\theta^*$  satisfying

$$\theta^* = \bar{\theta} + \alpha_1, \quad \varphi(A, \theta^*) = \pi + \alpha_1.$$

In light of this and considering the Taylor mean value theorem, one can get

$$\varphi(A, \bar{\theta} + \alpha) = \varphi(A, \theta^* - \alpha_1 + \alpha)$$

$$= \pi + \alpha_1 + \left. \frac{\partial \varphi(A, \theta)}{\partial \theta} \right|_{\theta=\hat{\theta}} (\alpha - \alpha_1), \quad (\text{B.2})$$

where  $\hat{\theta}$  is a real value satisfying  $\theta^* \leq \hat{\theta} \leq (\theta^* + \alpha_1 - \alpha)$ . It has been verified in [117] that  $\frac{\partial \varphi(A, \theta)}{\partial \theta} > -1$ , then the following inequalities can be ensured,

$$\varphi(A, \bar{\theta} + \alpha) > \pi + \alpha_1 + (\alpha - \alpha_1) = \pi + \alpha.$$

It means that  $\bar{\theta} \in \bar{\mathcal{S}}^*(A, \alpha)$  and then  $\underline{\mathcal{S}}(A^{-1}, \alpha) \subset \bar{\mathcal{S}}^*(A, \alpha)$ . Next, define the new function  $\tilde{\varphi}(\theta)$  which satisfies

$$\varphi(A, \theta + \tilde{\varphi}(\theta)) = \pi + \tilde{\varphi}(\theta). \quad (\text{B.3})$$

From (B.3) we can obtain the following derivative expression,

$$\frac{d\tilde{\varphi}(\theta)}{d\theta} = \frac{\frac{\partial \varphi(A, \theta)}{\partial \theta}}{1 + \frac{\partial \varphi(A, \theta)}{\partial \theta}} = 1 - \frac{1}{1 + \frac{\partial \varphi(A, \theta)}{\partial \theta}} < 1. \quad (\text{B.4})$$

With phase angle  $\tilde{\varphi}(\theta)$ , sets  $\underline{\mathcal{S}}(A^{-1}, \alpha)$  and  $\bar{\mathcal{S}}^*(A, \alpha)$  can be re-written in the following equivalent form

$$\begin{aligned} \underline{\mathcal{S}}(A^{-1}, \alpha) &= \{\theta | \theta = \theta^*, \tilde{\varphi}(\theta^*) \geq \alpha\}, \\ \bar{\mathcal{S}}^*(A, \alpha) &= \{\theta | \theta = \theta^* - \alpha_1 + \alpha, \tilde{\varphi}(\theta^*) = \alpha_1, \alpha_1 > \alpha\}. \end{aligned}$$

Similarly for any  $\bar{\theta} \in \bar{\mathcal{S}}^*(A, \alpha)$ , there exist the corresponding  $\alpha_1 \geq \alpha$  and  $\theta^*$  satisfying

$$\bar{\theta} = \theta^* - \alpha_1 + \alpha, \quad \tilde{\varphi}(\theta^*) = \alpha_1.$$

By Taylor's mean value theorem and the relation in (B.4), one has

$$\tilde{\varphi}(\bar{\theta}) = \tilde{\varphi}(\theta^* - \alpha_1 + \alpha) = \alpha_1 + \left. \frac{d\tilde{\varphi}(\theta)}{d\theta} \right|_{\theta=\hat{\theta}} (\alpha - \alpha_1) > \alpha, \quad (\text{B.5})$$

where  $\theta^* \leq \hat{\theta} \leq (\theta^* + \alpha_1 - \alpha)$ . It means that  $\bar{\theta} \in \underline{\mathcal{S}}(A^{-1}, \alpha)$  and then  $\bar{\mathcal{S}}^*(A, \alpha) \subset \underline{\mathcal{S}}(A^{-1}, \alpha)$ . Consequently, sets  $\bar{\mathcal{S}}^*(A, \alpha)$  and  $\underline{\mathcal{S}}(A^{-1}, \alpha)$  are equivalent. Then the following relation holds

$$\underline{\mathcal{S}}(A^{-1}, \alpha) = \bar{\mathcal{S}}^*(A, \alpha) = \{\theta | \theta = \theta^* - \alpha, \varphi(A, \theta^*) \geq \pi + \alpha\},$$

which can be also equivalently written as

$$\underline{\mathcal{S}}(A^{-1}, \alpha) = \{\theta | \theta = \theta^* - \alpha, \theta^* \in \bar{\mathcal{S}}(A, \alpha)\}.$$

The proof is completed. □

## B.2 Proof of Lemma 7

*Proof.* From Lemma 6, we get

$$\underline{\mathcal{S}}(A_i, 0) = \bar{\mathcal{S}}(A_i^{-1}, 0).$$

It means that, for a given  $\theta$ , if  $\varphi(A_i, \theta) \leq \pi$  then  $\varphi(A_i^{-1}, \theta) \geq \pi$ , consequently

$$\min \{ \varphi(A_i, \theta), \varphi(A_i^{-1}, \theta) \} \leq \pi \leq \max \{ \varphi(A_i, \theta), \varphi(A_i^{-1}, \theta) \}, \quad (\text{B.6})$$

for  $i = 1, 2, \dots, q$ . As a result we know that

$$0 < \hat{\varphi}_{\min}(\theta) \leq \pi \leq \hat{\varphi}_{\max}(\theta) < 2\pi. \quad (\text{B.7})$$

If for some  $\theta^*$  it holds that  $\hat{\varphi}_{\min}(\theta^*) = \pi$ , then

$$\min \{ \varphi(A_i, \theta^*), \varphi(A_i^{-1}, \theta^*) \} \geq \pi, \quad i = 1, 2, \dots, q.$$

Together with (B.6), we can assert that

$$\min \{ \varphi(A_i, \theta^*), \varphi(A_i^{-1}, \theta^*) \} = \pi, \quad i = 1, 2, \dots, q.$$

Certainly it means that at least one of  $\varphi(A_i, \theta^*)$  and  $\varphi(A_i^{-1}, \theta^*)$  is equal to  $\pi$ . Assuming that  $\varphi(A_i, \theta^*) = \pi$ , then there exists negative real number  $\lambda^*$  such that  $A_i x(\theta^*) = \lambda^* x(\theta^*)$ . Apparently  $A_i^{-1} x(\theta^*) = \frac{1}{\lambda^*} x(\theta^*)$ , which means  $\varphi(A_i^{-1}, \theta^*) = \pi$ . Overall we arrive at the result

$$\hat{\varphi}_{\min}(\theta) = \pi = \hat{\varphi}_{\max}(\theta).$$

Similarly the assumption  $\hat{\varphi}_{\max}(\theta^*) = \pi$  will infer the same result. From this point of view, one can assert that if one of  $\hat{\varphi}_{\min}(\theta)$  and  $\hat{\varphi}_{\max}(\theta)$  is equal to  $\pi$  for some variable  $\theta^*$ , then  $\hat{\varphi}_{\min}(\theta)$  and  $\hat{\varphi}_{\max}(\theta)$  must be equivalent to each other at  $\theta^*$ . In other words, the condition  $\hat{\varphi}_{\max}(\theta) \neq \hat{\varphi}_{\min}(\theta)$  for all  $\theta$  ensures the following relation

$$0 < \hat{\varphi}_{\min}(\theta) < \pi < \hat{\varphi}_{\max}(\theta) < 2\pi.$$

It means that both integrals in (4.14) are well defined. Before proceeding to any further analysis, let us make the following definitions

$$\bar{\mathcal{S}}_{\max}(\alpha) \triangleq \left\{ \theta \mid \hat{\varphi}_{\max}(\theta) \geq \frac{3\pi}{2} + \alpha \right\}, \quad \underline{\mathcal{S}}_{\max}(\alpha) \triangleq \left\{ \theta \mid \hat{\varphi}_{\max}(\theta) < \frac{3\pi}{2} - \alpha \right\},$$



$$\bar{\mathcal{S}}_{\min}(\alpha) \triangleq \left\{ \theta | \hat{\varphi}_{\min}(\theta) > \frac{\pi}{2} + \alpha \right\}, \quad \mathcal{S}_{\min}(\alpha) \triangleq \left\{ \theta | \hat{\varphi}_{\min}(\theta) \leq \frac{\pi}{2} - \alpha \right\}.$$

where  $\bar{\mathcal{S}}_{\max}(\alpha)$  means the domain of  $\hat{\varphi}_{\max}(\theta)$  with value above  $\frac{3\pi}{2}$ , similarly definitions for  $\mathcal{S}_{\max}(\alpha)$ ,  $\bar{\mathcal{S}}_{\min}(\alpha)$  and  $\mathcal{S}_{\min}(\alpha)$ . Alternatively the above sets can be constructed by the following expressions which are in the form of sets union,

$$\begin{aligned} \bar{\mathcal{S}}_{\max}(\alpha) &= \bigcup_{i=1}^r \bar{\mathcal{S}}(A_i, \alpha + \frac{\pi}{2}) \cup \bar{\mathcal{S}}(A_i^{-1}, \alpha + \frac{\pi}{2}), \quad \mathcal{S}_{\max}(\alpha) = \mathbb{R} \setminus \bar{\mathcal{S}}_{\max}(-\alpha), \\ \mathcal{S}_{\min}(\alpha) &= \bigcup_{i=1}^r \mathcal{S}(A_i, \alpha + \frac{\pi}{2}) \cup \mathcal{S}(A_i^{-1}, \alpha + \frac{\pi}{2}), \quad \bar{\mathcal{S}}_{\min}(\alpha) = \mathbb{R} \setminus \bar{\mathcal{S}}_{\min}(-\alpha). \end{aligned}$$

Considering (4.7), we may find that sets  $\mathcal{S}_{\min}(\alpha)$  and  $\bar{\mathcal{S}}_{\min}(\alpha)$  can be obtained by adding value  $\alpha + \frac{\pi}{2}$  to each element of sets  $\bar{\mathcal{S}}_{\max}(\alpha)$  and  $\mathcal{S}_{\max}(\alpha)$  respectively, that is

$$\mathcal{S}_{\min}(\alpha) = \left\{ \theta | \theta = \theta^* + \alpha + \frac{\pi}{2}, \theta^* \in \bar{\mathcal{S}}_{\max}(\alpha) \right\}, \quad (\text{B.8})$$

$$\bar{\mathcal{S}}_{\min}(\alpha) = \left\{ \theta | \theta = \theta^* + \alpha + \frac{\pi}{2}, \theta^* \in \mathcal{S}_{\max}(\alpha) \right\}. \quad (\text{B.9})$$

Denote the supremum and infimum values of  $\hat{\varphi}_{\max}(\theta)$  and  $\hat{\varphi}_{\min}(\theta)$  as

$$\begin{aligned} \hat{\varphi}_{\overline{\max}} &\triangleq \sup \{ \hat{\varphi}_{\max}(\theta) \}, \quad \hat{\varphi}_{\underline{\max}} \triangleq \inf \{ \hat{\varphi}_{\max}(\theta) \}, \\ \hat{\varphi}_{\overline{\min}} &\triangleq \sup \{ \hat{\varphi}_{\min}(\theta) \}, \quad \hat{\varphi}_{\underline{\min}} \triangleq \inf \{ \hat{\varphi}_{\min}(\theta) \}. \end{aligned}$$

From Lemma 6, intuitively one can find the following relations of the above supremum and infimum values,

$$\hat{\varphi}_{\overline{\max}} + \hat{\varphi}_{\underline{\min}} = 2\pi, \quad \hat{\varphi}_{\underline{\max}} + \hat{\varphi}_{\overline{\min}} = 2\pi. \quad (\text{B.10})$$

In addition, equations in (B.8) and (B.9) also indicate that the Lebesgue measures [100] of  $\bar{\mathcal{S}}_{\max}(\alpha)$  and  $\mathcal{S}_{\max}(\alpha)$  are equivalent to that of  $\mathcal{S}_{\min}(\alpha)$  and  $\bar{\mathcal{S}}_{\min}(\alpha)$  respectively, namely

$$\mu_L(\bar{\mathcal{S}}_{\max}(\alpha)) = \mu_L(\mathcal{S}_{\min}(\alpha)), \quad \mu_L(\mathcal{S}_{\max}(\alpha)) = \mu_L(\bar{\mathcal{S}}_{\min}(\alpha)).$$

Note that any  $\varphi(A_i, \alpha)$  or  $\varphi(A_i^{-1}, \alpha)$  is periodical with period  $2\pi$ , so  $\bar{\mathcal{S}}_{\max}(\alpha)$ ,  $\mathcal{S}_{\max}(\alpha)$ ,  $\bar{\mathcal{S}}_{\min}(\alpha)$  and  $\mathcal{S}_{\min}(\alpha)$  should also be periodical with period  $2\pi$ . Consequently the following equations also hold,

$$\mu_L(\bar{\mathcal{E}}_{\max}(\alpha)) = \mu_L(\mathcal{E}_{\min}(\alpha)), \quad \mu_L(\mathcal{E}_{\max}(\alpha)) = \mu_L(\bar{\mathcal{E}}_{\min}(\alpha)), \quad (\text{B.11})$$

with the new notations being defined as

$$\begin{aligned}\bar{\mathcal{E}}_{\max}(\alpha) &\triangleq \bar{\mathcal{S}}_{\max}(\alpha) \cap [0, 2\pi), & \mathcal{E}_{\max}(\alpha) &\triangleq \mathcal{S}_{\max}(\alpha) \cap [0, 2\pi), \\ \bar{\mathcal{E}}_{\min}(\alpha) &\triangleq \bar{\mathcal{S}}_{\min}(\alpha) \cap [0, 2\pi), & \mathcal{E}_{\min}(\alpha) &\triangleq \mathcal{S}_{\min}(\alpha) \cap [0, 2\pi).\end{aligned}$$

where  $\bar{\mathcal{E}}_{\max}(\alpha)$  describes the value of  $\bar{\mathcal{S}}_{\max}(\alpha)$  in the domain  $[0, 2\pi)$ , and similarly for  $\mathcal{E}_{\max}(\alpha)$ ,  $\bar{\mathcal{E}}_{\min}(\alpha)$  and  $\mathcal{E}_{\min}(\alpha)$ . It's true that the single integral of  $\tan(\theta)$  can be transformed as the double integral of  $\frac{1}{\cos^2 \theta}$ . Then by changing the order of double integral, we will get

$$\begin{aligned}& \int_0^{2\pi} \tan(\hat{\varphi}_{\max}(\theta) - \frac{3\pi}{2}) d\theta \\&= \int_0^{2\pi} \int_0^{\hat{\varphi}_{\max}(\theta) - \frac{3\pi}{2}} \frac{1}{\cos^2 \alpha} d\alpha d\theta \\&= \int_0^{\hat{\varphi}_{\max} - \frac{3\pi}{2}} \frac{1}{\cos^2(\alpha)} d\alpha \int_{\bar{\mathcal{E}}_{\max}(\alpha)} d\theta - \int_{\hat{\varphi}_{\max} - \frac{3\pi}{2}}^0 \frac{1}{\cos^2(\alpha)} d\alpha \int_{\mathcal{E}_{\max}(\alpha)} d\theta \\&= \int_0^{\hat{\varphi}_{\max} - \frac{3\pi}{2}} \frac{\mu_L(\bar{\mathcal{E}}_{\max}(\alpha))}{\cos^2(\alpha)} d\alpha - \int_{\hat{\varphi}_{\max} - \frac{3\pi}{2}}^0 \frac{\mu_L(\mathcal{E}_{\max}(\alpha))}{\cos^2(\alpha)} d\alpha.\end{aligned}\tag{B.12}$$

Considering (B.11) and (B.10), we may further obtain

$$\begin{aligned}& \int_0^{2\pi} \tan(\hat{\varphi}_{\max}(\theta) - \frac{3\pi}{2}) d\theta \\&= \int_0^{\frac{\pi}{2} - \hat{\varphi}_{\min}} \frac{\mu_L(\mathcal{E}_{\min}(\alpha))}{\cos^2(\alpha)} d\alpha - \int_{\frac{\pi}{2} - \hat{\varphi}_{\min}}^0 \frac{\mu_L(\bar{\mathcal{E}}_{\min}(\alpha))}{\cos^2(\alpha)} d\alpha \\&= \int_0^{\frac{\pi}{2} - \hat{\varphi}_{\min}} \frac{1}{\cos^2(\alpha)} d\alpha \int_{\mathcal{E}_{\min}(\alpha)} d\theta - \int_{\frac{\pi}{2} - \hat{\varphi}_{\min}}^0 \frac{1}{\cos^2(\alpha)} d\alpha \int_{\bar{\mathcal{E}}_{\min}(\alpha)} d\theta \\&= \int_0^{2\pi} \int_0^{\hat{\varphi}_{\min}(\theta) - \frac{\pi}{2}} \frac{-1}{\cos^2(\alpha)} d\alpha d\theta \\&= - \int_0^{2\pi} \tan(\hat{\varphi}_{\min}(\theta) - \frac{\pi}{2}) d\theta.\end{aligned}\tag{B.13}$$

Note that  $\cot(\theta) = -\tan(\theta - \frac{\pi}{2}) = -\tan(\theta - \frac{3\pi}{2})$ , we can thus confirm the following equality,

$$\int_0^{2\pi} \cot \hat{\varphi}_{\max}(\theta) d\theta + \int_0^{2\pi} \cot \hat{\varphi}_{\min}(\theta) d\theta = 0.$$

The proof is then completed. □

# Appendix C

## Explanation of the algorithms in Chapter 5

### C.1 Explanation of Algorithm 1

**Algorithm 1:** Vertices calculation method for type-1 T-S fuzzy system.

**Step 1.** Calculate the minimum and maximum value of  $h_i(x)$

$$h_{i \min} = \min_x \{h_i(x)\}, \quad h_{i \max} = \max_x \{h_i(x)\}$$

for all  $i = 1, 2, \dots, p$ .

**Step 2.** The minimum value of  $\bar{h}_q(x)$  should be 0. Referring to (5.8), we can calculate the maximum value of  $\bar{h}_q(x)$  as

$$\alpha_{qk} = \bar{h}_{(q+k)p \max} = \frac{1}{\delta} (h_{(q+k)p \max} - h_{(q+k)p \min}) \quad (\text{C.1})$$

for all  $q = 1, 2, \dots, p$  and  $k = 0, 1, \dots, p-1$ .

**Step 3.** Create new variable  $\beta_{qmk}$  as

$$\beta_{qm0} = \alpha_{q0} \quad \text{and} \quad \beta_{qmk} = \alpha_{q(m+k-1)p-1} \quad (\text{C.2})$$

for all  $q = 1, 2, \dots, p$ ,  $m = 1, 2, \dots, p-1$ , and  $k = 1, 2, \dots, p-1$ .

**Step 4.**

For all  $q = 1, 2, \dots, p$  and  $m = 1, 2, \dots, p-1$ ,

4.1 set  $k = 1$ .

4.2 check whether the condition  $\beta_{qmk} \geq 1 - \sum_{i=0}^{k-1} \beta_{qmi}$  is satisfied,

if  $\beta_{qmk} \leq 1 - \sum_{i=0}^{k-1} \beta_{qmi}$ , then set  $k = k + 1$  and repeat *Step 4.2*;

if  $\beta_{qmk} > 1 - \sum_{i=0}^{k-1} \beta_{qmi}$ , then set  $\beta_{qmk} = 1 - \sum_{i=0}^{k-1} \beta_{qmi}$ .

4.3 for  $i = k + 1, k + 2, \dots, p$ , set  $\beta_{qmi} = 0$ .

**Step 5.** Create new variable  $\gamma_{qmk}$  as

$$\gamma_{qm0} = \beta_{qm0}, \quad \text{and} \quad \gamma_{qmk} = \beta_{qm(k-m+1)p-1}$$

for all  $q = 1, 2, \dots, p$ ,  $m = 1, 2, \dots, p - 1$  and  $k = 1, 2, \dots, p - 1$ .

**Step 6.** Create new variable  $\tilde{\lambda}_{qmk}$  as

$$\tilde{\lambda}_{qmk} = \gamma_{qm[k-q]_p}$$

for all  $q = 1, 2, \dots, p$ ,  $m = 1, 2, \dots, p - 1$  and  $k = 1, 2, \dots, p$ .

**Step 7.** Create new variable  $\lambda_{qmk}$  as

$$\lambda_{qmk} = \delta \tilde{\lambda}_{qmk} + h_{k \min} \quad (\text{C.3})$$

for all  $q = 1, 2, \dots, p$ ,  $m = 1, 2, \dots, p - 1$  and  $k = 1, 2, \dots, p$ . And the final  $p \times (p - 1)$  vertices (checking points) should be

$$\lambda_{qm} = (\lambda_{qm1}, \lambda_{qm2}, \dots, \lambda_{qmp})$$

for all  $q = 1, 2, \dots, p$  and  $m = 1, 2, \dots, p - 1$ .

**Remark 10.** When the maximum values are used, all the original resized vertices (obtained by minimum values)

$$(h_{1 \min}, h_{2 \min}, \dots, 1 + h_{i \min} - \sum_{j=1}^p h_{j \min}, \dots, h_{p \min})$$

will disappear. Note that each original vertex is connected with  $p - 1$  edges, then  $p - 1$  new vertices will be created for each maximum value  $h_{i \max}$ . Step 4 is just the method used to calculate the location of those  $p \times (p - 1)$  new vertices. The “if” condition is used to check whether the new vertex is an intersection point of some maximum level surfaces  $h_i(x) = h_{i \max}$ . In such a case, we have  $\sum_{i=0}^{k-1} \beta_{qmi} \leq 1$  ( $k \geq 1$ ), and the new vertex will not be a point on the original polyhedron edges.

## C.2 Explanation of Algorithm 2

**Algorithm 2:** Vertices calculation method for interval type-2 T-S fuzzy system .

**Step 1.** Calculate the minimum and maximum values of possible  $h_i(x)$ ,

$$h_{i \min} = \min_{j=1}^{\kappa} \left\{ \min_x \{h_{i,j}(x)\} \right\}, \quad h_{i \max} = \max_{j=1}^{\kappa} \left\{ \max_x \{h_{i,j}(x)\} \right\}$$

for all  $i = 1, 2, \dots, p$ , where  $\kappa = 2^p$ .

The remaining **Steps 2 – 7** are the same as those of Algorithm 1. Similarly,  $p \times (p - 1)$  vertices  $(\lambda_{qm1}, \lambda_{qm2}, \dots, \lambda_{qmp})$  ( $q = 1, 2, \dots, p$  and  $m = 1, 2, \dots, p - 1$ ) will be obtained.

# Appendix D

## Values of the parameters in Chapter 6

Table D.1: Parameter values of the metamorphic palm

Category	Values of parameters
The mass of links	$m_2 = 33.85 \times 10^{-3} \text{ kg}$
	$m_3 = 93.59 \times 10^{-3} \text{ kg}$
	$m_4 = 97.58 \times 10^{-3} \text{ kg}$
	$m_5 = 33.85 \times 10^{-3} \text{ kg}$
The inertia tensor of links ( $\text{kg} \cdot \text{m}^2$ )	$I_2^2 = \begin{bmatrix} 4170.73 & 0.00 & 0.00 \\ 0.00 & 1072.71 & -761.23 \\ 0.00 & -761.23 & 4168.31 \end{bmatrix} \times 10^{-9}$
	$I_3^3 = \begin{bmatrix} 27476.85 & -1930.49 & 1537.38 \\ -1930.49 & 14659.30 & -11122.58 \\ 1537.38 & -11122.58 & 20770.61 \end{bmatrix} \times 10^{-9}$
	$I_4^4 = \begin{bmatrix} 31550.75 & 2135.61 & 1764.70 \\ 2135.61 & 16992.01 & 13025.86 \\ 1764.70 & 13025.86 & 22679.29 \end{bmatrix} \times 10^{-9}$
	$I_5^5 = \begin{bmatrix} 4170.73 & 0.00 & 0.00 \\ 0.00 & 1072.71 & 761.23 \\ 0.00 & 761.23 & 4168.31 \end{bmatrix} \times 10^{-9}$
The center of mass of links	$r_2^2 = [0.00, 14.61, 44.31] \times 10^{-3} \text{ m}$
	$r_3^3 = [2.40, 24.81, 37.77] \times 10^{-3} \text{ m}$
	$r_4^4 = [2.32, -25.65, 36.82] \times 10^{-3} \text{ m}$
	$r_5^5 = [0.00, -14.61, 44.31] \times 10^{-3} \text{ m}$

Category	Values of parameters
The arc angle length of links	$\alpha_1 = 120^\circ$
	$\alpha_2 = 42^\circ$
	$\alpha_3 = 80^\circ$
	$\alpha_4 = 80^\circ$
	$\alpha_5 = 42^\circ$

# Bibliography

- [1] C. A. Yfoulis and R. Shorten, “A numerical technique for the stability analysis of linear switched systems,” *International Journal of Control*, vol. 77, no. 11, pp. 1019–1039, 2004.
- [2] K. Tanaka, H. Yoshida, H. Ohtake, and H. O. Wang, “A sum-of-squares approach to modeling and control of nonlinear dynamical systems with polynomial fuzzy systems,” *IEEE Transactions on Fuzzy Systems*, vol. 17, no. 4, pp. 911–922, Aug 2009.
- [3] H. K. Lam and M. Narimani, “Quadratic-stability analysis of fuzzy-model-based control systems using staircase membership functions,” *IEEE Transactions on Fuzzy Systems*, vol. 18, no. 1, pp. 125–137, Feb 2010.
- [4] H. K. Lam, “Polynomial fuzzy-model-based control systems: Stability analysis via piecewise-linear membership functions,” *IEEE Transactions on Fuzzy Systems*, vol. 19, no. 3, pp. 588–593, Jun 2011.
- [5] A. Sala and C. Arino, “Relaxed stability and performance conditions for Takagi-Sugeno fuzzy systems with knowledge on membership function overlap,” *IEEE Transactions on Systems, Man, and Cybernetics, Part B: Cybernetics*, vol. 37, no. 3, pp. 727–732, Jun 2007.
- [6] Stuff4less.org, “Auto Gear Knob,” <https://sg.carousell.com/p/auto-gear-knob-149538118/>, [Online; accessed 17-September-2018].
- [7] S. Hedlund and A. Rantzer, “Optimal control of hybrid systems,” in *Proceedings of the 38th IEEE Conference on Decision and Control (Cat. No.99CH36304)*. IEEE, 1999.
- [8] Robotiq, “Robotiq 2-finger 85mm adaptive robot gripper for Universal robots (AGC-UR-KIT-002),” <https://www.thinkbotsolutions.com/shop/robotiq-2-finger-85>, [Online; accessed 18-September-2018].
- [9] Shadow Robot, “Shadow dexterous robotic hand,” <https://www.roscomponents.com/en/robotic-hands/117-shadow-dexterous-robotic-hand.html>, [Online; accessed 18-September-2018].



- [10] L. Xie, S. Shishkin, and M. Fu, “Piecewise Lyapunov functions for robust stability of linear time-varying systems,” *Systems & Control Letters*, vol. 31, no. 3, pp. 165–171, 1997.
- [11] R. N. Shorten and K. S. Narendra, “Necessary and sufficient conditions for the existence of a common quadratic Lyapunov function for a finite number of stable second order linear time-invariant systems,” *International Journal of Adaptive Control and Signal Processing*, vol. 16, no. 10, pp. 709–728, 2002. [Online]. Available: <https://onlinelibrary.wiley.com/doi/abs/10.1002/acs.719>
- [12] J. Sun, X. Zhang, G. Wei, and J. S. Dai, “Geometry and kinematics for a spherical-base integrated parallel mechanism,” *Meccanica*, vol. 51, no. 7, pp. 1607–1621, May 2016.
- [13] G. Chesi, P. Colaneri, J. C. Geromel, R. Middleton, and R. Shorten, “A non-conservative LMI condition for stability of switched systems with guaranteed dwell time,” *IEEE Transactions on Automatic Control*, vol. 57, no. 5, pp. 1297–1302, May 2012.
- [14] K. Wulff, “Quadratic and non-quadratic stability criteria for switched linear systems,” Ph.D. dissertation, Citeseer, 2004.
- [15] H. Lin and P. J. Antsaklis, “Hybrid dynamical systems: an introduction to control and verification,” *Foundations and Trends in Systems and Control*, vol. 1, no. 1, pp. 1–172, 2014.
- [16] L. A. Zadeh, “Outline of a new approach to the analysis of complex systems and decision processes,” *IEEE Transactions on Systems, Man, and Cybernetics*, vol. SMC-3, no. 1, pp. 28–44, 1973.
- [17] D. J. Leith, R. N. Shorten, W. E. Leithead, O. Mason, and P. Curran, “Issues in the design of switched linear control systems: A benchmark study,” *International Journal of Adaptive Control and Signal Processing*, vol. 17, no. 2, pp. 103–118, 2003. [Online]. Available: <https://onlinelibrary.wiley.com/doi/abs/10.1002/acs.741>
- [18] P. E. Allen, *Switched Capacitor Circuits*. Netherlands: Springer, 1984.
- [19] R. Goebel, R. G. Sanfelice, and A. Teel, “Hybrid dynamical systems,” *IEEE Control Systems*, vol. 29, no. 2, pp. 28–93, Apr 2009.
- [20] D. L. Pepyne and C. G. Cassandras, “Optimal control of hybrid systems in manufacturing,” *Proceedings of the IEEE*, vol. 88, no. 7, pp. 1108–1123, Jul 2000.

- [21] A. Balluchi, L. Benvenuti, M. D. di Benedetto, C. Pinello, and A. L. Sangiovanni-Vincentelli, “Automotive engine control and hybrid systems: challenges and opportunities,” *Proceedings of the IEEE*, vol. 88, no. 7, pp. 888–912, Jul 2000.
- [22] C. Tomlin, G. J. Pappas, and S. Sastry, “Conflict resolution for air traffic management: a study in multiagent hybrid systems,” *IEEE Transactions on Automatic Control*, vol. 43, no. 4, pp. 509–521, Apr 1998.
- [23] S. Engell, S. Kowalewski, C. Schulz, and O. Stursberg, “Continuous-discrete interactions in chemical processing plants,” *Proceedings of the IEEE*, vol. 88, no. 7, pp. 1050–1068, Jul 2000.
- [24] D. Liberzon, *Switching in Systems and Control*, ser. Systems & Control: Foundations & Applications. Basel: Birkhuser, 2003.
- [25] L. A. Zadeh, “Fuzzy sets,” *Information and Control*, vol. 8, no. 3, pp. 338–353, Jun 1965.
- [26] Wikipedia contributors, “Fuzzy control system — Wikipedia, The Free Encyclopedia,” 2018, [Online; accessed 18-September-2018]. [Online]. Available: [https://en.wikipedia.org/w/index.php?title=Fuzzy\\_control\\_system&oldid=847859909](https://en.wikipedia.org/w/index.php?title=Fuzzy_control_system&oldid=847859909)
- [27] E. H. Mamdani, “Advances in the linguistic synthesis of fuzzy controllers,” *International Journal of Man-Machine Studies*, vol. 8, no. 6, pp. 669–678, Nov 1976.
- [28] Mamdani, “Application of fuzzy logic to approximate reasoning using linguistic synthesis,” *IEEE Transactions on Computers*, vol. C-26, no. 12, pp. 1182–1191, Dec 1977.
- [29] T. Takagi and M. Sugeno, “Fuzzy identification of systems and its applications to modelling and control,” *IEEE Transactions on Systems, Man and Cybernetics*, vol. SMC-15, no. 1, pp. 116–132, Jan/Feb 1985.
- [30] K. Mehran, “Takagi-Sugeno fuzzy modeling for process control, industrial automation,” *Robotics and Artificial Intelligence (EEE8005)*, School of Electrical, Electronic and Computer Engineering, Newcastle University, 2008.
- [31] H. K. Lam, “A review on stability analysis of continuous-time fuzzy-model-based control systems: From membership-function-independent to membership-function-dependent analysis,” *Engineering Applications of Artificial Intelligence*, vol. 67, pp. 390–408, Jan 2018.

- [32] L. A. Zadeh, “The concept of a linguistic variable and its application to approximate reasoning — I,” *Information Sciences*, vol. 8, no. 3, pp. 199–249, Jan 1975.
- [33] J. Mendel, “Type-2 fuzzy sets and systems: an overview [corrected reprint],” *IEEE Computational Intelligence Magazine*, vol. 2, no. 2, pp. 20–29, May 2007.
- [34] E. J. Routh, *A treatise on the stability of a given state of motion: particularly steady motion*. Macmillan and Company, 1877.
- [35] W. R. Evans, “Control system synthesis by root locus method,” *Transactions of the American Institute of Electrical Engineers*, vol. 69, no. 1, pp. 66–69, Jan 1950.
- [36] H. Nyquist, “Regeneration theory,” *Bell System Technical Journal*, vol. 11, no. 1, pp. 126–147, Jan 1932.
- [37] R. K. R. Yarlagadda, *Analog and Digital Signals and Systems*. Springer US, 2010. [Online]. Available: [https://www.ebook.de/de/product/16829951/r\\_k\\_rao\\_yarlagadda\\_analog\\_and\\_digital\\_signals\\_and\\_systems.html](https://www.ebook.de/de/product/16829951/r_k_rao_yarlagadda_analog_and_digital_signals_and_systems.html)
- [38] N. P. Bhatia, G. P. Szeg, N. P. Bhatia, and G. P. Szeg, *Stability Theory of Dynamical Systems*. Springer Berlin Heidelberg, 2002.
- [39] H. Lin and P. J. Antsaklis, “Stability and stabilizability of switched linear systems: a survey of recent results,” *IEEE Transactions on Automatic Control*, vol. 54, no. 2, pp. 308–322, Feb 2009.
- [40] M. Bernal, T. M. Guerra, and A. Kruszewski, “A membership-function-dependent approach for stability analysis and controller synthesis of takagi–sugeno models,” *Fuzzy Sets and Systems*, vol. 160, no. 19, pp. 2776–2795, Oct 2009.
- [41] P. Gorce and J. G. Fontaine, “Design methodology approach for flexible grippers,” *Journal of Intelligent and Robotic Systems*, vol. 15, no. 3, pp. 307–328, 1996.
- [42] C. S. Lovchik and M. A. Diftler, “The Robonaut hand: a dexterous robot hand for space,” in *Proceedings of the 1999 IEEE International Conference on Robotics & Automation*, Detroit, Michigan, May 1999.
- [43] J. S. Dai, G. Wei, S. Wang, H. Luo, and J. Li, “An anthropomorphic hand with reconfigurable palm,” British Patent No. 201 110 026 001.X, 2011.
- [44] L. Cui and J. S. Dai, “Posture, workspace, and manipulability of the metamorphic multifingered hand with an articulated palm,” *Journal of Mechanisms and Robotics*, vol. 3, no. 2, pp. 1–7, 2011.

- [45] X. Yang, J. Sun, H.-K. Lam, and J. S. Dai, “Fuzzy model based stability analysis of the metamorphic robotic palm,” *IFAC-PapersOnLine*, vol. 50, no. 1, pp. 8630–8635, Jul 2017.
- [46] J. S. Dai and J. R. Jones, “Mobility in metamorphic mechanisms of foldable/erectable kinds,” *Journal of Mechanical Design*, vol. 121, no. 3, pp. 375–382, 1999.
- [47] J. S. Dai, D. Wang, and L. Cui, “Orientation and workspace analysis of the multifingered metamorphic hand–Metahand,” *IEEE Transactions on Robotics*, vol. 25, no. 4, pp. 942–947, Aug 2009.
- [48] R. A. Decarlo, M. S. Branicky, S. Pettersson, and B. Lennartson, “Perspectives and results on the stability and stabilizability of hybrid systems,” *Proceedings of the IEEE*, vol. 88, no. 7, pp. 1069–1082, Jul 2000.
- [49] D. Liberzon and A. S. Morse, “Basic problems in stability and design of switched systems,” *IEEE Control Systems*, vol. 19, no. 5, pp. 59–70, Oct 1999.
- [50] A. N. Michel, “Recent trends in the stability analysis of hybrid dynamical systems,” *IEEE Transactions on Circuits and Systems I: Fundamental Theory and Applications*, vol. 46, no. 1, pp. 120–134, 1999.
- [51] S. Boyd, L. E. Ghaoui, E. Feron, and V. Balakrishnan, *Linear Matrix Inequalities in System and Control Theory (Studies in Applied and Numerical Mathematics)*. Society for Industrial and Applied Mathematics, 1997.
- [52] J.-F. Bonnans, J. C. Gilbert, C. Lemarechal, and C. A. Sagastizbal, *Numerical Optimization*. Springer Berlin Heidelberg, 2006.
- [53] D. Liberzon and R. Tempo, “Common Lyapunov functions and gradient algorithms,” *IEEE Transactions on Automatic Control*, vol. 49, no. 6, pp. 990–994, Jun 2004.
- [54] R. Shorten, K. S. Narendra, and O. Mason, “A result on common quadratic Lyapunov functions,” *IEEE Transactions on Automatic Control*, vol. 48, no. 1, pp. 110–113, Jan 2003.
- [55] A. Polanski, “Lyapunov function construction by linear programming,” *IEEE Transactions on Automatic Control*, vol. 42, no. 7, pp. 1013–1016, Jul 1997.
- [56] B.-J. Rhee and S. Won, “A new fuzzy Lyapunov function approach for a Takagi-Sugeno fuzzy control system design,” *Fuzzy Sets and Systems*, vol. 157, no. 9, pp. 1211–1228, 2006, fuzzy Concepts Applied to Food Control Quality Control.

- [57] A. B. Godbehere and S. S. Sastry, “Stabilization of planar switched linear systems using polar coordinates,” in *Proceedings of the 13th ACM International Conference on Hybrid Systems: Computation and Control*, ser. HSCC ’10. New York, NY, USA: ACM, 2010, pp. 283–292.
- [58] Z. H. Huang, C. Xiang, H. Lin, and T. H. Lee, “Necessary and sufficient conditions for regional stabilisability of generic switched linear systems with a pair of planar subsystems,” *International Journal of Control*, vol. 83, no. 4, pp. 694–715, 2010.
- [59] Y. Yang, C. Xiang, and T. H. Lee, “Sufficient and necessary conditions for the stability of second-order switched linear systems under arbitrary switching,” *International Journal of Control*, vol. 85, no. 12, pp. 1977–1995, 2012.
- [60] —, “Necessary and sufficient conditions for regional stabilisability of second-order switched linear systems with a finite number of subsystems,” *Automatica*, vol. 50, no. 3, pp. 931–939, 2014.
- [61] M. Margaliot and G. Langholz, “Necessary and sufficient conditions for absolute stability: the case of second-order systems,” *IEEE Transactions on Circuits and Systems I: Fundamental Theory and Applications*, vol. 50, no. 2, pp. 227–234, Feb 2003.
- [62] L. Greco, F. Tocchini, and M. Innocenti, “A geometry-based algorithm for the stability of planar switching systems,” *International Journal of Systems Science*, vol. 37, no. 11, pp. 747–761, 2006.
- [63] J. P. Hespanha and A. S. Morse, “Stability of switched systems with average dwell-time,” in *Proceedings of the 38th IEEE Conference on Decision and Control (Cat. No.99CH36304)*, vol. 3, 1999, pp. 2655–2660.
- [64] J. P. Hespanha, “Stabilization through hybrid control,” *encyclopedia of life support systems (EOLSS)*, 2004.
- [65] J. Hespanha, “Uniform stability of switched linear systems: extensions of LaSalle’s invariance principle,” *IEEE Transactions on Automatic Control*, vol. 49, no. 4, pp. 470–482, Apr 2004.
- [66] M. Sugeno and G. T. Kang, “Structure identification of fuzzy model,” *Fuzzy Sets and Systems*, vol. 28, no. 1, pp. 15–33, Oct 1988.
- [67] E. Kim, M. Park, S. Ji, and M. Park, “A new approach to fuzzy modeling,” *IEEE Transactions on Fuzzy Systems*, vol. 5, no. 3, pp. 328–337, 1997.

- [68] S.-H. Tsai, “An improved fuzzy modeling method for a class of multi-input non-affine nonlinear systems,” *Journal of Optimization Theory and Applications*, vol. 157, no. 1, pp. 287–296, Oct 2012.
- [69] H.-K. Lam and F. H.-F. Leung, *Stability Analysis of Fuzzy-Model-Based Control Systems*. Springer Berlin Heidelberg, 2010.
- [70] H. O. Wang, K. Tanaka, and M. F. Griffin, “An approach to fuzzy control of nonlinear systems: stability and design issues,” *IEEE Transactions on Fuzzy Systems*, vol. 4, no. 1, pp. 14–23, 1996.
- [71] C.-L. Chen, P.-C. Chen, and C.-K. Chen, “Analysis and design of fuzzy control system,” *Fuzzy Sets and Systems*, vol. 57, no. 2, pp. 125–140, Jul 1993.
- [72] M. Johansson, A. Rantzer, and K.-E. Arzen, “Piecewise quadratic stability of fuzzy systems,” *IEEE Transactions on Fuzzy Systems*, vol. 7, no. 6, pp. 713–722, 1999.
- [73] G. Feng, “Controller synthesis of fuzzy dynamic systems based on piecewise lyapunov functions,” *IEEE Transactions on Fuzzy Systems*, vol. 11, no. 5, pp. 605–612, Oct 2003.
- [74] H. Ohtake, K. Tanaka, and H. O. Wang, “Switching fuzzy controller design based on switching Lyapunov function for a class of nonlinear systems,” *IEEE Transactions on Systems, Man and Cybernetics, Part B (Cybernetics)*, vol. 36, no. 1, pp. 13–23, Feb 2006.
- [75] H. K. Lam, M. Narimani, H. Li, and H. Liu, “Stability analysis of polynomial-fuzzy-model-based control systems using switching polynomial Lyapunov function,” *IEEE Transactions on Fuzzy Systems*, vol. 21, no. 5, pp. 800–813, Oct 2013.
- [76] H. K. Lam, C. Liu, L. Wu, and X. Zhao, “Polynomial fuzzy-model-based control systems: stability analysis via approximated membership functions considering sector nonlinearity of control input,” *IEEE Transactions on Fuzzy Systems*, vol. 23, no. 6, pp. 2202–2214, Dec 2015.
- [77] M. Narimani, H. K. Lam, R. Dilmaghani, and C. Wolfe, “LMI-based stability analysis of fuzzy-model-based control systems using approximated polynomial membership functions,” *IEEE Transactions on Systems, Man, and Cybernetics, Part B: Cybernetics*, vol. 41, no. 3, pp. 713–724, Jun 2011.
- [78] M. Narimani and H. K. Lam, “SOS-based stability analysis of polynomial fuzzy-model-based control systems via polynomial membership functions,” *IEEE Transactions on Fuzzy Systems*, vol. 18, no. 5, pp. 862–871, Oct 2010.

- [79] Marquez, *Nonlinear Control Systems: Analysis and Design*. John Wiley & Sons, 2003.
- [80] A. M. LYAPUNOV, “The general problem of the stability of motion,” *International Journal of Control*, vol. 55, no. 3, pp. 531–534, Mar 1992.
- [81] Keller-Ressel, Martin, “‘Lyapunov Function.’ From MathWorld—A Wolfram Web Resource, created by Eric W. Weisstein,” 2019, [Online; accessed 02-Janurary-2019]. [Online]. Available: <http://mathworld.wolfram.com/LyapunovFunction.html>
- [82] H. K. Khalil, *Nonlinear Systems, Third Edition*. Upper Saddle River, NJ: Prentice-Hall, 2002.
- [83] F. Blanchini, “Set invariance in control,” *Automatica*, vol. 35, no. 11, pp. 1747–1767, 1999.
- [84] O. N. Bobyleva, “Piecewise-linear lyapunov functions for linear stationary systems,” *Automation and Remote Control*, vol. 63, no. 4, pp. 540–549, 2002.
- [85] P. A. Parrilo, “Structured semidefinite programs and semialgebraic geometry methods in robustness and optimization,” Ph.D. dissertation, California Institute of Technology, 2000.
- [86] C. Arino and A. Sala, “Extensions to ‘stability analysis of fuzzy control systems subject to uncertain grades of membership’,” *IEEE Transactions on Systems, Man, and Cybernetics, Part B: Cybernetics*, vol. 38, no. 2, pp. 558–563, Apr 2008.
- [87] M. Narimani and H. K. Lam, “Relaxed LMI-based stability conditions for Takagi-Sugeno control systems using regional-membership-function-shape-dependent analysis approach,” *IEEE Transactions on Fuzzy Systems*, vol. 17, no. 5, pp. 1221–1228, Oct 2009.
- [88] E. I. Organick, *A Fortran IV Primer - 2nd Edition*. Addison-Wesley, 1967.
- [89] J. R. Wertz, *Spacecraft Attitude Determination and Control*. Netherlands: Springer, 1978.
- [90] Weisstein, Eric W, “‘Commutative.’ From MathWorld—A Wolfram Web Resource,” 2018, [Online; accessed 02-December-2018]. [Online]. Available: <http://mathworld.wolfram.com/Commutative.html>
- [91] A. L. Zelentsovsky, “Nonquadratic Lyapunov functions for robust stability analysis of linear uncertain systems,” *IEEE Transactions on Automatic Control*, vol. 39, no. 1, pp. 135–138, Jan 1994.

- [92] F. A. Valentine, *Convex Sets*. New York, NY: McGraw-Hill, 1965.
- [93] R. A. Horn and C. R. Johnson, *Matrix Analysis, 2nd Edition*. Cambridge: Cambridge University Press, 2012.
- [94] A. Berman and R. Plemmons, *Nonnegative Matrices in the Mathematical Sciences*. Society for Industrial and Applied Mathematics, 1994. [Online]. Available: <https://epubs.siam.org/doi/abs/10.1137/1.9781611971262>
- [95] L. Farina and S. Rinaldi, *Positive Linear Systems: Theory and Applications*. New York, NY: Wiley Interscience Series, 2000.
- [96] V. S. Bokharaie, “Stability analysis of positive systems with applications to epidemiology,” Ph.D. dissertation, National University of Ireland Maynooth, Jan 2012. [Online]. Available: <http://eprints.maynoothuniversity.ie/3733/>
- [97] F. Blanchini, P. Colaneri, and M. E. Valcher, “Co-positive Lyapunov functions for the stabilization of positive switched systems,” *IEEE Transactions on Automatic Control*, vol. 57, no. 12, pp. 3038–3050, Dec 2012.
- [98] L. Gurvits, R. Shorten, and O. Mason, “On the stability of switched positive linear systems,” *IEEE Transactions on Automatic Control*, vol. 52, no. 6, pp. 1099–1103, Jun 2007.
- [99] M. Akar, A. Paul, M. G. Safonov, and U. Mitra, “Conditions on the stability of a class of second-order switched systems,” *IEEE Transactions on Automatic Control*, vol. 51, no. 2, pp. 338–340, Feb 2006.
- [100] E. W. Weisstein, “Lebesgue measure,” *From MathWorld—A Wolfram Web Resource*, 2018.
- [101] A. Sala and C. Arino, “Local stability of open- and closed-loop fuzzy systems,” in *Proceedings of the 2006 IEEE International Symposium on Intelligent Control*, Munich, Germany, Oct 2006.
- [102] K. Tanaka and H. O. Wang, *Fuzzy Control Systems Design and Analysis*. New York: Wiley, 2001.
- [103] X. Yang, H. K. Lam, and L. Wu, “Novel membership-function-dependent stability condition for T-S fuzzy systems,” in *Proceedings of 2016 IEEE World Congress on Computational Intelligence*, Vancouver, Canada, Jul 2016, pp. 2199–2205.
- [104] S. Coupland and R. Joh, “Geometric type-1 and type-2 fuzzy logic systems,” *IEEE Transactions on Fuzzy Systems*, vol. 15, no. 1, pp. 3–15, Feb 2007.



- [105] J. M. Mendal, R. I. John, and F. Liu, “Interval type-2 fuzzy logic systems made simple,” *IEEE Transactions on Fuzzy Systems*, vol. 14, no. 6, pp. 808–821, Dec 2006.
- [106] Q. Lu, P. Shi, H. K. Lam, and Y. Zhao, “Interval type-2 fuzzy model predictive control of nonlinear networked control systems,” *IEEE Transactions on Fuzzy Systems*, vol. 23, no. 6, pp. 2327–2328, Dec 2015.
- [107] H. Li, L. Wu, H. K. Lam, and Y. Gao, *Analysis and Synthesis for Interval Type-2 Fuzzy-Model-Based Systems*. Singapore: Springer, 2016.
- [108] T. Wang, S. Tong, J. Yi, and H. Li, “Adaptive inverse control of cable-driven parallel system based on Type-2 fuzzy logic systems,” *IEEE Transactions on Fuzzy Systems*, vol. 23, no. 5, pp. 1803–1816, Oct 2015.
- [109] D. G. Luenberger, *Linear and Nonlinear Programming*, 2nd ed. Springer, 2003.
- [110] R. R. Stoll, *Set Theory and Logic*. Dover books on advanced mathematics, Dover Publications, 1979.
- [111] S. Hu *et al.*, *Principles of Automatic Control [in Chinese]*. Beijing: Science Press, 2001.
- [112] F. H. Ghorbel, O. Chetelat, R. Gunawardana, and R. Longchamp, “Modeling and set point control of closed-chain mechanisms: Theory and experiment,” *IEEE Transactions on Control Systems Technology*, vol. 8, no. 5, pp. 801–815, 2000.
- [113] R. Murray-Smith and T. A. Johansen, *Multiple Model Approaches to Modelling and Control*. London: Taylor and Francis, 1997.
- [114] M. W. Spong, S. Hutchinson, and M. Vidyasagar, *Robot Modeling and Control*. New York: John Wiley & Sons, 2006.
- [115] D. C. Planchard and M. P. Planchard, *SolidWorks 2013 Tutorial*. SDC Publications, 2013.
- [116] E. Emmanouil, G. Wei, and J. S. Dai, “Spherical trigonometry constrained kinematics for a dexterous robotic hand with an articulated palm,” *Robotica*, 6 2015.
- [117] X. Yang, H. K. Lam, and L. Wu, “Necessary and sufficient stability condition for second-order switched systems: a phase function approach,” *International Journal of Control*, pp. 1–14, Sep 2017.

- [118] —, “Membership-dependent stability conditions for type-1 and interval type-2 T-S fuzzy systems,” *Fuzzy Sets and Systems*, Feb 2018.